FIFTH RARE EARTH RESEARCH CONFERENCE

AUGUST 30, 31, SEPTEMBER 1, 1965

Book One

spectra symposium session S-1 and spectra session S-2

sponsored by Institute for Atomic Research, Iowa State University and Air Force Office of Scientific Research - Directorate of Chemical Sciences

CONTENTS

Spectra Symposium S-1 and Spectra Session S-2

ORBITAL ENERGY DIFFERENCES AND CHEMICAL BONDING IN RARE EARTHS

Chr. Klixbüll Jørgensen

Cyanamid European Research Institute,
Cologny (Geneva), Switzerland

ABSTRACT

The absorption spectra of lanthanide compounds show three types of transitions: internal transitions in the $4f^q$ configuration, where the very small shifts induced by the ligands (the nephelauxetic effect) allow conclusions on weak covalent bonding; transitions 4f → 5d producing broader and more intense absorption bands; and electron transfer bands λ → 4f strongly dependent on the reducing character of the ligands. A common theory for the variation with the number q of 4f electrons of the two latter categories explains why the wavenumbers are particularly low for q = 8 and q = 6, respectively. The behaviour of metallic alloys is discussed, and parenthetical remarks made about the 5f elements. The reluctance of lanthanides to change their oxidation state is connected with the very large effect of repulsion between 4f electrons.

Recent theoretical interpretation of rare earth absorption and luminescence spectra can be used in two different ways: for the spectroscopist, it is a most fascinating case of pseudo-atomic spectroscopy and an example of how to apply group theory; for the chemist, it is possible to draw conclusions about the extent of covalent bonding and to understand the conditions for formation of metallic or nonmetallic compounds. Here, I am concentrating on the second aspect, because much chemical speculation can be clarified by comparison with the newly established experiment facts.

The broad absorption bands are the main subject of the rest of the paper; their wavenumbers are rather dependent on the neighbor atoms, the ligands, and their width is caused by the Franck-Condon principle acting on different electron configurations where the internuclear distances at equilibrium would be different, and usually larger than in the ground configuration $4f^q$. On the other hand, the narrow line groups caused by transitions to excited J-levels belonging to $4f^q$ as well do not shift much when the ligands are varied. Many authors have collaborated the last twelve years in identifying a large number

of such levels.[1,2] The most frequent attempts to describe the fine-structure of each J-level are based on the electrostatic model of the ligand field; however, a closer analysis shows that the only condition for the apparent success of ligand field theory is the consistent occurrence of seven slightly different (to the extent of some hundred cm^{-1}) one-electron energies of the partly filled f shell. Actually, it is possible to predict these small energy differences by a theory of weak σ-anti-bonding effects involving fewer parameters than the conventional electrostatic model and being physically far more plausible.[3,4] It would be highly desirable to extend this description in terms of σ-anti-bonding effects to other chromophores MX_N of known symmetry, such as the C_2-site[5] in the C-type oxide M_2O_3. Another quantitative argument for the presence of weak covalent bonding is the nephelauxetic effect[6] first observed by Ephraim in 1926 that the interelectronic repulsion parameters separating the J-levels are roughly one percent smaller in relatively covalent compounds, such as anhydrous chlorides, bromides, iodides or complexes of organic ligands, compared to the aqua ions (in solution or hydrated salts) and the fluorides. In order to separate this minute effect $d\beta$ it is necessary[7] to write for the wavenumber of the baricenter of each J-level:

$$\sigma_{compound} - \sigma_{aqua} = d\sigma - (d\beta)\,\sigma_{aqua} \qquad (1)$$

where it is assumed that the J-level energy differences all are decreased by the same percentage $d\beta$ relative to the aqua ion (the corresponding gaseous ions M^{+3} are, unfortunately, not known; they probably have $d\beta$ about - 0.01) and $d\sigma$ represents the "ligand field" stabilization of the lowest sub-level of the compound, relative to the lowest sub-level of the aqua ion. The parameters of interelectronic repulsion definitely decrease when the 4f shell expands (because of lower effective charge of the central ion) or participates in anti-bonding molecular orbitals. However, we realize that the Hartree-Fock 4f radial functions[8] predict values of these parameters roughly 50% larger than the observed ones. This may be explained by special difficulties for the one-electron description[1]. It is satisfactory that neutron diffraction experiments on erbium(III) compounds indicate a 4f radial function nearly coincident with the Hartree-Fock calculation for isolated Er^{+3}. It is surprising that oxides[7,9] show a very pronounced nephelauxetic effect, $d\beta$ frequently being between 0.04 and 0.02, and nearly as large as the relatively very covalent sulfides[10] and cyclopentadienides.[11] One reason may be anomalously short M-O distances, because it is known from high-pressure experiments[12] that the nephelauxetic effect increases under such circumstances. Another reason may be the variable diagonal element of ionization energy of the oxide ligand, which is very strongly dependent on the Madelung energy of the solid. A last phenomenon regarding internal $4f^q$ transitions to be mentioned is the strong variation of the intensity of absorption bands corresponding to transitions $J \rightarrow J-2$ (and insofar Russell-Saunders coupling obtains, $L \rightarrow L-2$ and S invariant). These are called hypersensitive pseudo-quadrupole transitions because of the quadrupole-like selection rules.[13]

The 4f → 5d transitions in lanthanide compounds are not the only case known of approximate nl → n'l' transitions in chemistry; 5f → 6d, 5s → 5p and 6s → 6p transitions are also known; and the ionic halides show even, to a certain approximation, strong(np) → (n+1 s) absorption bands. In X-ray absorption and emission spectra, the phenomenon is very frequent. However, the 4f → 5d transitions are interesting by having so relatively low wavenumbers. They are the lowest in divalent lanthanides such as Sm(II), Eu(II) and Yb(II)[14, 15] and have been identified by McClure and Kiss[16] in all divalent lanthanides in dilute solution in solid CaF_2. In trivalent aqua ions, Ce(III) and Tb(III) show these transitions within the easily accessible wavenumber range below 50000 cm^{-1}, and Pr(III) just on the limit.[17, 18]

It is possible to construct a theory[17] for the characteristic variation of both 4f → 5d and electron transfer (filled M. O. concentrated on the ligand) → 4f transitions. Previously, the electron transfer bands were not known of lanthanide complexes, though, according to private communication from Professor K. W. Sykes, Dr. A. G. Davies observed such bands in 1957. The experimental difficulty is that most ligands, which are sufficiently strongly reducing to produce electron transfer bands in lanthanide complexes, are either coloured because of internal transitions in the ligands or do not displace water from the aqua ions. Bromides in nearly anhydrous ethanol and dialkyldithiocarbamates extracted in dichloroethane show such bands, which are very broad and relatively weak.[17] Their wavenumbers vary in a characteristic way with the central ion

$$Eu(III) < Yb(III) < Sm(III) < Tm(III) < \ldots . \qquad (2)$$

similar to the chemical tendency to be reduced to M(II). Actually, the aqua ions[19] of Eu(III) show an electron transfer band at 53200 cm^{-1} and of Yb(III) about 59000 cm^{-1}. Barnes and Day[20, 21] studied a variety of anions bound to lanthanides and found remarkably low wavenumbers of the sulfate complexes: $EuSO_4^+$ 41700, $YbSO_4^+$ 44500 and $SmSO_4^+$ 48100 cm^{-1}. Normally, SO_4^{--} is not considered to be particularly reducing, but it is known[22] to undergo photochemical oxidation to SO_4^- above 55000 cm^{-1}. Another interesting phenomenon is the relatively low wavenumbers of the electron transfer bands of ethanol solvates(Eu(III) 44100 cm^{-1}) though it is not easy to make a distinction from the effects of possibly coordinated ClO_4^-. In gaseous state, C_2H_5OH has the ionization energy[23] 16000 cm^{-1} below that of H_2O. Hartmann[24] made similar comments on the electron transfer spectra of VCl_3 in alcohols, though here, it is difficult to avoid interference with chloride complexes. It is possible to rationalize the positions of electron transfer bands in all five transition groups by means of the concept[1] of optical electronegativities, x_{opt}. If corrected for spinpairing energy, the values of x_{opt} vary linearly in a given transition group with a given oxidation number[25, 26] as function of increasing number q. The spinpairing energy (due to differences in interelectronic repulsion) for the average of all terms with the same S is:

$$\underline{D}\left[\frac{3}{4}\, q\left(1 - \frac{q-1}{4\underline{\ell}+1}\right) - \underline{S}\,(\underline{S}+1)\right] \qquad (3)$$

where the parameter D is proportional to the average value of the reciprocal radius $< r^{-1} >$ of the partly filled shell. Eq. (3) expresses the stability of half-filled shells and hence, it explains the particularly low wavenumbers of the $4f \rightarrow 5d$ transitions in $4f^8$ systems such as Tb(III) and of $\lambda \rightarrow 4f$ electron transfer transitions in $4f^6$ systems such as Eu(III), whereas the wavenumbers are particularly high both of $4f \rightarrow 5d$ and $\lambda \rightarrow 4f$ transitions in $4f^7$ systems such as Gd(III). If the spin-pairing energy(3) was the only effect superposed a linear, gradual stabilization of the 4f orbitals as function of increasing q, the energy differences would fall on two straight lines making a jump 8D at the half-filled shell. However, there occur a few other, less important, effects which can be treated by Racah's theory[27] of inter-electronic repulsion in the configurations f^q and by a first-order relativistic treatment in terms of Lande's parameter ζ_{nf}. The actual variation of the wavenumbers of the lowest $\lambda \rightarrow 4f$ transition is expected to be (changing from the ground configuration $4f^q$ to $4f^{q+1}$):

$$W - q(E-A) + k_1\underline{D} + k_2\underline{E}^3 + k_3\,\zeta_{nf} \qquad (4)$$

and the variation of the lowest $4f^q \rightarrow 4f^{q-1}5d$ transition:

$$W_2 + (q-1)\,(E-A)_2 + k_4\underline{D} + k_5\underline{E}^3 + k_6\,\zeta_{nf} \qquad (5)$$

where Table 1 gives the coefficients k_n. The wavenumbers W and W_2 are just standards of reference for comparison within a given series, where only q is varied. The symbols (E-A) and $(E-A)_2$ indicate that the gradually increasing stabilization of the 4f orbital energy can be written as the difference between the increase E of the core attraction and the increase A(of the type F^0) of interelectronic repulsion in the 4f shell. One of the reasons why (E-A) and $(E-A)_2$ are different is that we neglect the repulsion between 4f and 5d electrons; McClure and Kiss [6] have given explicit expressions for this interaction. It is worth noting that the spin-pairing parameter $\underline{D}$ is equivalent to Racah's $\left(\frac{9}{8}\underline{E}^1\right)$ and that $\underline{E}^1 \sim 14.7\,\underline{F}_2$ and $\underline{E}^3 \sim 1.48\,\underline{F}_2$ in terms of the Slater-Condon-Shortley parameter $\underline{F}_2$ used by many authors. Though eqs. (4) and (5) seem to involve many parameters, the great advantage is that D (or $\underline{E}^1$), $\underline{E}^3$ and ζ_{4f} already are well determined from the internal transitions in the 4f shell. However, the values of (E-A), $(E-A)_2$ and D given in Table 2 cannot usually be taken seriously better than ± 10%. Since D is strongly fixed by comparison with the known values for the internal 4f transitions, the wavenumbers of which do not vary much with the ligands, it has been estimated and is given in brackets in Table 2 when only two data were available, or when three observations gave unreasonable values of D by the strict application of three equations

with three unknown parameters. Table 3 gives the numerical values of $\underline{E}^3$ and ζ_{nf}.

The hexahalides of trivalent lanthanides MX_6^{-3} were not previously known, but Ryan[30] has recently studied them in a solvent consisting of a mixture of acetonitrile and succinonitrile. The only MX_6^{--} known is $CeCl_6^{--}$, and hence, only W can be given in Table 2. It may be remembered that $\lambda \rightarrow$ 5f and 5f $\rightarrow$ 6d transitions have been identified in U(IV), Np(IV) and Pu(IV) hexahalides[32] and that the 5f group elements exhibit an evolution of the optical electronegativities intermediate between the 4f and the three d groups.[33] Recently, electron transfer spectra of neptunium(IV) aqua, methanol, sulfate and chloride complexes have been further studied.[34]

W is expected to be a linear function of the optical electronegativity $\underline{x}_{opt}$ of the ligands, and actually, it has approximately the form

$$W = W_0 + (30000\ cm^{-1})\ \underline{x}_{opt} \qquad (6)$$

where $W_0 = -15000\ cm^{-1}$ for trivalent lanthanides and $W_0 = -65000\ cm^{-1}$ for quadrivalent lanthanides. This is a much larger variation with the oxidation number than in the d groups[26] where W_0 only decreases some 15000 cm^{-1} for each unit of increase of oxidation number (keeping q and the ligands constant). In the compressed hexahalides[30] MX_6^{-3} with unusually short M-X distances, W_0 seems to be only - 18000 cm^{-1}.

I may warn you that electron transfer spectra of lanthanides are only observable under rather special conditions. Impurities of Fe(III) or less frequently, of Ti(IV), Cu(II), Pt(IV)(from crucibles) and Pb(II) may imitate the broad relatively weak bands. The lanthanides are characterized by magnetic moments, which in nearly all cases correspond to an integral number of electrons in the partly filled 4f shell. Hence, it is possible to define an oxidation state even in metallic alloys (such as $NdCd_{11}$ containing Nd(III) but UCd_{11} containing U(IV)[35]) and black, low-energy-gap semiconductors where the internal 4f-transitions cannot be observed. Professor K. A. Jensen has proposed to write such oxidation states derived from spectroscopic and magnetic measurements with sharp brackets M[II] and M[III] in the cases where they would be different from the Stock nomenclature. It is now well known that even the metallic elements are Eu[II] and Yb[II] but for instance Gd[III] and Er[III] in this sense. The situation is entirely different in the d transition groups where antiferromagnetic interactions can be extremely strong even in compounds with normal visible absorption spectra(e.g. of many oxides and halides). However, many low-energy-gap semiconductors[36] still have magnetic moments corresponding to well-defined S which is not usually the case for metallic compounds. Goodenough[37] proposed a criterion for localized magnetic moments occurring when the closest distance between transition group atoms is larger than 2.5 times the average radius of the partly filled shell.

In this connection, it is very interesting that LaS, CeS, PrS, NdS, GdS, TbS, DyS, HoS, ErS and TmS are metals containing roughly one conduction electron and the number of 4f electrons corresponding to M[III] whereas SmS, EuS and YbS are non-metallic M(II) compounds.[38] The parameters[29] given in Table 2 for MS satisfy the condition that the non-metallic monosulfides have $4f^q$ groundstates and that the metals would have had $4f^{q-1}5d$ groundstates if it were not for the larger average radius of the 5d shell transforming itself into a delocalized conduction band. Metallicity can also be caused by non-stoichiometric composition; a very interesting case is the metallic $Ce_{3-x}S_4$ becoming non-metallic for the stoichiometric value x=0.333 but retaining the same crystal structure.[39] The metallic transition sometimes can be extremely sharp; thus,[40] NdSe and $Nd_{1-x}Sm_xSe$ are metallic for $x < 0.11$ but is distinctly metallic for $x > 0.13$. The diiodides LaI_2, CeI_2 and GdI_2 are metallic alloys whereas NdI_2, SmI_2, EuI_2, TmI_2 and YbI_2 are strongly coloured, non-metallic compounds, and PrI_2 a somewhat uncertain intermediate case.[41,42] The parameters adapted to McClure and Kiss' M(II) in in dilute solution in fluorite[16] given in Table 2 predict that La(II), Ce(II), Gd(II) and Tb(II) have $4f^{q-1}5d$ goundstates and that $4f^3$ of Pr(II) is only 2000 cm^{-1} below $4f^25d$ in agreement with the behaviour of the undiluted MI_2 (and quite different from the gaseous Pr^{++}, where the lowest energy level of the configuration $4f^3$ occurs[43,44] 12850 cm^{-1} below the lowest level of $4f^25d$). When comparing gaseous ions M^{+z} and compounds, two opposite tendencies act. At one hand, the energy difference between 4f and 5d tends to decrease in complexes[45] (this is also true for 6s → 6p in Tl(I), Pb(II), Bi(III))[52] and at the other hand, the relative σ-anti-bonding character[3,19] of the five 5d orbitals is rather different in chromophores MX_N of various symmetries, and may shift the position of the first 4f → 5d absorption band some 10000 cm^{-1}.

The mononitrides MN all have magnetic moments[46] corresponding to M[III] though they show metallic conductivity. This may be caused by weak deviations from stoichiometry, or by "accidental metallicity" (occurring e.g. in Bi or CoS_2 where only a small fraction of an electron p r atom is involved in the conduction[36]). There is optical evidence[47] that the stoichiometric mononitrides, at least DyN, HoN and ErN, would be semiconductors with a relatively large energy gap. However, MP and MAs, which also crystallize in NaCl lattice, are genuinely black. It is interesting to note that many chalcogenides ME_x are black with metallic brillance and has a very high electric conductivity, but for x=1.50 it is black like smoke and only semiconducting.[48] The lanthanides are particularly interesting by showing extreme transition group properties. The d^q configurations show intermediate properties with respect to delocalization of the partly filled shell etc. between $5f^q$ and the p^q configurations existing in a certain sense in complexes of Se(II), Br(III), Te(II), I(III) and Xe(IV)(q=2) and I(I) and Xe(II)(q=4). One may go as far as to say that the 4f shell shows internal transitions which have been shifted from the X-ray region into the visible. The 4f electrons have enormously large integrals of attraction by the core potential[8] and correspondingly small average distance from the nucleus, but the interelectronic repulsion between the 4f electrons (of the F^0 type) is so large as to cancel

the attraction nearly completely and to obtain ionization energies comparable to those of the loosest bound electrons (with far larger $< r >$) of other atoms. However, a consequency of this cancellation is that the 4f ionization energy increases unusually rapidly as function of the ionic charge + z. This explains the great reluctance of the lanthanides to change oxidation number to the highly reducing M(II) or the highly oxidizing M(IV). Another consequency is the necessity of the presence of one or more 5d and 6s electrons in the isolated M^o, M^+, and Gd^{+2}. Hence, Ce(II), Gd(II) and Tb(II)[16] in CaF_2 are, like the gaseous molecule[29] TiO, among the rare examples in chemistry of the simultaneous presence of two partly filled shells. This situation does not appear in undiluted compounds, because one of the two shells delocalizes to a conduction band in all known cases. There is no contradiction[49] between the presence of 5f electrons in Th^{+3}, Pa(IV), U(III), U(IV),... and the higher and more variable oxidation numbers compared with the lanthanides. The quantitative difference is caused by the cancelling core attraction and interelectronic repulsion just mentioned and can be expressed empirically by the values[2] $W_2 \sim 0$ for M(III) aqua ions, $W_2 \sim 33000$ cm^{-1} for M(IV) aqua ions, and $W \sim 60000$ and $W_2 \sim 18000$ cm^{-1} for M(IV) hexabromides.[22] Actually, there is no necessary connection between the presence of f electrons and a tendency towards the oxidation state + 3. There is very little positive evidence for any measurable influence of the 4f electrons on the chemical bonding in lanthanide complexes, though minute effects such as the "gadolinium break" may perhaps be caused by the weakly pronounced (but quite verified) M. O. formation of the 4f shell. An alternative contribution may be the 5d bonding possibly being influenced by the half-filled shell effects discussed here. However, we remember that the mechanism of the invariant oxidation number of elements such as beryllium or aluminum is different from that of holmium: Be(II) and Al(III) would loose electrons from a very strongly bound inner shell, if oxidized, and gain electrons in an external shell of weak electron affinity if reduced. The lanthanides loose or gain 4f electrons; but the ionization energy is much larger than the electron affinity because of the small average radius of the partly filled 4f shell and the concomitant huge effects of interelectronic repulsion. A closer analysis shows that this is also the fundamental reason for the tendency towards localized 4f shells in metallic materials. Table 4 gives a numerical, qualitative model of the differences between 4f and 3d elements; the concept of ionization energy of chemical species is discussed p. 236 of ref. 52.

REFERENCES

1. Jørgensen, C.K. "Orbitals in Atoms and Molecules". Academic Press, London, 1962.
2. Jørgensen, C.K. "Lanthanides and 5f Group Elements". Academic Press, London, 1965.
3. Jørgensen, C.K., Pappalardo, R. and Schmidtke, H.-H., J. Chem. Phys. 39, (1963) 1422.
4. Schäffer, C. E. and Jørgensen, C.K., Mol. Phys.
5. Kisliuk, P., Krupke, W.F. and Gruber, J.B., J. Chem. Phys. 40, (1964) 3606, and Gruber, J. B., Krupke, W. F. and Poindexter, J. M., ibid. 41 (1964) 3363.
6. Jørgensen, C.K., Progress Inorg. Chem. 4, (1962) 73.
7. Jørgensen, C.K., Pappalardo, R. and Rittershaus, E., Z. Naturforsch. 19a, (1964) 424.
8. Freeman, A. J. and Watson, R. E., Phys. Rev. 127, (1962) 2058.
9. Jørgensen, C.K., Pappalardo, R. and Rittershaus, E., Z. Naturforsch. 20a, (1965) 54.
10. Jørgensen, C.K., Pappalardo, R. and Flahaut, J., J. chimie phys.
11. Pappalardo, R., Helv. Phys. Acta 38, (1965) 178. 62, (1965) 444.
12. Drickamer, H. G. and Zahner, J. C., Advanc. Chem. Phys. 4, (1962) 161.
13. Jorgensen, C.K. and Judd, B. R. Mol. Phys. 8, (1964) 281.
14. Butement, F. D. S., Trans. Faraday Soc. 44, (1948) 617.
15. Kaplyanskii, A. A. and Feofilov, P. P., Optics and Spectroscopy 13, (1962) 129.
16. McClure, D. S. and Kiss, Z., J. Chem. Phys. 39, (1963) 3251.
17. Jørgensen, C. K., Mol. Phys. 5, (1962) 27
18. Cohen, S.H., Iwamoto, R. T. and Kleinberg, J., J. Phys. Chem. 67, (1963) 1275.
19. Jørgensen, C.K. and Brinen, J.S., Mol. Phys. 6, (1963) 629.
20. Barnes, J. C., J. Chem. Soc. 1964 3880.
21. Barnes, J.C. and Day, P., J. Chem. Soc. 1964 3886.
22. Barrett, J., Fox, M.F. and Mansell, A.L., Nature 200, (1963) 257.
23. Al-Joboury, M.I. and Turner, D.W., J. Chem. Soc. 1964 4434.
24. Hartmann, H., Z. Naturforsch. 6a, (1951) 781.

25. Jørgensen, C.K., Mol. Phys. 6, (1963) 43.

26. Jørgensen, C.K., Proceed. 8. I. C. C. C. Vienna, September 1964, p. 67.

27. Racah, G., Phys. Rev. 76, (1949) 1352.

28. Dieke, G.H., Crosswhite, H.M. and Dunn, B., J. Opt. Soc. Amer. 51, (1961) 820.

29. Jørgensen, C.K., Mol. Phys. 7, (1964) 417.

30. Ryan, J.L. and Jørgensen, C.K.,

31. Asprey, L.B. and Hoppe, R., private communication

32. Ryan, J. L. and Jørgensen, C.K., Mol. Phys. 7, (1963) 17.

33. Jørgensen, C.K., Proceed. Tihany Conference on Coordination Chemistry, September 1964, Hungarian Academy of Sciences, Budapest.

34. Gainar, I. and Sykes, K.W., J. Chem. Soc. 1964 4452.

35. Cafasso, F.A., Feder, H.M. and Gruen, D.M., J. Chem. Phys. 38, (1963) 1256.

36. Hulliger, F. and Mooser, E., Progress Chem. Solids.

37. Goodenough, J.B., "Magnetism and the Chemical Bond". Interscience, New York, 1963.

38. McClure, J.W., J. Phys. Chem. Solids 24, (1963) 871.

39. Cuttler, M. and Leavy, J.F., Phys. Rev. 133, (1964) A 1153.

40. Reid, F.J., Matson, L.K., Miller, J.F. and Himes, R.C., J. Phys. Chem. Solids 25, (1964) 969.

41. Corbett, J.D., Druding, L.F., Burkhard, W.J. and Lindahl, C.B., Discuss. Faraday Soc. 32, (1961) 79.

42. Dworkin, A.S., Bronstein, H.R. and Bredig, M.A., J. Phys. Chem. 66, (1962) 1201. and 67, (1963) 2715.

43. Sugar, J., J. Opt. Soc. Amer. 53, (1963) 831.

44. Trees, R.E., J. Opt. Soc. Amer. 54, (1964) 651.

45. Jørgensen, C.K., Mat. fys. Medd. Dan. Vid. Selsk. 30, (1956) No. 22.

46. Didchenko, R. and Gortsema, F.P., J. Phys. Chem. Solids 24, (1963) 863.

47. Sclar, N., J. Appl. Phys. 35, (1964) 1534.

48. Flahaut, J., private communication.

49. Jørgensen, C.K., Mol. Phys. 2, (1959) 96.

50. Carnall, W.T. and Wybourne, B.G., J. Chem. Phys. 40, (1964) 3428.

51. Conway, J.G., J. Chem. Phys. 41, (1964) 904.

52. Jørgensen, C.K., "Absorption Spectra and Chemical Bonding in Complexes". Pergamon Press (U.S. distributor: Addison-Wesley) Oxford 1962.

Table 1. The coefficients applied in eqs. (4) and (5).

q =	0	1	2	3	4	5	6	7	8	9	10	11	12	13	14
k_1 =	0	$-8/13$	$-16/13$	$-24/13$	$-32/13$	$-40/13$	$-48/13$	$+48/13$	$+40/13$	$+32/13$	$+24/13$	$+16/13$	$+8/13$	0	-
k_2 =	0	-9	-12	0	+12	+ 9	0	0	- 9	-12	0	+12	+ 9	0	-
k_3 =	-2	-1	-1/2	0	+1/2	+ 1	+ 2	-3/2	- 1	-1/2	0	+1/2	+ 1	+ 3/2	-
k_4 =	-	0	$+8/13$	$+16/13$	$+24/13$	$+32/13$	$+40/13$	$+48/13$	$-48/13$	$-40/13$	$-32/13$	$-24/13$	$-16/13$	$-8/13$	0
k_5 =	-	0	+ 9	+12	0	-12	- 9	0	0	+9	+12	0	-12	-9	0
k_6 =	-	+2	+ 1	$+1/2$	0	$-1/2$	- 1	-2	$+3/2$	+ 1	$+1/2$	0	$-1/2$	-1	$-3/2$

Table 2. The parameters of eqs. (4) and (5) for different environments of lanthanides M(II), M(III) and M(IV).

gaseous M^{++}	W_2 = 8000	$(E-A)_2$ = 3600	[D=5500]	ref. 17, 28
gaseous M^{+3}	W_2 = 50000	$(E-A)_2$ = 5000	[D=6700]	ref. 17, 28
M(II) in CaF_2	W_2 = -17000	$(E-A)_2$ = 3800	D=5200	ref. 29
MS solid	W_2 = -25000	$(E-A)_2$ = 3000	[D=5200]	ref. 29
$M(H_2O)_9^{+3}$	W = 90000	(E-A) = 2800	[D=6500]	ref. 19
	W_2 = 33000	$(E-A)_2$ = 5000	D=6500	
M_2O_3 solid	W = 75000	(E-A) = 3000	D=6500	ref. 9
	W_2 = 21000	$(E-A)_2$ = 3800	D=5200	
MSO_4^+ in water	W = 80000	(E-A) = 3000	[D=6500]	ref. 20
MCl^{++} in ethanol	W = 78000	(E-A) = 3150	D=7000	ref. 20
MCl_6^{-3} in nitriles	W = 74000	(E-A) = 3200	[D=6500]	ref. 30
MBr^{++} in ethanol	W = 70000	(E-A) = 3000	D=6500	ref. 17
	W_2 = 31000	$(E-A)_2$ = 4700	D=6200	
MBr_6^{-3} in nitriles	W = 66000	(E-A) = 3100	[D=6500]	ref. 30
MCl_6^{--}	W = 25000	-	-	ref. 30
Cs_3MF_7 solid	W = 54000	(E-A) = 5600	[D=7800]	ref. 31

Table 3. The parameters $\underline{E}^3$ and ζ_{nf} in cm^{-1} determined from internal transitions in the partly filled f shell. The slightly less certain values for 5f elements in the oxidation states M(III)[50] and M(IV)[51] have recently been estimated by comparative studies.

$4f^q$, q =		$\underline{E}^3$	ζ_{nf}	$5f^q$, q =		$\underline{E}^3$	ζ_{nf}
3	Pr^{++}	410	650	3	U(III)	290	1670
6	Sm(II)	480	1050	4	Np(III)	330	2070
13	Tm(II)	-	2510	5	Pu(III)	350	2290
2	Pr(III)	460	730	6	Am(III)	380	2550
3	Nd(III)	490	880	7	Cm(III)	410	2950
4	Pm(III)	520	1030	2	U(IV)	300	1870
5	Sm(III)	550	1180	3	Np(IV)	330	2190
6	Eu(III)	~600	1360	4	Pu(IV)	360	2430
7	Gd(III)	~600	1540	5	Am(IV)	410	2820
8	Tb(III)	~600	1720	6	Cm(IV)	450	3040
9	Dy(III)	~600	1920				
10	Ho(III)	620	2080				
11	Er(III)	640	2380				
12	Tm(III)	670	2620				
13	Yb(III)	-	2950				

Table 4. The spectroscopic ionization energies I_{n+1}, the sum of Madelung-like and chemical bonding terms E_M, and the resulting chemical ionization energies $C_{n+1} = I_{n+1} - E_M$, all in eV. A chemical species is only stable if C_{n+1} is larger than 3 eV, and if the corresponding electron affinity C_n is smaller than 9 eV. The example is purely qualitative, suggesting why M(II), M(III) and M(IV) exist for a typical 3d element, and only M(III) of a typical 4f element.

	$3d^q$			$4f^q$		
	I_{n+1}	E_M	C_{n+1}	I_{n+1}	E_M	C_{n+1}
$M \rightarrow M^+$	6	5	1	-	4	-
$M^+ \rightarrow M^{+2}$	18	15	3	4	12	-8
$M^{+2} \rightarrow M^{+3}$	30	25	5	22	20	+2
$M^{+3} \rightarrow M^{+4}$	42	35	7	40	28	12
$M^{+4} \rightarrow M^{+5}$	54	45	9	58	36	22

OPTICAL SPECTROSCOPY OF RARE EARTH COMPOUNDS

by

K.H.Hellwege

Institut für Technische Physik, Technische Hochschule Darmstadt.

Abstract

New results covering the following fields are presented: The term schemes of Nd^{3+} and Tb^{3+} ions have been investigated up to 40 000 cm^{-1}; the absorption spectrum of the $^2F_{5/2} \rightarrow {}^2F_{7/2}$ transition in unhydrous $CeCl_3$ has been analyzed. An extensive study of magnetically ordered compounds has been undertaken ($GdCl_3$, DyAlG, ErIG, DyIG, HoIG); the internal fields for these compounds have been obtained in the ordered state. In $La(Er)Cl_3$ an example for the correlation of linewidth of fluorescence lines and the ORBACH coefficient is given.

Introduction.

The main fields in our present spectroscopic investigations of rare earth compounds are: The completion of the level schemes of the trivalent rare earth ions; linewidth of absorption and fluorescence lines, properties of magnetically ordered compounds. In the following section we shall give some recent results in all three fields.

II. Experimental procedure.

For the spectroscopic investigations we used four spectrographs: a 6 m ROWLAND concave grating, a 3,5 m and a 2 m EBERT mounting spectrograph and a prism spectrograph for the infrared investigations. The crystals were placed in conventional glass or metal dewars either

directly in liquid nitrogen or liquid helium or fastened to a copper block which itself was cooled by the cooling liquid. The spectra were photographed or directly photorecorded with a multiplier or a PbS photoresistor.

III. Term schemes of the trivalent rare earth ions.

The term schemes of the trivalent rare earth ions have by now all been completed up to about 30 000 cm^{-1} [1]. At higher energies in some cases the term density becomes so large that the analysis of the spectra gets very complicated. We have analyzed the ultraviolet absorption spectra of Nd^{3+} [2] and Tb^{3+} [3] salts. In the case of Nd^{3+} it was possible to assign all observed linegroups to theoretical terms. For Tb^{3+} the analysis was much more difficult because of the large term density in the investigated spectral range. Yet it was possible to attribute some of the observed line groups to theoretical terms. Fig. 1 shows the term schemes for all trivalent rare earth ions in their present state.

In $CeCl_3$ [4] the transition $^2F_{5/2} \rightarrow {}^2F_{7/2}$ was investigated in order to obtain the crystal field parameters in this compound. The crystal field level scheme deduced from our measurements is shown in fig. 2. The crystal field parameters with which we could best fit the observed levels are: $A_2^0 \langle r^2 \rangle = 64{,}5\ cm^{-1}$, $A_4^0 \langle r^4 \rangle = -41{,}0\ cm^{-1}$, $A_6^0 \langle r^6 \rangle = -64{,}1\ cm^{-1}$ and $A_6^6 \langle r^6 \rangle = 399{,}1 cm^{-1}$.

IV. Magnetically ordered compounds.

The spectroscopic investigation of magnetically ordered compounds can yield useful information about the internal fields in the ordered state, the level schemes in the ordered state and the effect on the ordered state

of an applied external magnetic field.

a) Rare Earth Iron Garnets.

WICKERSHEIM and WHITE [5] were the first to investigate a rare earth iron garnet (YbIG) by optical spectroscopy. We have performed a study of the iron garnets of Er, Ho, and Dy [6]. It was possible to determine the level schemes of these three garnets (fig. 3). The ground term level schemes are in agreement with those from other investigations, i.e. the far infrared spectroscopy of SIEVERS and TINKHAM [7] and the specific heat measurements of HARRIS and MEYER [8]. From the splittings of the excited $^4S_{3/2}$ term in ErIG and the excited $^6F_{3/2}$ term in DyIG it was possible to determine the exchange fields acting in the ordered state on the rare earth ions. They are $(285 \pm 3o).1o^3$ oe and $(3o5 \pm 5o).1o^3$ oe for ErIG and DyIG respectively as compared to $285 \cdot 1o^3$ oe and $327 \cdot 1o^3$ oe [9] deduced from a magnetization measurement.

b) Dysprosium Aluminium Garnet (DyAlG).

DyAlG has a very large anisotropic splitting factor ($g_z = 18,2$, $g_x = g_y = 0$) which causes an antiferromagnetic ordering of this compound at 2,49 °K [10]. We investigated the transitions $^6H_{15/2} \rightarrow {}^6F_{5/2}$, $^6F_{3/2}$ [11][12] in this compound in the ordered and paramagnetic state. In the ordered state the KRAMERS doublets are split by the internal fields. Fig. 4 gives a photorecording of the whole transition $^6H_{15/2} \rightarrow {}^6F_{5/2}$ at various temperatures. The ground term splittings are proportional to the magnetization curve of DyAlG. Fig. 5 shows the optically measured points ($o = {}^6H_{15/2} \rightarrow {}^6F_{5/2}$ $\times = {}^6H_{15/2} \rightarrow {}^6F_{3/2}$) as compared with the curve which is a result from a neutron diffraction measurement [13]. The splitting of the lowest doublet of the $^6H_{15/2}$ term in the

ordered state is $\Delta W = (5,2 \pm o,5) cm^{-1}$ which is to be compared with the value 5,4 cm^{-1} of COOKE et al [14], and with two theoretical values [14] 4,9 cm^{-1} and 5,46 cm^{-1}.

c) Gadoliniumchloride($GdCl_3$).

$GdCl_3$ orders ferromagnetically [15] at 2,2 °K. The optical measurements [16] yield a value of the internal field $H_{eff} = (8,5 \pm 2,o)\ 1o^3$ oe extrapolated to o °K. The value of the exchange field deduced from a magnetization measurement is $H_{ex} = (8,2)\ 1o^3$ oe [15].

V. Linewidth and ORBACH-relaxation.

A correlation exists between the linewidth in special optical transitions and the ORBACH coefficient in paramagnetic relaxation [17] as can be deduced from fig.6. The linewidth of the A-line is given by the strain broadening. The linewidth of the E-line is given by strain broadening plus the broadening of the II $^4I_{15/2}$ level by spontaneous emission of phonons; the rate for spontaneous emission of phonons on the other hand is measured in paramagnetic relaxation experiments by the ORBACH coefficient. The results of an experiment of Er(5%) $LaCl_3$ are [18]: Γ (A) = o,34 cm^{-1}, Γ(E) = o,39 cm^{-1} which yields Γ (II) = o,o5 cm^{-1}. On the other hand the relaxation time measurement [18] yields $\tau^{-1} = \Gamma(II)\ 2\pi c \cdot \exp(-\Delta/kT) = 1.4 \times 1o^{10} \cdot \exp(-54.5/T)$ that is Γ (II) = o,o7 cm^{-1} in good agreement with the above figure.

This work was supported by the Deutsche Forschungsgemeinschaft.

Literature

1) DIEKE, G.H. Proc. of the 1th int.Conf. on Paramag. Resonance, Acad.Press(New York)1963, p 237

2) HELLWEGE, K.H., S. HÜFNER, M. SCHINKMANN, to be published

3) HELLWEGE, K.H., S. HÜFNER, H. SCHMIDT, to be published

4) HELLWEGE, K.H., E. ORLICH, G.SCHAACK, to be published

5) WICKERSHEIM, K.A. and M.L. WHITE, Phys.Rev.Lett.4, 123 (1960)

6) HÜFNER, S., and H.SCHMIDT, to be published

7) SIEVERS, A.J., and M.TINKHAM, Phys.Rev.129,1995(1963)

8) HARRIS, A.B., and H. MEYER, Phys.Rev.127, 101(1962)

9) CASPARI, M.E.,A.KOICKI, S.KOICKI, and G.T.WOOD, Phys.Letters 11,195(1964)

10)BALL, M.,M.T.HUTCHINGS, M.J.M.LEASK, and W.P.WOLF, Proc. 8th Int.Conf.Low Temp.Phys.248(1964)

11)HELLWEGE, K.H., S.HÜFNER, M.SCHINKMANN, and H.SCHMIDT Phys.Letters 12,107(1964)

12)HÜFNER, S, M.SCHINKMANN, and H.SCHMIDT, to be published

13)HERPIN, A. et P.MERIEL: C.R.(Paris) 259,2416(1964)

14)COOKE, A.H., K.A.GEHRING, M.J.M.LEASK,D.SMITH, and J.H.M.THORNLY, Phys.Rev.Lett.,14,685(1965)

15)WOLF, W.P., M.J.M.LEASK, B.MANGUM, and A.F.G. WYATT, J.Phys.Soc.Jap.17, Suppl.BI, 487 (1962)

16)HÜFNER,S., M.SCHINKMANN, and H.SCHMIDT, to be published

17)YEN, W.M., W.C. SCOTT, and P.L. SCOTT, Phys.Rev.137, A 1109 (1965)

18)HELLWEGE, K.H., P. HILL, S.HÜFNER, M.SCHINKMANN, and G.WEBER, to be published.

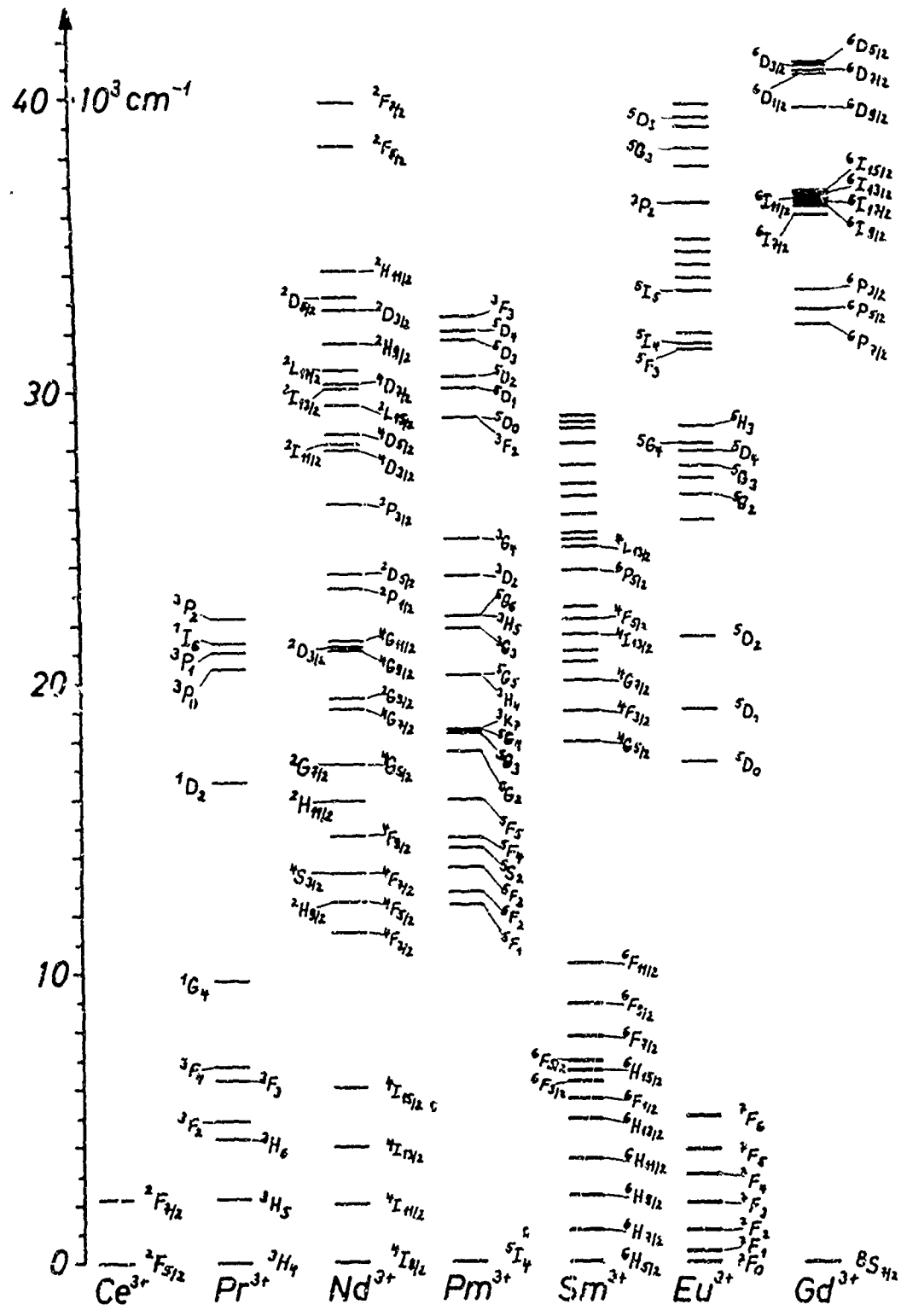

Fig.1: Term scheme of the trivalent rare earth ions;
a) Ce^{3+} to Gd^{3+}.

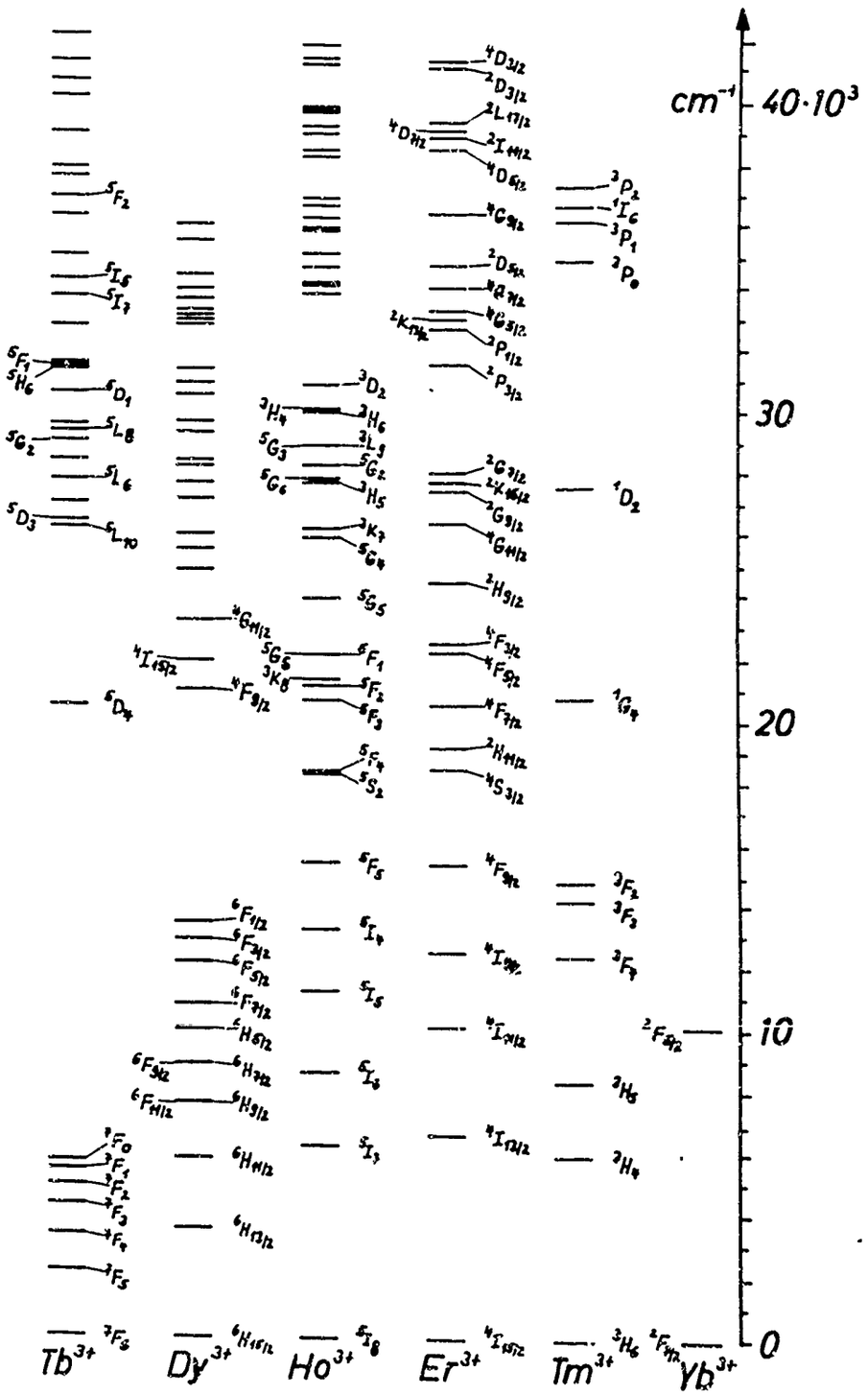

Fig.1: Term scheme of the trivalent rare earth ions;
b) Tb^{3+} to Yb^{3+}

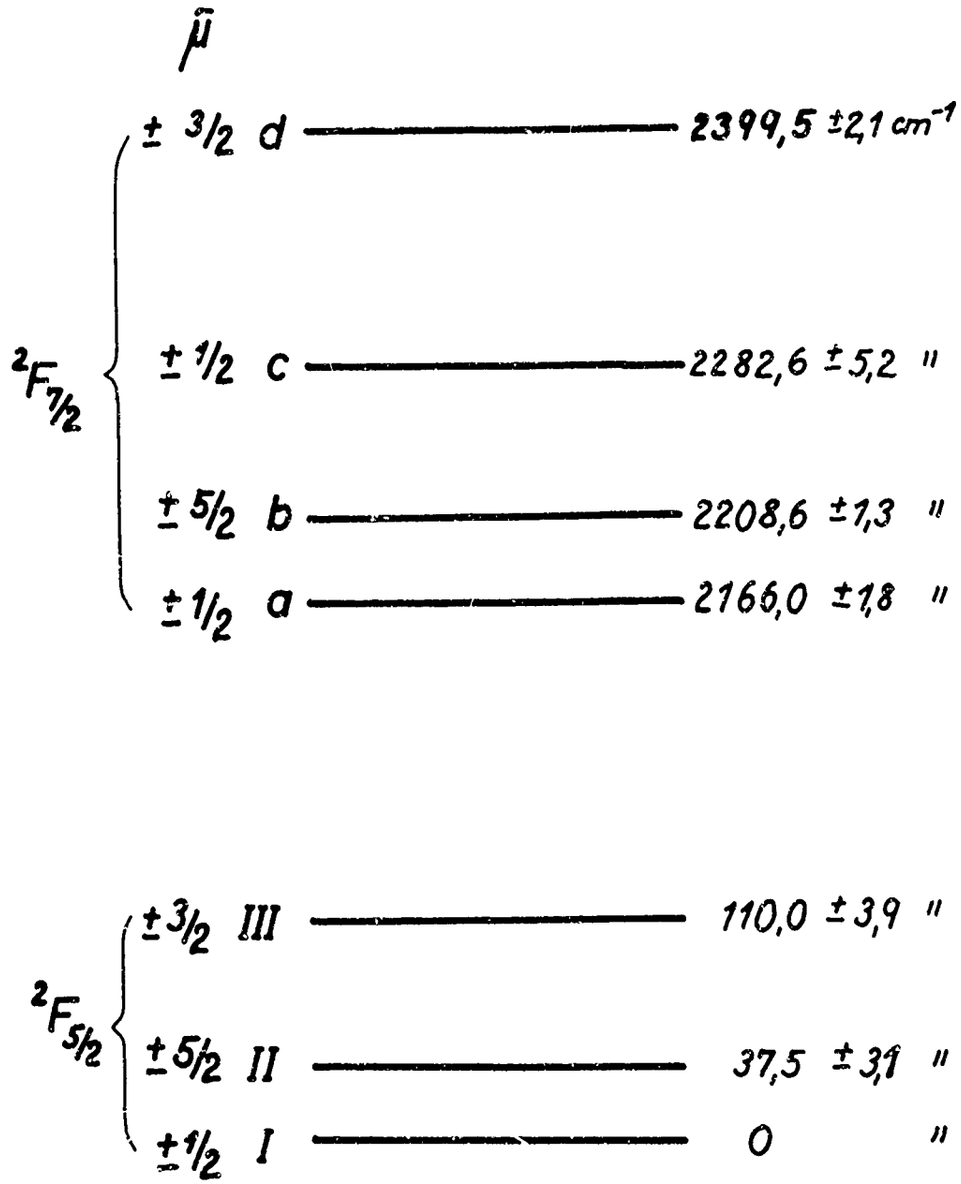

Fig.2: Level scheme of the $^2F_{5/2}$ and $^2F_{7/2}$ terms in $CeCl_3$

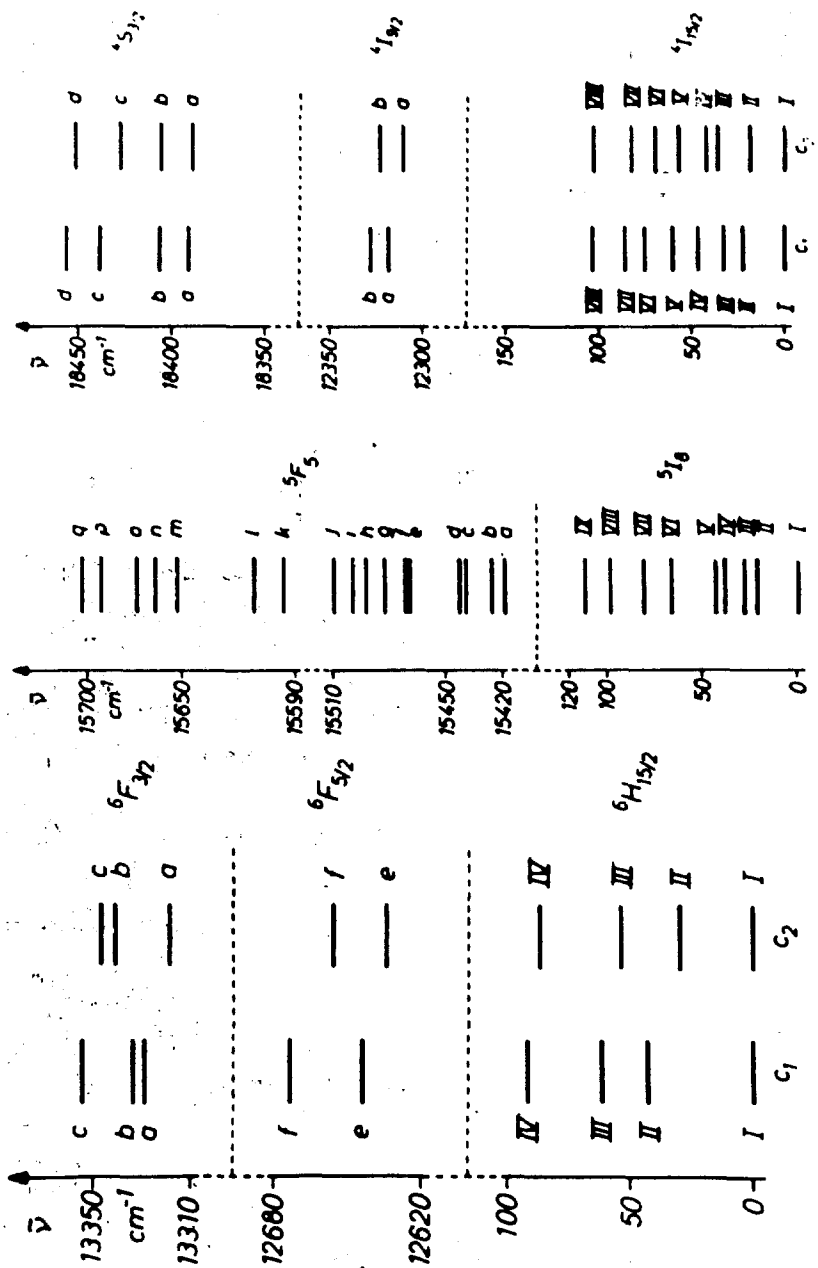

Fig.3: Level schemes of ErIG, HoIG and DyIG.

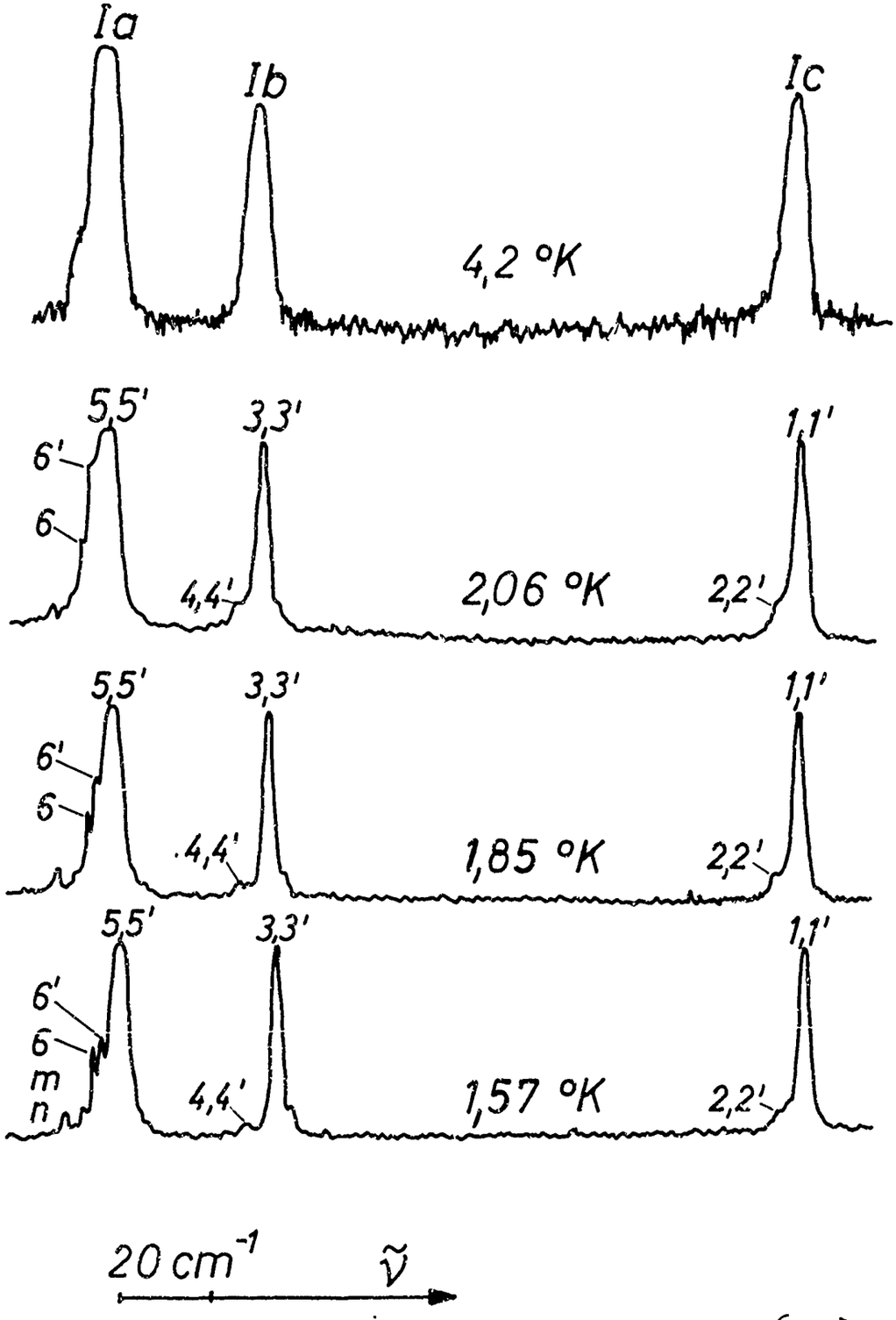

Fig.4: Photorecording of the complete transition $^6H_{15/2} \rightarrow {}^6F_{5/2}$ in the paramagnetic and antiferromagnetic state.

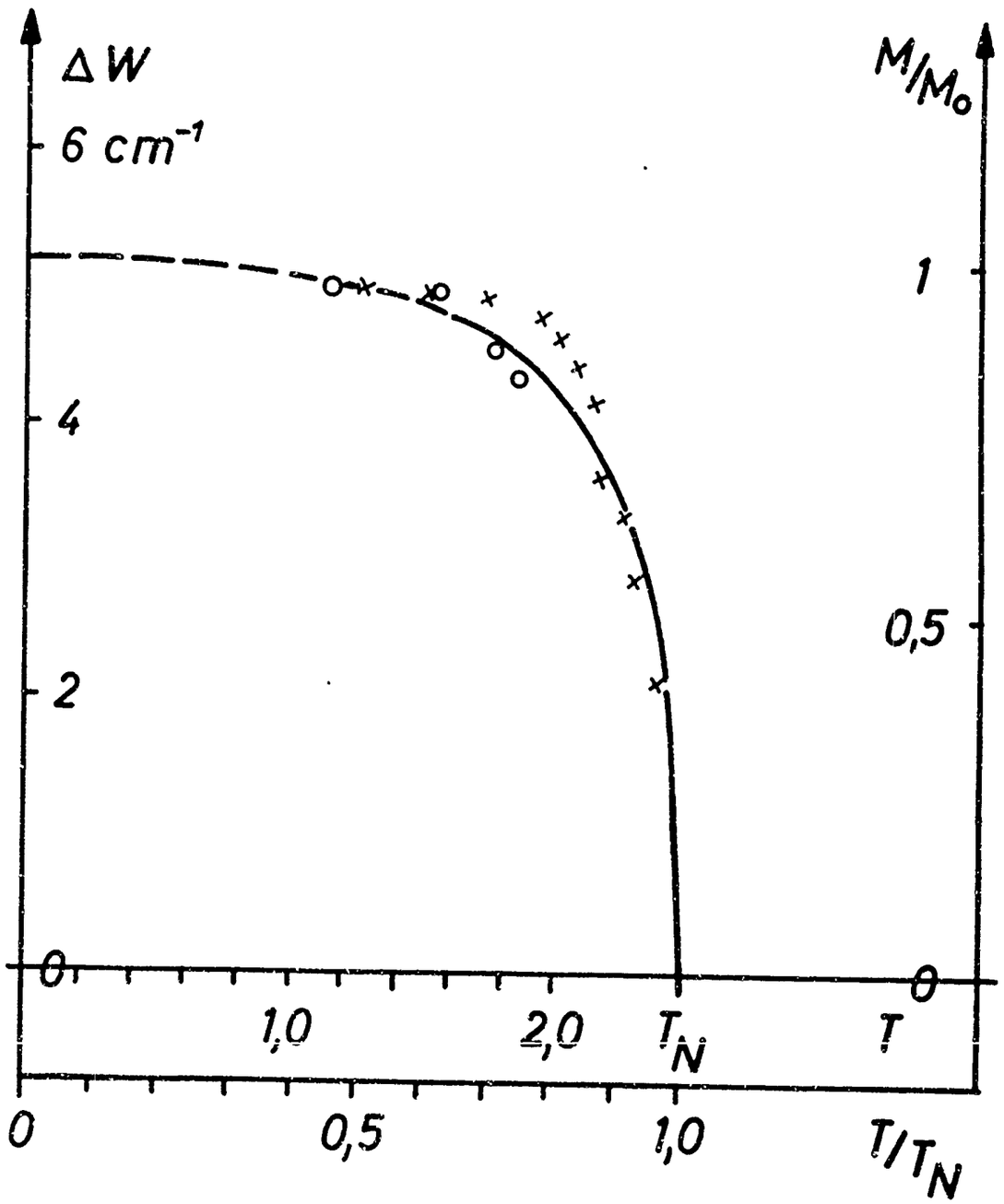

Fig.5: Magnetization curve of DyAlG o = $^6H_{15/2} \rightarrow {}^6F_{5/2}$
x = $^6H_{15/2} \rightarrow {}^6F_{3/2}$; the straight line is the square root of the neutron intensity.

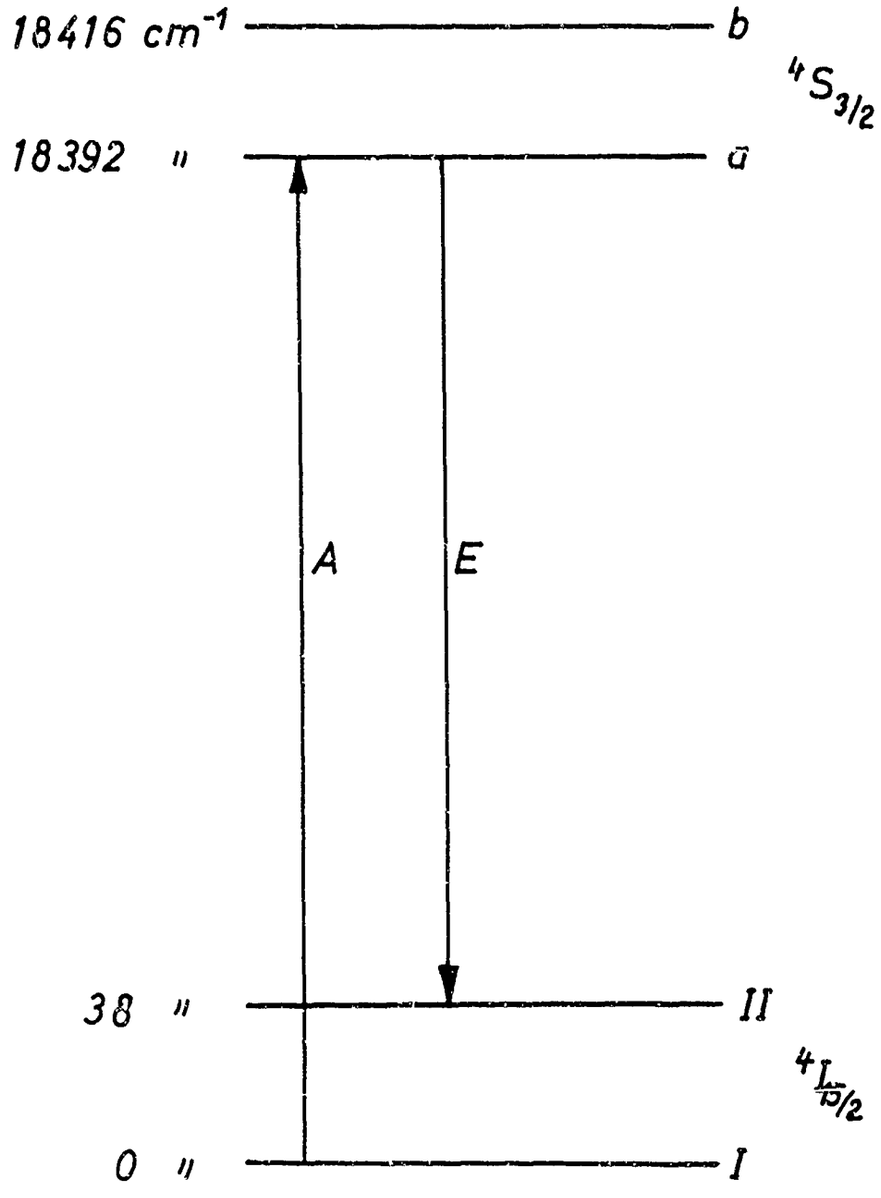

Fig.6: Energy level diagram of the two lowest crystal field levels of the $^4H_{15/2}$ ground state and the $^4S_{3/2}$ excited state in (Er)$LaCl_3$.

INTERACTIONS OF RARE EARTH IONS WITH THEIR CRYSTALLINE ENVIRONMENTS

R. E. Watson

Bell Telephone Laboratories, Inc.
Murray Hill, New Jersey
and
Brookhaven National Laboratories
Upton, Long Island, New York

ABSTRACT

The speaker will inspect the current status of our understanding of the interaction of rare earth ions with crystalline environments. Emphasis will be placed on the electrostatic interactions, though some features of the associated magnetic problem will be considered. Comparisons will be made with transition metal crystal field theory, a topic which is traditionally thought to be more complicated, but which, in fact, is simpler and better understood than the rare earth case.

2, 2' - DIPYRIDYL COMPLEXES OF RARE EARTHS - II CHANGE IN FLUORESCENCE INTENSITIES OF EUROPIUM AND TERBIUM CHELATES ON LIGAND SUBSTITUTION

S. P. Sinha

Cyanamid European Research Institute
Cologny (Geneva), Switzerland

ABSTRACT

A semiquantitative comparison of fluorescence intensities of unsubstituted and para dimethyl substituted dipyridyl chelates of trivalent europium and terbium is presented. The electron donating methyl groups increase the overall intensity for both europium and terbium chelates. However, in case of europium the intensity ratio $\eta_{Dimp/Dip}$ for the two transitions from ^5D_o to $^7F_1$ and $^7F_2$ levels are not of the same order of magnitude. The $\eta_{Dimp/Dip}$ values for all transitions of terbium are roughly the same.

Recently[1] we have demonstrated the effect of para CH_3-groups on the spectrum of substituted neodymium-bis-dipyridyl chelate and it has been concluded that the increase in electron density around the nitrogen atoms of the ligand due to + I effect is responsible for greater red shift in Nd-bis-(4, 4'-dimethyl-2, 2'-dipyridyl) chloride chelate compared to the unsubstituted one. Two recent papers[2, 3] describe the substitution effect of the ligand on the fluorescence intensity, quantum yield, spectral

line splittings and shifts of various substituted β -diketonate chelates of europium and terbium. Electron donating substituents in the proper position of the ligand increase the fluorescence yield while the reverse effect is obtained with electron withdrawing groups.[3] In europium doped tungstates VAN UITERT[4] has shown dependence of fluorescence intensity of europium with the bond energy between europium and oxygen atoms of the first coordination sphere. It has also been shown[5] that the radiationless intramolecular energy transfer in complexes containing Eu-O covalent bond is more efficient than that of Eu-O ionic bond. We have previously[6] noticed approximately fifteen fold increase in $^5D_o \rightarrow {}^7F_2$ transition of trivalent europium on changing the ligand from phthalate $[C_6H_4(COO)_2^{--}]$ to naphthalate $[C_{10}H_6(COO)_2^{--}]$ in the anionic complexes. This significant enhancement of fluorescence, besides many reasons, may be due to the presence of highly conjugated ligand (i. e. the naphthalate moiety) which imperts some quasiaromatic nature to the chelate ring. However, the non-fluorescent nature of terbium naphthalate has been explained[7] on the basis that the triplet state lies below the $^5D_4$ resonance level of terbium ion.

In this paper a semiquantitative treatment and a comparison of the relative fluorescence intensities of europium and terbium dipyridyl and para dimethyl substituted chelates are presented.

RESULTS AND DISCUSSION

The relevant portions of the fluorescence spectra of 4, 4'-dimethyl substituted and unsubstituted chelates of europium and terbium are presented in Figs. 1 and 2. The experimental conditions (such as slit width,

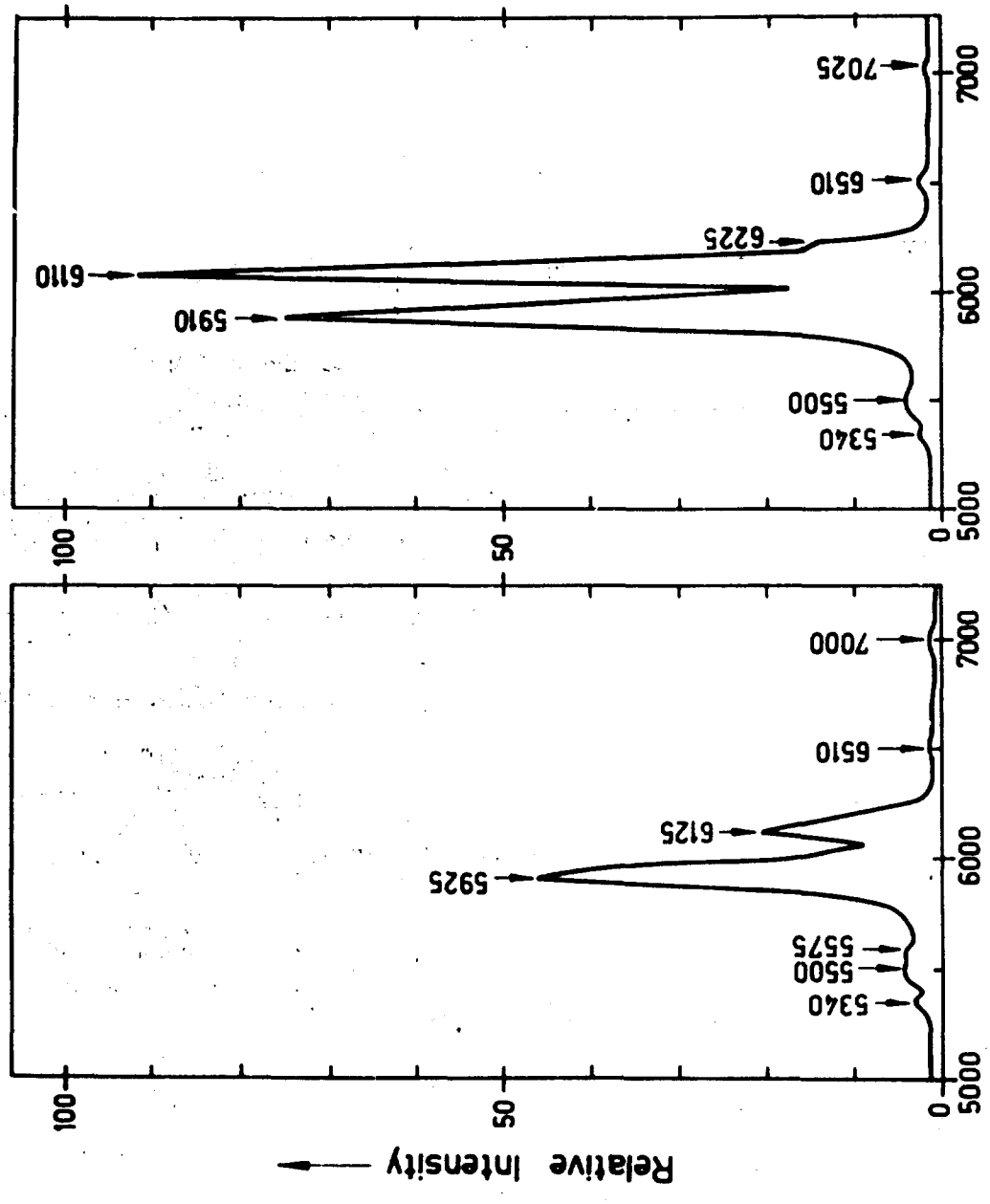

Fig. 1. Fluorescence spectra of $Eu(Dip)_2Cl_3 \cdot 2H_2O$ and $Eu(Dimp)_2Cl_3 \cdot 2H_2O$.

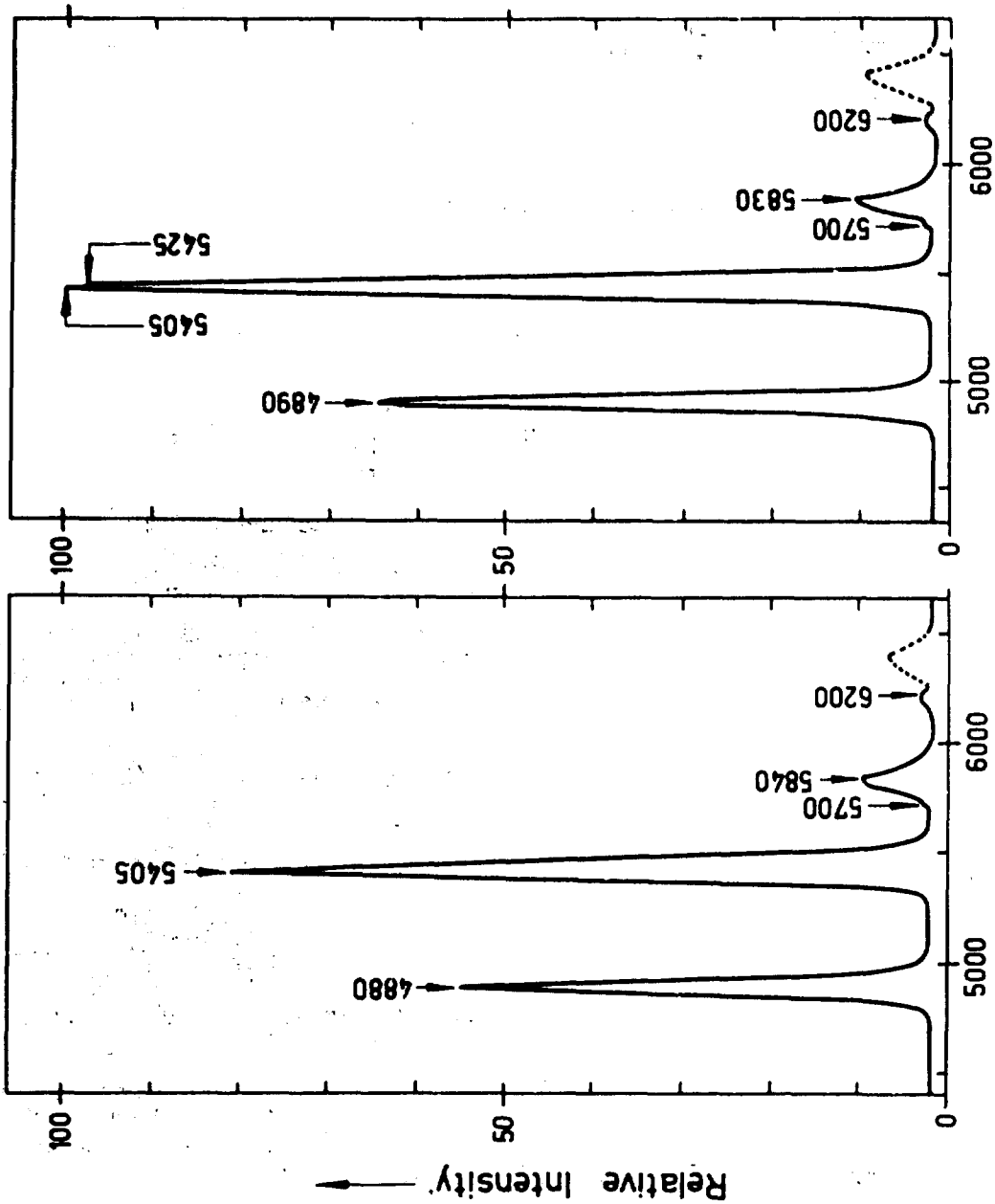

Fig. 2. Fluorescence spectra of $Tb(Dip)_2(NO_3)_3$ and $Tb(Dimp)_2(NO_3)_3$ The dotted portion shows the second order contribution of the excitation radiation.

sensitivity etc.) for each set of experiments were kept constant for comparison. In case of europium a direct comparison of intensities of $^5D_o \rightarrow {}^7F_1$ and $^5D_o \rightarrow {}^7F_2$ transitions of individual chelates is difficult because the transition around 16900 cm^{-1} contains second order contribution from the excitation radiation and it is quite difficult to extract the real contribution of Eu^{3+} ion transition. However, we can compare the spectra of dipyridyl(Dip) chelates of both europium and terbium with that of the 4, 4'-dimethyl substituted dipyridyl(Dimp) chelates under the same experimental conditions as is done in here. The intensity ratio η (defined as the ratio of intensity of the Dimp-chelate to Dip-chelate) is a measure of increment of fluorescence intensity due to substitution.

Eu^{3+} chelates: Table 1 clearly shows an overall enhancement of fluorescence intensity of Eu^{3+} ion in $Eu(Dimp)_2Cl_3 \cdot 2H_2O$ chelate. The intensity ratio $\eta_{^5D_o \rightarrow {}^7F_2}$ (Dimp/Dip) has a value ~ 3.7 and $\eta_{^5D_o \rightarrow {}^7F_1} \sim 1.4$ (allowing errors as indicated in the preceeding paragraph). These values point out two importand facts. (1) The electron donating CH_3-groups in the para position of the ligand increase electron density (+ I effect)* around the nitrogen coordination sites of dipyridyl and hence possibly through a better orbital overlap of ligand-metal bond results effective energy transfer with consequent increase in fluorescence. Increase in ionic fluorescence of europium in dibenzoylmethide chelates with electron donating substituents and the expected opposite effect in presence of electron withdrawing groups have been observed by FILIPESCU et al.[3] (2) The difference of η values for the two transitions of europium

*Methyl groups are also capable of supplying electron density to the conjugated system by resonance (+R) effect.

originating from the same resonance level (^5D_o) suggests that the transition probabilities to the ^7F levels are not of the same order of magnitude and is very sensitive to the change of environments around the europium ion.

The decrease in halfwidth for the transitions from ^5D_o to $^7F_1$ and $^7F_2$ speaks for the narrowing of the transitions of europium in Dimp-chelate and is substituent dependent. Components of $^5D_o \rightarrow {}^7F_2$ transition at 16556, 16460, 16366 (maximum) and 16194 cm^{-1} for the Dimp-chelate have been observed at room temperature. The position of maximum of $^5D_o \rightarrow {}^7F_2$ transition experiences very minor change with para CH_3-substitution. The separation between $^5D_1$ and ^5D_o levels in the Dimp-chelate is somewhat smaller than that of the Dip-chelate.

Tb^{3+} chelates: A comparison of the fluorescence data of the Dip-chelate with the Dimp one is made in Table 2. The overall increase in fluorescence intensity is again apparent for the Dimp-chelate. However, one interesting point in this case is that the η value for all observed bands are roughly the same and has an average value of 1.16. It appears that in case of terbium chelates once the energy reaches the resonance level ($^5D_4$), the fluorescent transition probability from the resonance level to the lowlying ^7F states is approximately the same. The same conclusion can be reached by comparing $\eta_{\frac{^5D_o \rightarrow {}^7F_5}{^5D_o \rightarrow {}^7F_6}}$ values for Dimp (1.69) and Dip (1.68) chelates of terbium. In this case such comparison is feasible because the second order contribution of the excitation source lies outside the terbium transitions concerned (see Fig. 2).

EXPERIMENTAL

The complexes $Eu(Dip)_2Cl_3 \cdot 2H_2O$, $Eu(Dimp)_2Cl_3 \cdot 2H_2O$, $Tb(Dip)_2(NO_3)_3$ and $Tb(Dimp)_2(NO_3)_3$ were prepared by reacting the hydrated europium and terbium salts with the ligands in commercial absolute ethanol as described previously [1, 8].

Fluorescence Measurements

The solid state fluorescence spectra were recorded with an AMINCO spectrophotofluorometer[9] using 0.2 mm groove sandwich cell (106-QS) at room temperature. The comparison spectra were recorded on the same chart paper under the identical experimental conditions. The europium chelates were excited by monochromatic radiation of 2950 Å. Two 1 mm slits were used for the excitation monochromator and slits of 2 and 0.5 mm were used for the emission monochromator. The rotary turret for slit selection for the photomultiplier was ~0.05. The photometer sensitivity control was adjusted at 14 x 0.03. In these experiments the second order contribution of the excitation radiation around 5900 Å complicated the measurements of fluorescence intensity for the $^5D_o \rightarrow {}^7F_1$ transition of Eu^{3+}. The terbium chelates were excited by 3200 Å radiation and the slits and rotary turret settings were exactly the same as used for europium chelates. Only the photometer sensitivity was different and was adjusted at 10 x 0.03. The second order contribution lies beyond (6400 Å) the fluorescence transitions of Tb^{3+} (see the dotted portion of the spectrum in Fig. 2).

REFERENCES

(1) S. P. SINHA, J. Inorg. Nucl. Chem. 27, 115 (1965).

(2) F. HALVERSON, J. S. BRINEN and J. R. LETO, J. Chem. Phys. 41, 2752 (1964).

(3) N. FILIPESCU, W. F. SAGER and F. A. SERAFIN, J. Phys. Chem. 68, 3324 (1964).

(4) L. G. VAN UITERT, J. Chem. Phys. 37, 981 (1962) and references therein.

(5) L. G. VAN UITERT, J. Electrochem. Soc. 107, 803 (1960).

(6) S. P. SINHA, C. K. JØRGENSEN and R. PAPPALARDO, Z. Naturforsch. 19a, 434 (1964).

(7) S. P. SINHA, Z. Naturforsch. 20a, 319 (1965).

(8) S. P. SINHA, Spectrochim. Acta 20, 879 (1964).

(9) S. P. SINHA, Z. Naturforsch. 20a, (1965).

Table 1. DETAILS OF FLUORESCENCE SPECTRUM OF EUROPIUM CHELATES AT 300°K

Fluorescent transitions Å	cm^{-1}	$d\bar{\nu}$ [a] cm^{-1}	Halfwidth $\Delta\bar{\nu}$ cm^{-1}	Relative Intensity [b] I_{max} Arbitrary units	$I_{max} X \Delta\bar{\nu}$	Assignment
A. $Eu(Dip)_2Cl_3 \cdot 2H_2O$						
5340	18726	~529	-	weak	-	$^5D_1 \rightarrow {}^7F_1$
5500 } 5575 }	18182 } 17937 }	~819	-	weak	-	$^5D_1 \rightarrow {}^7F_2$
5925	16877	1015	428	44.8 [c]	19174	$^5D_o \rightarrow {}^7F_1$
6125	16326	655	305	19	5795	$^5D_o \rightarrow {}^7F_2$
6510	15360	-	-	very weak	-	$^5D_o \rightarrow {}^7F_3$
7000	14285	-	-	very weak	-	$^5D_o \rightarrow {}^7F_4$
B. $Eu(Dimp)_2Cl_3 \cdot 2H_2O$						
5340	18726	~529	-	weak	-	$^5D_1 \rightarrow {}^7F_1$
5550	18182	~819	-	weak	-	$^5D_1 \rightarrow {}^7F_2$
5910	16920	1024	358	74 [c]	26492	$^5D_o \rightarrow {}^7F_1$
6110	16366	724	241	90	21690	$^5D_o \rightarrow {}^7F_2$

contd.

Table 1. Contd.

6225	16064	-	-	-	-	$^5D_1 \rightarrow {}^7F_4$
6510	15360	-	-	very weak	-	$^5D_o \rightarrow {}^7F_3$
7025	14234	-	-	very weak	-	$^5D_o \rightarrow {}^7F_4$

[a] d $\bar{\nu}$ denotes the width of the spectral range covered by the entire band and the values are approximate.

[b] The values of relative intensities are in arbitrary units and I_{max} is expressed as the vertical height of the peak on the linear scale of the chart paper.

[c] The intensity of this peak contains second order contribution from the excitation source as well as the fluorescence of europium.

Table 2. DETAILS OF FLUORESCENCE SPECTRUM OF TERBIUM CHELATES AT 300°K

Fluorescent transitions Å	$\bar{\nu}$ cm^{-1}	d $\bar{\nu}$ [a] cm^{-1}	Halfwidth $\Delta\bar{\nu}$ cm^{-1}	Relative Intensity[b] I_{max} Arbitrary units	$I_{max} X \Delta\bar{\nu}$	Assignment
A. $Tb(Dip)_2(NO_3)_3$						
4880	20492	~833	~314	53.5	16799	$^5D_4 \rightarrow {}^7F_6$
5405	18501	~760	~356	79.5	28302	$^5D_4 \rightarrow {}^7F_5$
5700 Sh	17544	~737	~324	7.5	2430	$^5D_4 \rightarrow {}^7F_4$
5840	17123					
6200	16130	-	-	very weak	-	$^5D_4 \rightarrow {}^7F_3$
B. $Tb(Dimp.)_2(NO_3)_3$						
4890	20450	~833	~314	63	19782	$^5D_4 \rightarrow {}^7F_6$
5045	18501	~760	~340	98.5	33490	$^5D_4 \rightarrow {}^7F_5$
5425	18433					
5700	17544	~737	~324	8.5	2754	$^5D_4 \rightarrow {}^7F_4$
5830	17152					
6200	16130	-	-	very weak	-	$^5D_4 \rightarrow {}^7F_3$

a, b see the explanations in Table 1.

COORDINATION AND CHEMICAL EQUILIBRIUM IN CHELATE LASER MATERIALS

H. Samelson, C. Brecher, and A. Lempicki

General Telephone & Electronics Laboratories Inc.
Bayside, New York

ABSTRACT

Chelated rare earth ions have been found to exist in solution in a multiplicity of molecular structures, differing in the number and geometrical arrangement of coordinating ligands. Eight-fold coordination is the most common, but changes in temperature, solvent, or substituent groups may alter the coordination in either direction. Furthermore, most chelates dissociate progressively further as their concentration is lowered. The ramifications of such behavior on their luminescence and laser applications will be discussed.

I. INTRODUCTION

The use of rare earth chelates in liquid lasers has given increased impetus to the investigation of their coordination chemistry. This has been the subject of considerable research interest.[1] It had generally been thought that the structure of the trivalent rare earth coordination compounds paralleled that of the corresponding d-type transition metal ions. Indeed, the octahedral coordination typical of the latter has been accepted in much of the recent literature as being equally valid for the rare earths. However, for some time now evidence has been accumulating that the coordination chemistry of these ions is not so easily explained. Thompson[2] and Choppin[3] have found chemical evidence that four bidentate ligands can coordinate with lanthanide ions. Charles[4] has reported a number of europium chelates for which the coordination number may be greater than six. Hoard[5] and his coworkers have shown that coordinations as high as ten can be found. In our own work[6] and in that of Bauer, Blanc and Ross[7] and Melby, Rose, Abramson and Caris,[8] coordination numbers of eight and nine have been unequivocally established.

The extremely intense fluorescence emission from many europium β-diketone chelates in solution is the basis for their successful application in liquid lasers. This application has raised many questions about the quantum efficiency of the fluorescence and the path of the energy

migration from its absorption in the ligand singlet band to its ultimate appearance as ion fluorescence. The investigation of these problems, however, is hampered by the fact that these europium chelates dissociate in solution. This dissociation process depends not only on the chemical nature of the ligand, but on the solvent as well. Since the spectroscopic properties observed arise from a mixture of species, the characterization of the energy transfer phenomena requires a detailed knowledge of the species present in solution.

In this paper we will discuss the solution chemistry of two different β-diketone chelates of europium, the benzoylacetonate and the benzoyltrifluoroacetonate. The emission of both the tris and tetrakis forms are studied at various concentrations in a number of commonly used solvents and their behavior characterized. In addition, a method for obtaining the dissociation constants of the chelates will be described, and this method will be used to obtain these constants for one particular system.

II. EXPERIMENTAL

A. Materials

The chelates used in this work, the tetrakis and tris benzoylacetonates and benzoyltrifluoroacetonates, were prepared by standard methods described elsewhere.[6] For the tetrakis compounds which require a neutralizing positive charge, the cation present was piperidinium. These compounds were analyzed for europium, and the agreement with the expected formula was always within 0.2%. There were four solvents used in this work and these are listed in Table I. The detailed determination of the stability constants was done only for the benzoylacetonate in the mixed alcohol solvent and dilution studies in the first three solvents. The last solvent medium is included because it has an interesting, and as yet unexplained, influence on the structure of the tetrakis benzoylacetonate chelate.

B. Apparatus

The experiments to be described were the determination of the fluorescence spectrum performed under steady illumination and flash experiments to determine the existence of laser action. The apparatus for the latter has been described elsewhere in considerable detail.[9]

The apparatus for the measurement of the fluorescence emission spectra is shown in Fig. 1. The output of an AH-6 Hg arc lamp was filtered and focused on the sample. At the same time this output was monitored by a phototube so that the variations in the lamp output could be corrected for. The sample tube was kept in a dewar, and the temperature controlled to within 0.2°C by a flow of pre-cooled nitrogen gas. The fluorescence output was focused on the entrance slit of a Jarrell-Ash 0.5 m Ebert monochromator. The monochromator output

TABLE I

Solvent	Composition	Preparation
Mixed alcohol	3:1 mixture by volume of ethanol and methanol	Absolute ethanol (USI) and spectroscopic grade methanol used directly.
EPA	5:5:2 volume mixture of ethanol, 2 methylpentame and di-ethyl ether	Absolute ethanol (USI). Other reagents, spectroscopic grade.
Nitrile	1:1:1 volume mixture of isobutyro-, n butyro- and propionitriles	All reagents distilled and mixture stored over anhydrous $CaSO_4$ until ready for use.
Mixed alcohol – sodium acetate	Solvent 1 + anhydrous sodium acetate	Prepared as used.

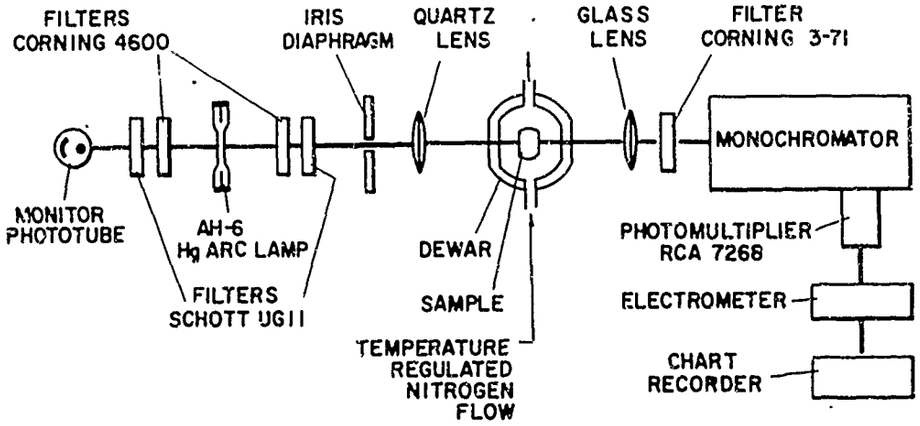

Fig. 1. Experimental arrangement for the measurement of fluorescence emission spectra.

was detected by an RCA 7268 photomultiplier and recorded. The straight-through optics are particularly suited to these experiments since the intense absorption of the ligands provide a sharp fluorescent image of the exciting arc, which is then focused on the entrance slit of the monochromator. Meaningful intensity comparisons can be made as long as this image is at the focus of the lens. In the more dilute solutions there is considerable penetration of the exciting radiation and this tends to result in a diffuse image of significant depth. This diffuseness introduces geometrical effects, making intensity comparisons much more difficult. In all the work used for quantitative determinations either the absorption was sufficiently intense to result in a sharp fluorescent image line or appropriate corrections were made.

III. EXPERIMENTAL RESULTS

The results of the fluorescence experiments are interpreted in terms of the energy level structure of the europium ion. The principal emission that is most easily detected is that due to the $^5D_0 - {}^7F_2$ transition in the 6100-6250 Å region. The $^5D_0 - {}^7F_1$ and $^5D_0 - {}^7F_0$ transitions at 5850-5950 Å, and 5800 Å, respectively, are more than an order of magnitude less intense but nevertheless easily detectable. At low temperature the emission lines are quite sharp and the structure of the fluorescence is easily discernible. This emission has two important properties. The first is that the $^5D_0 - {}^7F_0$ transition is not split by fields of any symmetry, and therefore multiple emission lines in this region are evidence of multiple species. Moreover, there is little overlap between the lines even if they are separated by as little as 4 Å and the intensities can be interpreted quantitatively. The second important property of the emission is that the structure of the fluorescence from the $^5D_0 - {}^7F_2$ transition is characteristic of the coordination symmetry. Although the breadth and overlap of the lines in this transition vitiates their use in a quantitative manner, they can, nevertheless, be used to identify the structure of a given species.

In the subsequent discussion we will exploit these two properties, first quantitatively to evaluate the relative amounts of the various species present in solution from which one can ascertain the dissociation constants; second, qualitatively in a more general discussion of the solution chemistry.

A. Determination of Dissociation Constants

The dissociation constants of the benzoylacetonate chelates of europium were determined in the mixed alcohol solvent at -180°C. A series of solutions with constant 0.01 M europium concentration but varying ligand concentration was prepared. This was done by using appropriate volumes of solutions of europium tetrakis benzoylacetonate and anhydrous europium chloride, both in the mixed alcohol solvent. Equivalent spectra were obtained if the solutions were prepared by mixing appropriate amounts of piperidinium benzoylacetonate and europium chloride only, but the former method was somewhat more convenient.

Some of the spectra obtained are shown in Fig. 2. It is readily seen that as the ratio of europium to benzoylacetonate is varied, the number and wavelength of the principal emission lines in the $^5D_0 - {}^7F_0$ region changes. In all there are four distinct lines, each corresponding to a given chelate species. The emission from the free europium ion is too weak to be detected at the concentration used with the method of excitation described.

The emission in the $^5D_0 - {}^7F_2$ region of the spectrum also undergoes rather marked changes with the variation in metal ion-to-ligand ratio. As can be seen, these emissions are quite characteristic for each of the

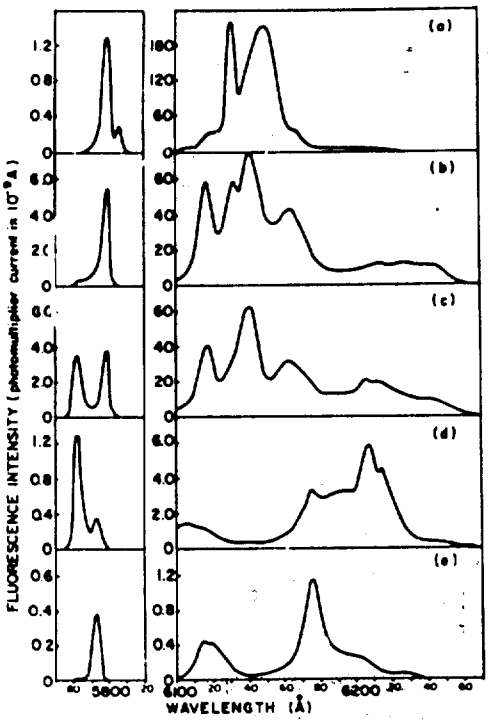

Fig. 2. Emission spectra used for calculating the dissociation constants of europium benzoylacetonate in alcohol. Europium concentration: 0.01 M. Benzoylacetonate concentration: (a) 0.04, (b) 0.03, (c) 0.025, (d) 0.01, (e) 0.005.

chelate compounds and can serve to identify them. The intensities of the individual lines, however, cannot be measured precisely because there is far too much overlap between the lines of each species. Thus for quantitative work one is limited to the transitions in the $^5D_0 - ^7F_0$ region alone.

To a very good approximation the absorption of ultraviolet radiation by europium chelates is determined by the absorption characteristics of the ligand. In fact, there is good evidence[6] that the absorption constant on a per ligand basis is constant. If it is further assumed that all the exciting radiation is absorbed, then the number of photons absorbed per cm^2 per sec by a species having n ligands per molecule is given by

$$P_n = P_0 \frac{nC_n}{C_\ell} \tag{1}$$

where P_0 is the incident flux density and C_n is the concentration of the species with n ligands and C_ℓ is the total concentration of ligand, free and combined.

The intensity, I_n, of the emission from the species with concentration C_n is proportional to P_n:

$$I_n = A_n P_n = A_n P_0 \frac{nC_n}{C_\ell} \tag{2}$$

If I_n^0 is defined as the intensity obtained when $nC_n = C_\ell$, then

$$I_n = I_n^o \frac{nC_n}{C_l} \quad . \tag{3}$$

If the I_n^o are known and I_n measured, then C_n can be determined. Because there is always some dissociation, the I_n^o's have to be determined by an iterative procedure.

Starting with spectrum b of Fig. 2 and assuming this solution to be entirely the tris species, a tentative value of I_3^o is obtained. Using this value, along with material balance considerations, the spectra a, b, and c, and Eq. (3), one can, by an iteration procedure, rapidly converge on a consistent set of values for I_4^o, I_3^o, I_2^o, K_4 and K_3. Using I_2^o and the spectra d and e, one can then find I_1^o, K_2 and K_1. These values are listed in Table II. The equilibrium constant for each step in the dissociation is defined as $K_n = (C_{n-1} C_B)/C_n$ where C_n and C_{n-1} follow from previous definitions and C_B is the concentration of free benzoylacetonate anion. These constants have been calculated on the basis of concentration and not activities, and are estimated to have a probable error of 10%. The I_n^o values depend, of course, on the particular experimental arrangement employed, but their ratios are generally applicable to the system itself.

TABLE II

n	K_n	I_n^o
1	1.20×10^{-8}	0.40
2	2.66×10^{-6}	9.62
3	1.30×10^{-6}	5.80
4	1.17×10^{-3}	0.45

This technique is complementary to other methods for determining stability constants. It depends on an easily interpretable emission spectrum and may thus be limited only to europium chelates. In addition to this, not only must the particular chelates be fluorescent, but the lines must be sharp. It is therefore essentially limited to low temperature application in a solvent system that glasses readily and provides sharp emission lines. However, within these limitations, the spectroscopic method described here will produce information not obtainable by any other means.

B. Behavior of Chelate Solutions on Dilution

With the existence of equilibria having dissociation constants as large as those found for the europium benzoylacetonate chelates, the relative proportions of the various species present in a solution will be depen-

dent on the concentration even at the concentrations normally used in fluorescence experiments. Furthermore, the equilibria will also depend on the solvent itself and will shift as the solvent is altered. To study these effects, two chelates of europium, the benzoylacetonate and the benzoyltrifluoroacetonate, were selected because of interest in their laser application. The solvents were chosen because of the prevalence of their use in either fluorescence studies or as a laser host medium.

The behavior of the tris and tetrakis europium benzoylacetonate chelates in the mixed alcohol solvent on dilution from 10^{-2} to 10^{-5} M is shown in Figs. 3a and b. This behavior is what would be expected on the basis of the equilibrium constants already determined. In each case there is a gradual increase in dissociation so that at the lower concentration the solute consists not of the starting compound, but of species having one or two fewer β-diketone ligands. The tris and tetrakis benzoyltrifluoroacetonates exhibit a different sort of behavior in this solvent as shown in Figs. 4a and b. For this ligand the tetrakis compound is completely dissociated into the tris even at the highest concentration, since the spectra obtained from both compounds are identical except for intensity. The spectrum of the tris compound is about 1/3 more intense than that of the tetrakis because the dissociated ligand absorbs energy but does not lead to fluorescence. Dilution does not alter the spectrum but decreases the intensity. For this ligand then, only the tris form is stable in this solvent; the equilibrium constants for the other forms must be extremely high.

In the nitrile mixture, which is a highly coordinating solvent, a markedly different sort of behavior is observed as seen in Figs. 5 and 6. Both the tris and tetrakis benzoylacetonates are less stable here than in alcohol and by 10^{-4} M the chelates have dissociated nearly completely into free ligand and free ion. It should also be noted at 10^{-2} M the spectrum of the tetrakis chelate is not the same as that in alcohol. For the benzoyltrifluoroacetonate, Figs. 6a and b, the spectra of the tetrakis and tris compounds are different at the highest concentration and the tris spectrum shows the presence of a small amount of the tetrakis. As the solutions are diluted, the tetrakis spectrum does not alter except in intensity, while that of the tris is converted to the tetrakis. In this coordinating solvent then, the lower chelate species are essentially unstable and the tetrakis form has a smaller dissociation constant than the tris form.

EPA is a solvent commonly used for fluorescence experiments and the results of dilution experiments in this solvent are shown in Figs. 7 and 8. In the case of both the tris and tetrakis benzoylacetonates there are at least four species present in solution even at concentrations as high as 10^{-2} M. As the concentration is decreased, the relative amounts of the lower coordination components increase until at 10^{-4} M it is difficult, if at all possible, to identify the chelate components with any degree of confidence. With the benzoyltrifluoroacetonate, both the tetrakis and tris compounds produce solutions that are mixtures of the

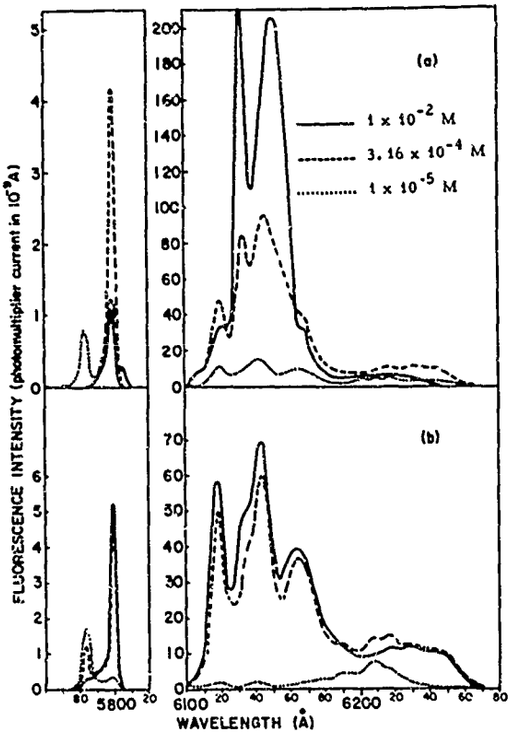

Fig. 3. Benzoylacetonate chelates of Eu in mixed alcohol solvent at -180°C: (a) tetrakis chelate, (b) tris chelate.

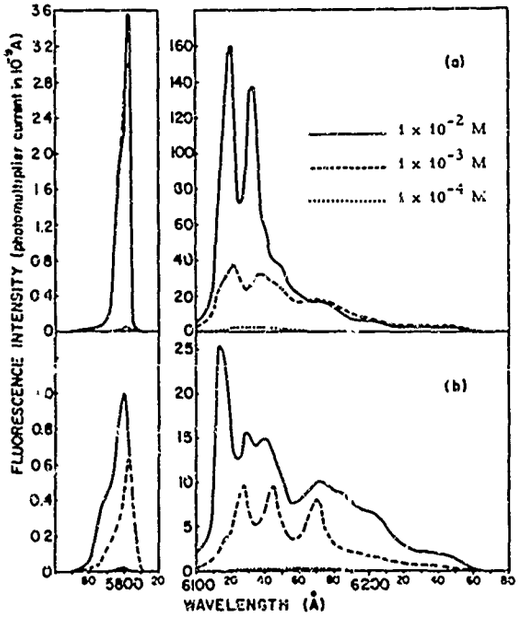

Fig. 5. Benzoylacetonate chelates of Eu in nitrile solvent at -180°C: (a) tetrakis compound, (b) tris compound.

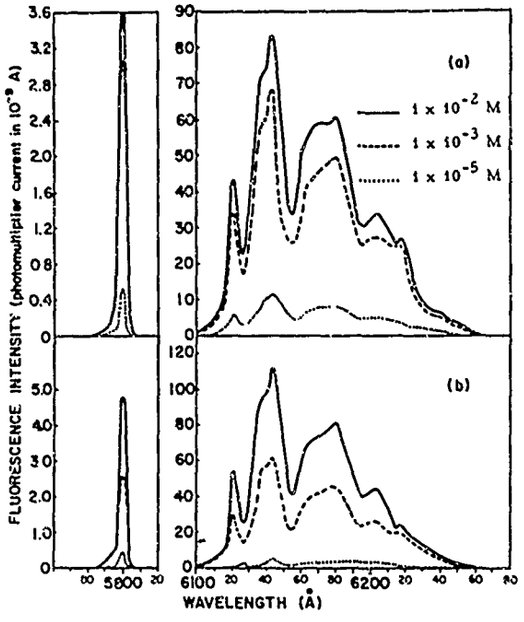

Fig. 4. Benzoyltrifluoroacetonate chelates of Eu in mixed alcohol solvent at -180°C: (a) tetrakis chelate, (b) tris chelate.

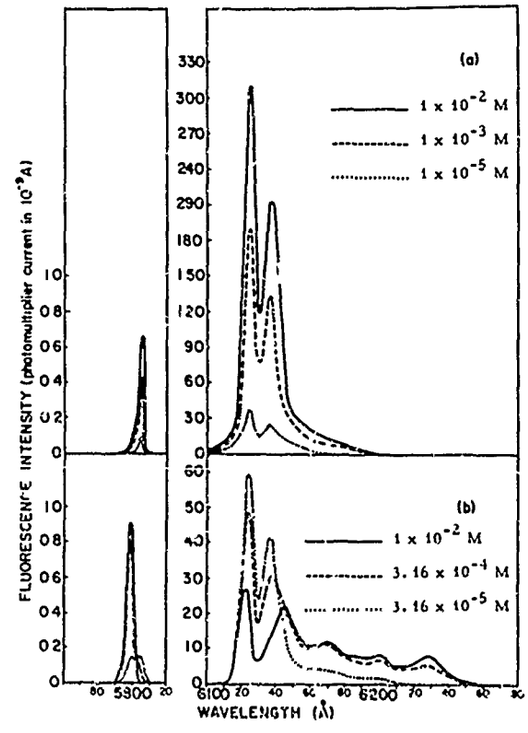

Fig. 6. Benzoyltrifluoroacetonate chelates of Eu in nitrile solvent at -180°C: (a) tetrakis compound, (b) tris compound.

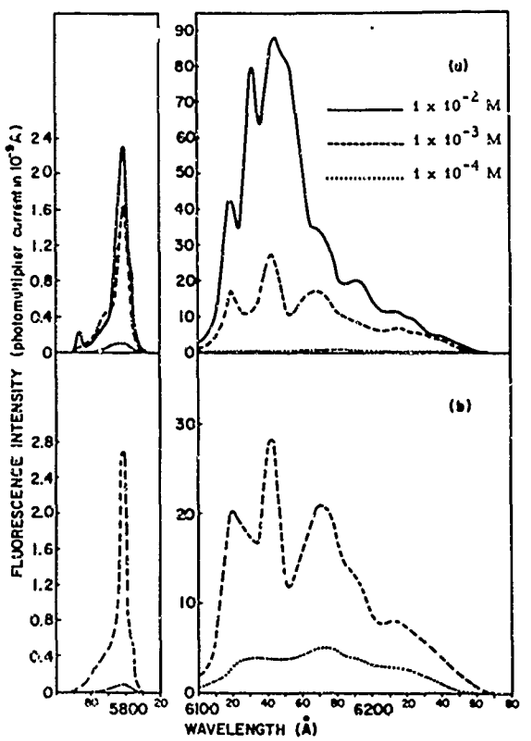

Fig. 7. Benzoylacetonate chelates of Eu in EPA solvent at -180°C: (a) tetrakis compound, (b) tris compound.

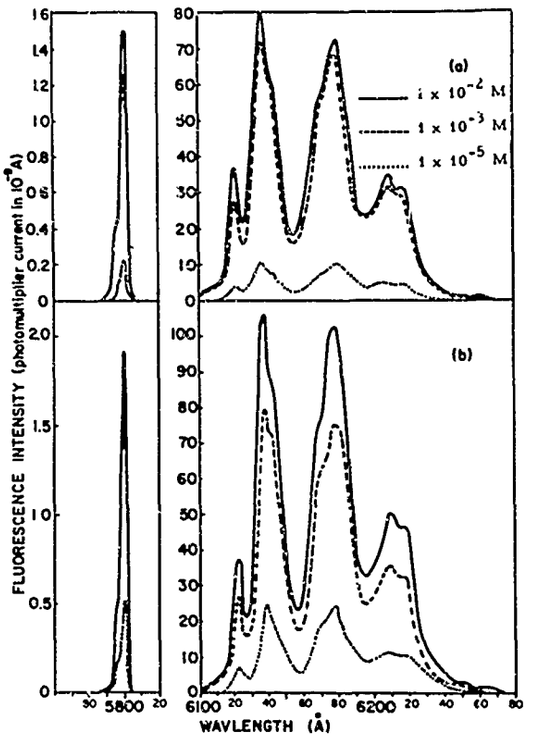

Fig. 8. Benzoyltrifluoroacetonate chelates of Eu in EPA solvent at -180°C: (a) tetrakis compound, (b) tris compound.

tris and bis species. The relative amounts of these remain unchanged on dilution from 10^{-2} M to 10^{-5} M.

C. Structural Considerations

Thus far the solvent has been considered as having an effect only on the stability of the various complexes. However, its influence is more deeply felt. In the tetrakis chelates the metal ion resides in a cage of eight oxygens. With the available metal orbitals, two possible arrangements of these oxygens are dodecahedral and antiprismatic. The solvent can play a key role in determining this structure. In alcohol, for example, it has been shown[6, 10] that the emission spectrum of europium tetrakis benzoylacetonate in the $^5D_0 - ^7F_2$ region is consistent with a dodecahedral structure of symmetry D_{2d}. In the nitrile solvent, on the other hand, the emission spectrum is more consistent with a structure belonging to the symmetry group C_4. Nitriles can coordinate strongly through the nitrogen, and in so doing will distort the dodecahedral structure toward an Archimedean antiprismatic one since the latter allows the nitrogen to approach the central ion more closely. The coordinated nitrile group produces an overall nine-fold coordination and lowers the site symmetry from D_4 to C_4. This has been discussed in some detail previously.[6]

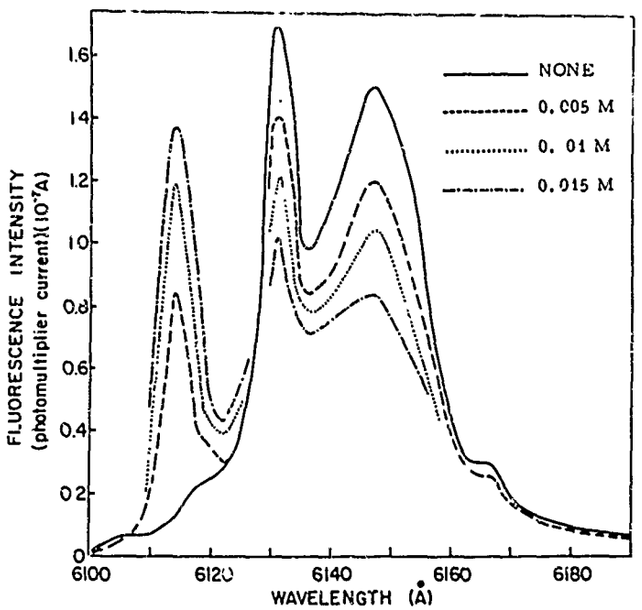

Fig. 9. Europium tetrakis benzoylacetonate (0.01 M) in mixed alcohol solvent at -150°C containing various concentrations of sodium acetate.

An even more intriguing case occurs when the alcohol solvent is altered by the addition of sodium acetate. The change in this case is a more general one as is seen in Fig. 9. The spectrum of the tetrakis benzoylacetonate is altered so that a single emission line in the $^5D_0 - ^7F_2$ spectral region becomes increasingly more dominant, consistent with a gradual conversion to a structure having a symmetry of the antiprism alone or D_4. This symmetry can be achieved by coordinating either two or none of the singly charged cations to a chelate molecule, but the question has not yet been resolved.

IV. INFLUENCE ON LASER ACTION

The dissociation and structural factors have a strong influence on the laser capability of these compounds. As of this writing, one highly significant point that has emerged is that only the tetrakis chelates, and no tris or lower coordinated forms, have been made to exhibit laser action. Thus, the dissociation of the tetrakis chelate to the tris chelate can only be deleterious. Even in those cases where such dissociation can be reversed by additional chelate anion, there is not much advantage since the non-useful absorption is also increased. From the point of view of the laser, the solvent effects can be much more useful. Thus, while the tetrakis benzoyltrifluoroacetonate dissociates to a far greater extent than the benzoylacetonate in alcohol, it dissociates much less than the latter, indeed hardly at all, in the nitrile. Such a complete reversal of behavior of the tetrakis benzoyltrifluoroacetonate chelate makes it possible to achieve laser action in the nitrile solvent. In fact,

the nitrile is such a good solvent medium for the benzoyltrifluoroacetonate that this chelate retains its fluorescence intensity and undissociated nature even at room temperature, enabling the room temperature chelate laser to become a reality.[11]

Furthermore, the effect of the solvent is not limited to the dissociation equilibrium, since the tetrakis form itself is markedly dependent on the nature of the solvent. Indeed, the europium tetrakis benzoylacetonate can be made to show laser action in three distinct forms, the dodecahedral, the antiprismatic, and the antiprism adduct, at wavelengths of 6130, 6114, and 6126 Å, respectively. This is achieved by merely changing the solvent. Thus the very structure of the lasing molecule itself is readily altered by interactions with the solvent, making it possible to attain some degree of frequency tuning of the laser emission by chemical means.

V. SUMMARY

The interaction of europium β-diketone chelates and the solvent depends on the nature of both the ligand and the solvent. In this work a beginning has been made toward an understanding of this interaction. It has been shown that the dissociation constants of these chelates can be determined from fluorescence measurements. It has also been pointed out that because of the dissociation problem, great care must be exercised when comparing and interpreting fluorescence data, particularly when these are obtained from dilute solutions. By an awareness of these problems it should be possible to study energy transfer phenomena and fluorescence efficiency with greater control over the structural and chemical parameters. In this way more meaningful comparisons can be made and a greater insight into the laser behavior of these compounds can be obtained.

REFERENCES

1. T. Moeller, D. F. Martin, L. C. Thompson, R. Ferrus, G. R. Feistel and W. S. Randall, Chem. Rev. 65, 1 (1965).
2. L. C. Thompson and J. A. Loraas, J. Inorg. Chem. 2, 89 (1963).
3. G. R. Choppin and J. A. Chopoorian, J. Inorg. Nucl. Chem. 22, 97 (1961).
4. R. G. Charles and A. Perotto, J. Inorg. Nucl. Chem. 26, 373 (1964).
5. J. L. Hoard, M. D. Lind and B. K. Lee, Fourth Rare Earth Research Conference, Session III, April 1964. J. L. Hoard and J. V. Silverton, Inorg. Chem. 2, 235, 243 (1963).
6. C. Brecher, H. Samelson and A. Lempicki, J. Chem. Phys. 42, 1081 (1965).

7. H. Bauer, J. Blanc and D. L. Ross, J. Am. Chem. Soc. 86, 5125 (1964).

8. L. R. Melby, N. J. Rose, E. Abramson and J. C. Caris, J. Am. Chem. Soc. 86, 5117 (1965).

9. A. Lempicki, H. Samelson and C. Brecher, J. Chem. Phys. 41, 1214 (1964).

10. C. Brecher, A. Lempicki and H. Samelson, J. Chem. Phys. 41, 279 (1964).

11. H. Samelson, A. Lempicki, C. Brecher and V. A. Brophy, Appl. Phys. Lttrs. 5, 173 (1964).

OPTIMUM ACTIVATOR CONCENTRATIONS IN RARE-EARTH OXIDE PHOSPHORS

R. C. Ropp

Westinghouse Electric Corporation
Lamp Division - Bloomfield, N. J.

ABSTRACT

The intensity of fluorescence of rare-earth activators in rare-earth oxide phosphors is an inverse function of the degree of ground-state splitting which occurs, and also of the degree of resonance energy interaction between ions within the lattice. Such phenomena probably account for the completely different optimum concentration observed for the various activators studied.

The number of papers dealing with yttrium and gadolinium oxide phosphors has increased of late, but little has been presented regarding the relationship between concentration and emission intensity for the various rare-earth activators in these matrices. In this respect, Eu^{+3} is unique because of the relatively high concentrations which may be accommodated without affecting emission intensities.

The phosphors were prepared by coprecipitation of the rare-earth oxalates, as has been reported previously[1]. The precipitate was calcined at temperatures ranging from 1000-1400°C for one to four hours in air, depending upon the composition. Brightness measurements were made by illuminating the surface of a powder plaque with the radiation (2537Å) from a regulated low-pressure mercury discharge lamp and comparing the response (by means of a 1P28 photomultiplier and a Photovolt Model 520M power supply) with that of an arbitrary standard phosphor whose emission band coincided with the rare-earth emission.

In Y_2O_3- and Gd_2O_3-based phosphors, it was shown previously[1] that only Sm^{+3}, Eu^{+3}, Tb^{+3} and Dy^{+3} gave fluorescence of any appreciable intensity. Such intensity was a function of the wavelength employed for excitation.

In order to obtain a comparison of intensity of emission, as a function of activator concentration, it was necessary to obtain the relative measurement of the various members in a series. The easiest method proved to be measurement of plaque brightness. Although the Sm^{+3}, Eu^{+3}, Tb^{+3} and Dy^{+3} activators produced considerable differences of intensity in response to 2537Å excitation, as

shown in Table I, the measurements proved sufficient for relative comparison.

TABLE I

Relative Brightness of Rare-Earth Activators

Rare-Earth Activator (.05 mol/mol Y_2O_3)	% 2537Å Response	Major Excitation Band Angstroms	Standard Employed	Peak Emission Angstroms
Sm^{+3}	8	2080	$Ca_5(F,Cl)(PO_4)_3$:Sb:Mn	5850
Eu^{+3}	92	2537 *	Y_2O_3:$Eu_{.075}$	6125
Tb^{+3}	49	3060 *	Zn_2SiO_4:Mn	5280
Dy^{+3}	10	2080	$Ca_5(F,Cl)(PO_4)_3$:Sb:Mn	5850

*depending upon activator concentration.

The brightest phosphor in each series was then chosen and the other members were read in terms of it. This gave the results shown in Figure I which presents the effect of activator concentration on relative plaque brightness. The optimum concentrations found are given in Table II.

TABLE II

Optimum Activator Concentration in Y_2O_3

Activator	Optimum Concentration (mols per mol)	Ratio
Sm^{+3}	0.0015	1
Eu^{+3}	0.1500	100
Tb^{+3}	0.0250	17
Dy^{+3}	0.0100	7

One of the major differences found for Eu^{+3}- and Tb^{+3}-activated phosphors was the existance of a broad excitation band, due to a perturbed activator state, which was not found in Sm^{+3}- or Dy^{+3}-activated phosphors. The relative peak heights were a function of the activator content, as shown in Figure II for Eu^{+3} in Y_2O_3. Such behavior was not observed in the Sm^{+3}- or Dy^{+3}-activated phosphors[1].

Another difference noted was the relative brightness as a function of host sensitization. Matrix excitation of Y_2O_3 phosphors may be obtained at 2080Å[2]. When excitation of the optimized phosphors is achieved by means of a cadmium lamp, which has a spectral line at 2288Å, the results shown in Figure III are obtained. Note that the Eu^{+3} and Tb^{+3} phosphors are up to six times brighter than the corresponding Sm^{+3} or Dy^{+3} phosphors. Since these results are also a measure of host sensitization, it is obvious that the efficiency of energy transfer from host to activator center varies considerably. Host sensitiza-

tion occurs for Eu^{+3} or Tb^{+3}, but to a much smaller degree for Sm^{+3} or Dy^{+3}.

This aspect was investigated in more detail, with the results shown in Table III. The relative number of photons emitted (N_o) was measured by employing an excitation beam of constant energy at a 2080Å wavelength. This produced matrix excitation, with subsequent energy transfer and emission by the rare-earth activator. The emission lines observed were integrated, resulting in an average energy of emission which is specified both as energy and wavelength. Calculation of the luminosity then showed the same general results given in Figure III. Note that Tb^{+3}-, Sm^{+3}- and Dy^{+3}-activated phosphors do emit about the same relative number of photons. However, because of the higher luminosity of the Tb^{+3} photons, the emission brightness is greater than Sm^{+3}, for example. The Eu^{+3}-activated phosphor is four times more efficient than the other materials. Indeed, measurements of Y_2O_3:Eu^{+3} have shown this phosphor to possess a quantum efficiency of 92% under 2537Å excitation, and Eu^{+3} has been observed[3] to possess quantum efficiencies close to, or in excess of, 100%.

TABLE III

Calculation of Relative Brightness of Phosphors Based on Y_2O_3

	Y_2O_3:Eu .15		Y_2O_3:Tb .025		Y_2O_3:Sm .0015		Y_2O_3:Dy .01	
	$\bar{\nu}$ (cm^{-1})	I	$\bar{\nu}$ (cm^{-1})	I	$\bar{\nu}$ (cm^{-1})	I	$\bar{\nu}$ (cm^{-1})	I
1. Emission Observed	15,900	.04	15,800	.03	14,710	.06	14,640	.05
	16,100	.03	16,000	.03	14,850	.07	14,920	.04
	16,400	.62	16,130	.02	15,120	.06	17,110	.19
	16,600	.10	16,720	.03	16,000	.11	17,430	.47
	17,100	.14	17,170	.03	16,390	.18	20,440	.09
	17,500	.05	17,810	.03	17,050	.11	20,660	.10
	18,900	.02	18,180	.23	17,430	.11	21,140	.06
			18,420	.36	17,680	.20		
			20,220	.04	18,420	.03		
			20,390	.06	20,440	.03		
			20,610	.05	20,660	.03		
			20,770	.07	20,769	.03		
			20,930	.02				
2. Average Energy of Emission ($\sum(\bar{\nu} \times I)$)	16,430 cm^{-1} (6086Å)		18,495 cm^{-1} (5384Å)		16,577 cm^{-1} (6032Å)		17,940 cm^{-1} (5574Å)	
3. Color	Red		Green		Red-Orange		Yellow-Green	
4. Relative Number of Photons Emitted (N_o)	100		38		23		24	
5. Electron Volts	2.04		2.30		2.05		2.22	

TABLE III - (Continued)

	Y_2O_3:Eu.15	Y_2O_3:Tb.025	Y_2O_3:Sm.0015	Y_2O_3:Dy.01
6. Calculated Intensity (N_o x e.v.)	204	87	47	53
7. Luminosity Factor (f)	.5156	.9603	.5926	.9995
8. Calculated Luminosity (L_c)	106	84	28	53

Spectra of the rare earths have been observed to consist mainly of electric dipole transitions, although some magnetic dipole transitions have also been noted[4,5]. It might be possible to explain the experimental intensity differences observed in terms of emission involving electric dipole transitions (Eu^{+3}) as opposed to those involving magnetic dipole transitions (Tb^{+3}, Sm^{+3} and Dy^{+3}). However, while it is possible that quenching interactions, which occur between rare-earth ions of different species, are associated with mutual relationships of their energy levels, as proposed by Van Uitert and Iida[6], these factors do not fully explain the quenching interactions observed between similar species nor the differences determined for the optimum activator concentrations. Neither do they explain the differences observed for quenching effects of other rare earths on Eu^{+3} emission in Y_2O_3. Results for Y_2O_3:Eu.05:RE_x systems are shown in Figure IV.

Therefore, there are at least two factors which need to be explained:

1. Fluorescence-quenching between similar species.
2. Fluorescence-quenching between unlike rare earths.

As shown by the absence of lattice frequencies in their emission spectra[7], Eu^{+3} and Tb^{+3} do not interact as strongly with their environment as the rare-earth ions which have H or I ground states. Thus, it would be expected that the latter ions would behave quite differently, particularly Eu^{+3} whose emitting level, $^5D_0$, and ground state level, $^7F_0$, are not affected by the crystal field.

Only a few measurements have been made on the ground-state splitting of the rare-earths in a crystalline field. The most extensive of these involves the garnets, $Y_3Al_5O_{12}$ and $Y_3Ga_5O_{12}$. Table IV shows the measured results as found by various investigators.

TABLE IV

Ground-State Splitting of Rare-Earth Activators

Activator	Ground State (LSJ Term)	Matrix	Energy Differences of Stark Levels cm^{-1}	Reference
Eu^{+3}	$^7F_0$	$Y_3Ga_5O_{12}$	None	8
Sm^{+3}	$^6H_{5/2}$	$Y_3Ga_5O_{12}$	45	8
		$LaCl_3$	66	9
Tb^{+3}	$^7F_6$	$Y_3Ga_5O_{12}$	15	8
		$Y_3Ga_5O_{12}$	54	10
		$Y_3Al_5O_{12}$	74	10
		$Y_3Al_5O_{12}$	70	11
Dy^{+3}	$^6H_{15/2}$	$Y_3Ga_5O_{12}$	48	8
		$LaCl_3$	141	9
Er^{+3}	$^4I_{15/2}$	$Y_3Al_5O_{12}$	564	12
		Y_2O_3	510	13
Nd^{+3}	$^4I_{9/2}$	$Y_3Al_5O_{12}$	848	14
Tm^{+3}	$^3H_6$	Y_2O_3	797	13

Note that the same order of magnitude prevails, regardless of the matrix in which the rare earth finds itself. Thus, the values for rare earths are not likely to be much different for Y_2O_3 as compared to $Y_3Al_5O_{12}$ or $Y_3Ga_5O_{12}$. Note also the reciprocal relationship between ground-state splitting (Stark components) and fluorescent intensity found previously for Y_2O_3 phosphors[1]. This simple fact could account for differences observed in optimum activator concentrations. For example: Quenching between Eu^{+3}-Eu^{+3} pairs does not occur at concentrations one hundred times higher than that observed for Sm^{+3}-Sm^{+3} pairs, yet the presence of Sm^{+3} at a 1:100 ratio in Y_2O_3:Eu causes a considerable quenching of Eu^{+3} emission intensity. Thus, even the low degree of ground-state splitting for Eu^{+3} or Tb^{+3} does not fully explain the observed effects.

It may be concluded that the two factors affecting the fluorescent intensity of rare-earth emission in the oxides are (a) the degree of ground-state

splitting and (b) the amount of quantum mechanical resonance energy transfer which occurs between unlike ions. The crystalline field, according to its symmetry properties, removes the degeneracy of a given state, producing Stark levels (2J + 1). When a significant degree of ground-state splitting occurs, vibronic coupling of both the excited and ground states occurs, resulting in dissipation of excitation energy by phonon processes. Such phenomena probably account for the low optimum activator concentration determined for Sm^{+3} and Dy^{+3}, since a minimum of vibronic coupling is mandatory to obtain fluorescence. When concentrations are increased above the optimum, interactions between centers increase rapidly and phonon vibrational dissipation of energy occurs. Eu^{+3} and Tb^{+3}, being much less affected by the lattice field, can be tolerated at much higher concentrations before fluorescence-quenching begins to occur.

It is interesting to calculate the number of cation sites occupied by the activator per unit cell, assuming random distribution. There are thirty-two cation sites per unit cell[15], twenty-four of which have C_2 symmetry. Table V shows the calculated sites occupied as a function of activator.

TABLE V

Comparison of Sites Occupied in Y_2O_3 Matrix

Activator	Optimum Concentration (mols/mol)	Sites Occupied per Unit Cell	Sites Occupied per 5-Unit Cells
Eu^{+3}	0.1500	12.0	60
Tb^{+3}	0.0250	2.0	10
Sm^{+3}	0.0015	1.2	6
Dy^{+3}	0.0100	.8	4

Note that even the Eu^{+3} activator occupies only a fraction of the total available sites. In fact, just half of the sites having C_2 symmetry are occupied. Because there are three times as many C_2 sites as S_6 sites, one would expect nine C_2 sites and three sites having S_6 symmetry if random distribution occurred. Whether all possess C_2 symmetry is unknown. Note that only one Sm^{+3} center per unit cell (80 atoms) can be tolerated without producing losses in fluorescent intensity.

The other factor of resonance energy transfer between unlike ions within the lattice also affects luminescence adversely. For Eu^{+3} or Tb^{+3}, dipole-dipole or dipole-quadrupole resonance energy transfer between unlike ions causes a significant loss of intensity due to the increased degree of lattice vibronic coupling at the other rare-earth ion site.

Some factors which remain to be explained include (a) lack of host-sensitization in the weakly emitting phosphors, (b) lack of excitation "activator band" for Dy^{+3} and Sm^{+3}, (c) the mechanism of lattice energy exchange with the activator center, (d) the degree of exchange-coupling between two centers, either identical or different cations, (e) the total mechanism of fluorescence-quenching and the paths which energy dissipation can take, and (f) the nature of the spectroscopic transitions within the various activator centers.

ACKNOWLEDGMENT

The author is indebted to E. Chen and G. Grasso for preparation of samples, and to E. E. Gritz for technical aid in the evaluation of materials.

REFERENCES CITED

1. R. C. Ropp, "Proceedings of Third Rare Earth Conference," p. 481 Gordon and Breach, N. Y. (1964).
2. R. C. Ropp, J. Electrochem. Soc., 112, 181 (1965).
3. R. C. Ropp, Unpublished results.
4. E. V. Sayer and S. Freed, J. Chem. Phys., 24, 1213 (1956).
5. K. H. Hellwege, U. Johnson, H. G. Kahle and G. Schaack, Z. Phys. 148, 112 (1957).
6. L. G. Van Uitert and S. Iida, J. Chem. Phys., 37, 986 (1962).
7. G. H. Dieke and L. A. Hall, J. Chem. Phys., 25, 465 (1957).
8. S. P. Keller and G. D. Petit, Phys. Rev., 121, 1639 (1961).
9. J. D. Axe and G. H. Dieke, J. Chem. Phys., 37, 2364 (1962).
10. J. A. Koningstein, USASR Report, AD-D 411-484, Bell Tel. Labs. (April 1963).
11. J. A. Koningstein, Phys. Rev., 136, A717 (1964).
12. J. A. Koningstein, Phys. Rev., 136, A726 (1964).
13. J. B. Gruber, W. F. Krupke and J. M. Poindexter, J. Chem. Phys., 41, 3363 (1964).
14. J. A. Koningstein and J. E. Geusix, Phys. Rev., 136, A711 (1964).
15. L. Pauling and M. D. Shappell, Z. Krist., 75, 128 (1930).

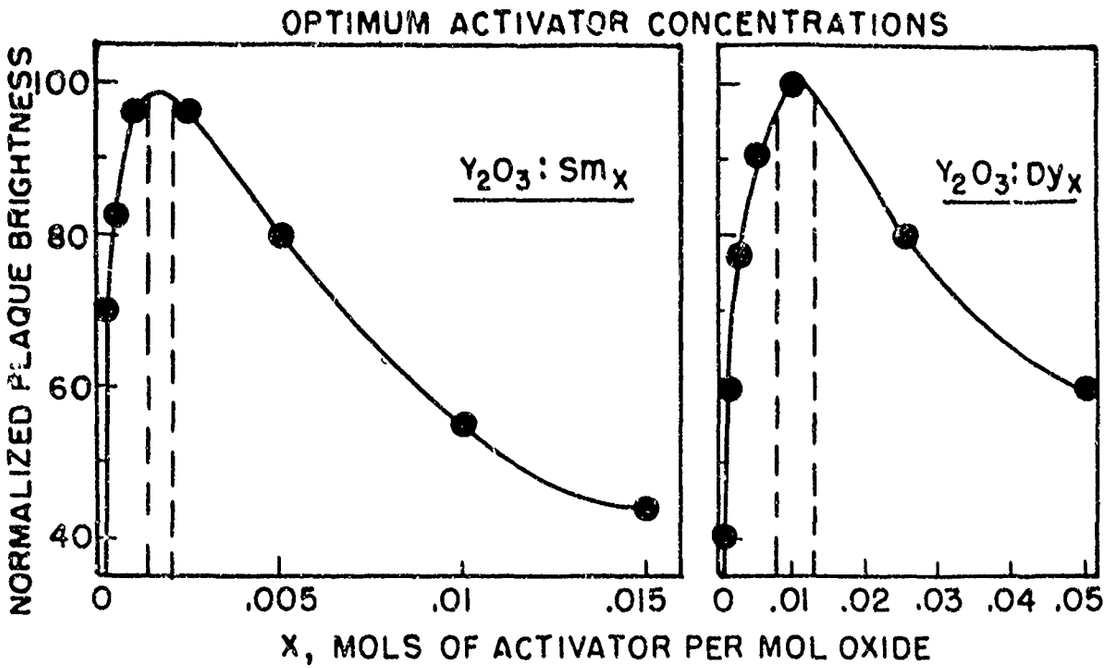
OPTIMUM ACTIVATOR CONCENTRATIONS
NORMALIZED PLAQUE BRIGHTNESS
100
80
60
40
$Y_2O_3:Sm_x$
$Y_2O_3:Dy_x$
0
.005
.01
.015
0
.01
.02
.03
.04
.05
X, MOLS OF ACTIVATOR PER MOL OXIDE

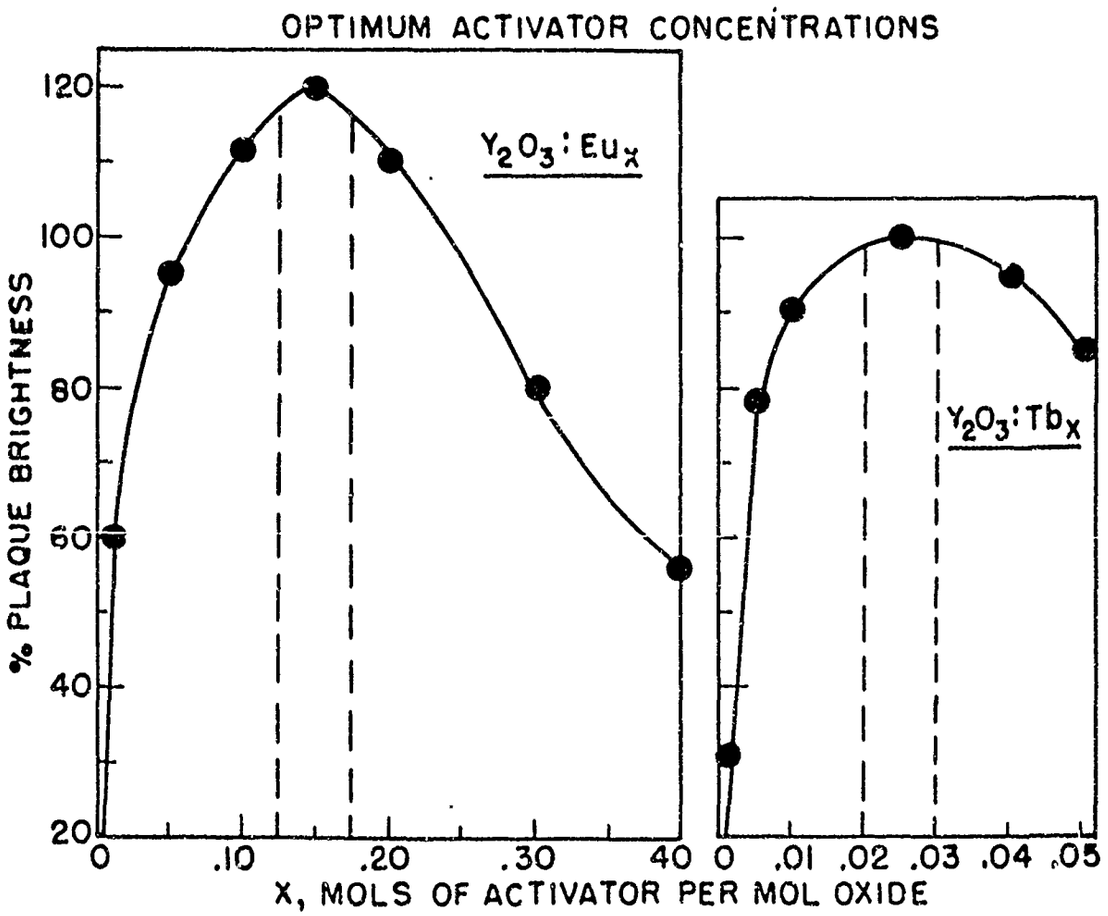
OPTIMUM ACTIVATOR CONCENTRATIONS
% PLAQUE BRIGHTNESS
120
100
80
60
40
20
$Y_2O_3:Eu_x$
$Y_2O_3:Tb_x$
0
.10
.20
.30
40
0
.01
.02
.03
.04
.05
X, MOLS OF ACTIVATOR PER MOL OXIDE

FIG. 1

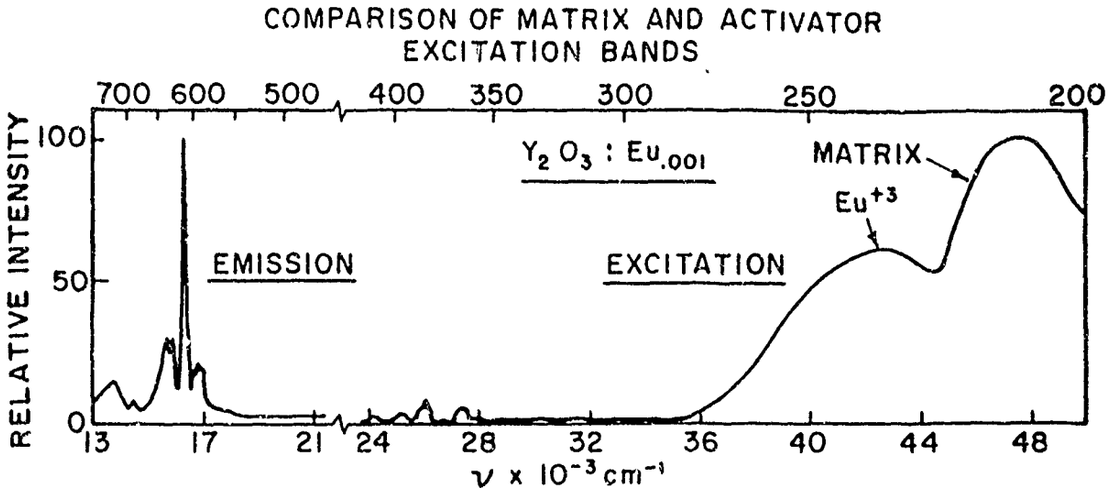
COMPARISON OF MATRIX AND ACTIVATOR
EXCITATION BANDS
700 600 500 400 350 300 250 200
RELATIVE INTENSITY
100
50
0
$Y_2O_3 : Eu_{.001}$
MATRIX
Eu^{+3}
EMISSION
EXCITATION
13 17 21 24 28 32 36 40 44 48
$\nu \times 10^{-3}\,cm^{-1}$

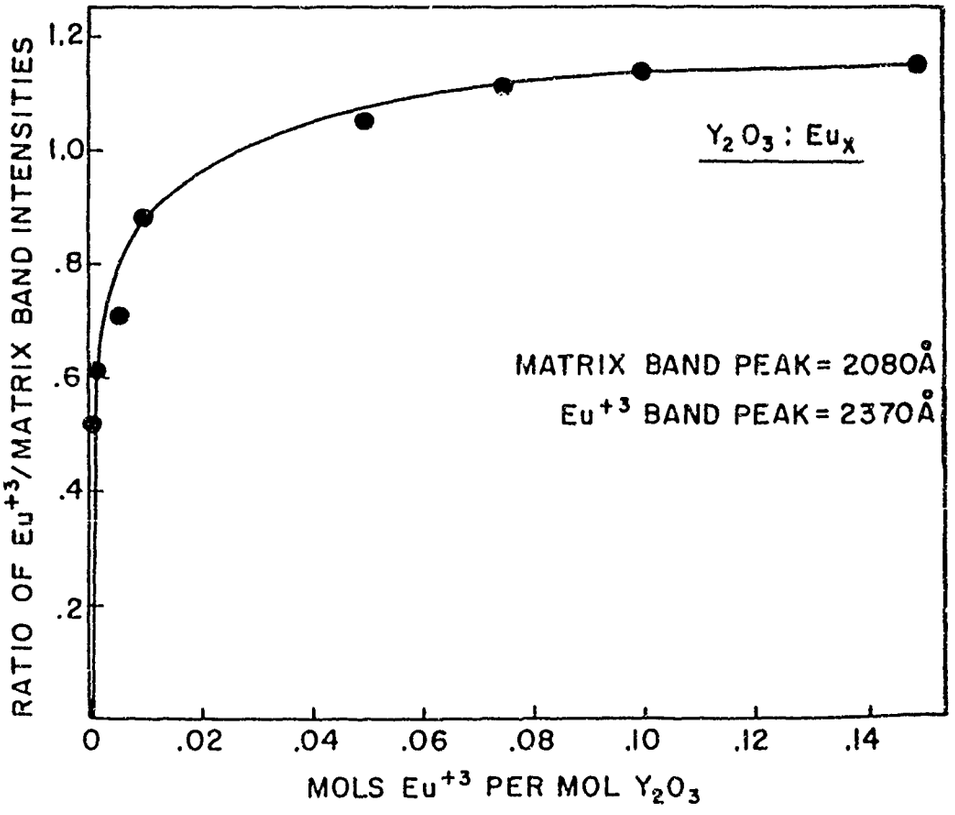
RATIO OF Eu^{+3}/MATRIX BAND INTENSITIES
1.2
1.0
.8
.6
.4
.2
$Y_2O_3 : Eu_X$
MATRIX BAND PEAK = 2080Å
Eu^{+3} BAND PEAK = 2370Å
0 .02 .04 .06 .08 .10 .12 .14
MOLS Eu^{+3} PER MOL Y_2O_3

FIG. 2

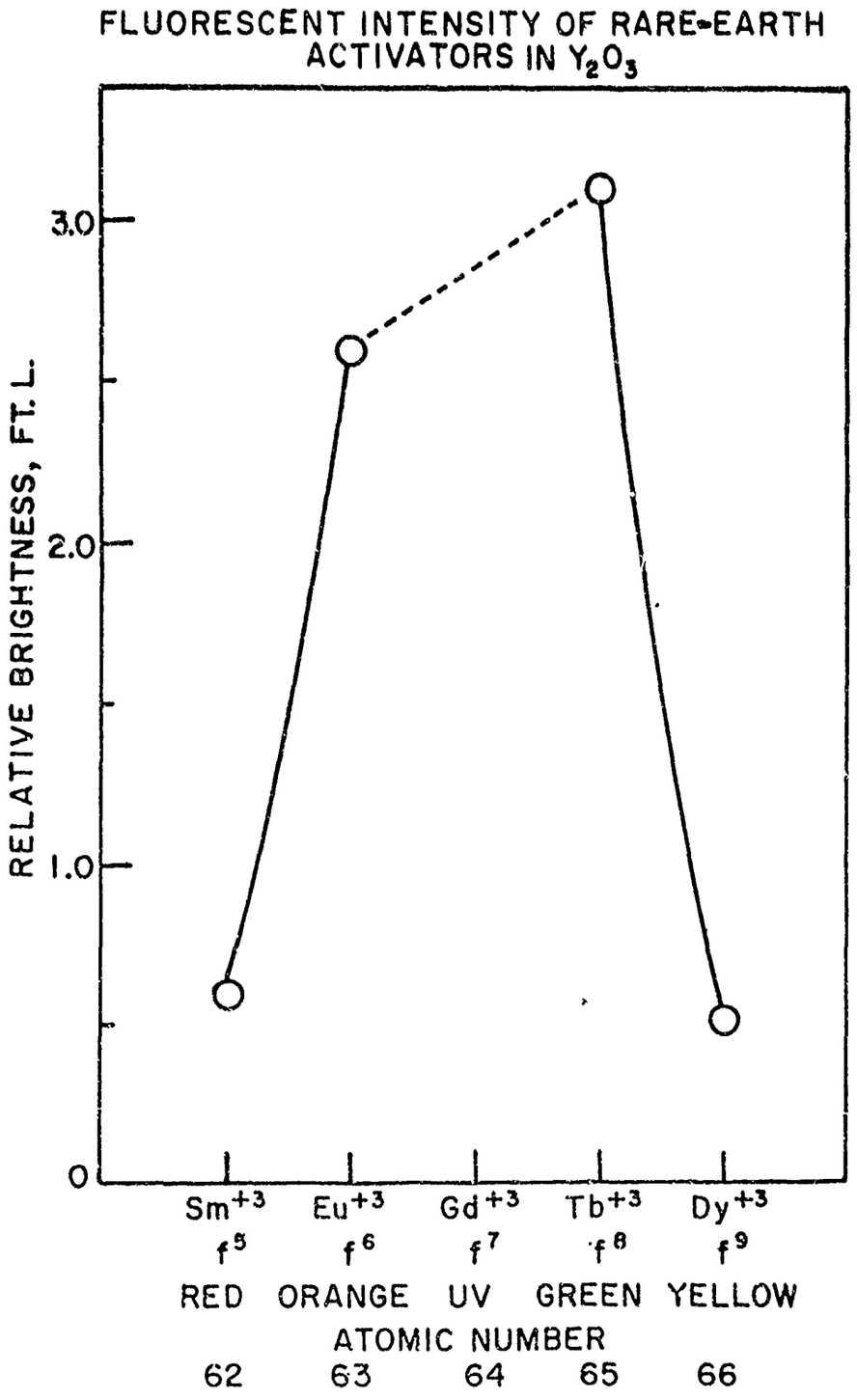
FLUORESCENT INTENSITY OF RARE-EARTH ACTIVATORS IN Y_2O_3
RELATIVE BRIGHTNESS, FT. L.
3.0
2.0
1.0
0
Sm^{+3} Eu^{+3} Gd^{+3} Tb^{+3} Dy^{+3}
f^5 f^6 f^7 f^8 f^9
RED ORANGE UV GREEN YELLOW
ATOMIC NUMBER
62 63 64 65 66

FIG. 3

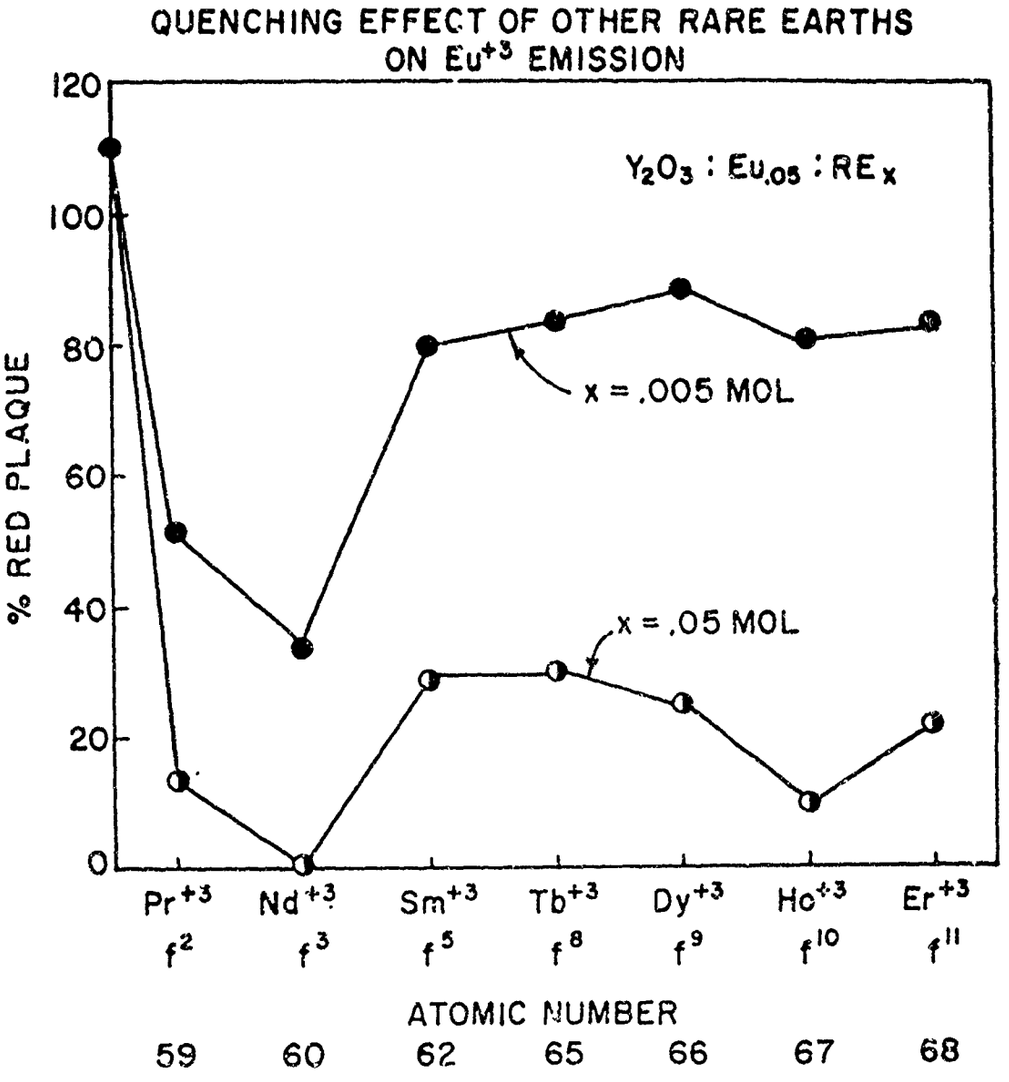
QUENCHING EFFECT OF OTHER RARE EARTHS
ON Eu+3 EMISSION
Y2O3 : Eu.05 : REx
x = .005 MOL
x = .05 MOL
% RED PLAQUE
120
100
80
60
40
20
0
Pr+3 f2
Nd+3 f3
Sm+3 f5
Tb+3 f8
Dy+3 f9
Ho+3 f10
Er+3 f11
ATOMIC NUMBER
59 60 62 65 66 67 68

FIG. 4

EFFICIENCY OF Eu^{+3} FLUORESCENCE IN OXYGEN-DOMINATED HOST LATTICES

Hans J. Borchardt

Central Research Department
E. I. du Pont de Nemours & Company
Wilmington, Delaware

ABSTRACT

The efficiency of Eu^{+3} fluorescence in a variety of rare earth oxygen-dominated host materials was measured under excitation by 2537 Å UV at 25°C. It was found to be of the same order as that of the commercial phosphor magnesium arsenate:Mn in all such hosts. To account for the insensitiveness of efficiency to the nature of the host lattice, it is proposed that europium-oxygen states are excited directly and that the corresponding absorption coefficient is of a magnitude to make this the dominant absorption process. Independent evidence for europium-oxygen charge-transfer absorption is given.

INTRODUCTION

It has been known since the turn of the century that Eu^{+3} gives rise to a red fluorescence when incorporated in a wide variety of hosts[1]. Such materials had not been considered as practical phosphors until recently, however[2]. It was first pointed out by the writer that Eu^{+3} (and Tb^{+3}), in certain oxygen-containing hosts, fluoresces with an efficiency comparable to that of commercial phosphors[3]. High efficiency fluorescence of Eu^{+3}-doped oxides has since been reported by other workers[4,5,6,7] as has the practical utilization of such materials in color television[2]. It is the purpose of this paper (1) to show that high efficiency Eu^{+3} fluorescence is not the property of a few isolated hosts but rather that it occurs generally in host lattices of a type that will be specified, and (2) to offer a plausible explanation for the generality of the phenomenon.

The high efficiency fluorescence was first observed[8] with Eu^{+3}-doped rare earth tungstates of stoichiometry $R_2(WO_4)_3$ and R_2WO_6. R is one of the elements Sc, Y, La, Gd, and Lu. It is believed that these elements are not directly involved in the fluorescence process but function only as diluents to reduce quenching interactions between europium ions[8]. After this finding with tungstates, molybdates and then a wide variety of other rare earth oxygen-dominated hosts were investigated. It was from these data that the generalization regarding europium fluorescence in oxygen-dominated hosts emerged.

EXPERIMENTAL

Preparation of Materials

The compositions listed in Table I were prepared in most instances by direct reaction of Eu_2O_3, the oxide of one of the above-cited rare earths, and a third oxide. The powders were mixed on a Crescent "Wig-L-Bug" and fired in air in platinum-lined boats. Sample weights were approximately 1.5 g. The materials were generally prefired at 500-600° for one to two hours, then ground and fired a second time at high temperatures. The maximum firing temperatures are listed in Table I. $(Y_{1-x}Eu_x)_2O_3$ compositions were prepared both by direct reaction of the constituent oxides and by coprecipitation of the oxalates. A considerably higher quantum efficiency was obtained with the coprecipitated materials and the results given herein are for materials prepared in that fashion.

To assure that all the compositions are single phases, the pseudobinary phase diagrams of the systems R_2O_3-MO_x (for example, Y_2O_3-SrO) were determined in part. This work will not be described herein. In those cases where the host lattice has previously been reported, a reference to prior work is given in Table I.

Measurement of Relative Emission Intensities

The emission intensities were measured relative to that of magnesium arsenate, manganese activated. The latter was obtained from the National Bureau of Standards as "NBS Standard Sample 1030". A quantum efficiency of 0.71 has been reported for "NBS Standard Sample 1030" by Bril and van Meurs-Hoekstra[9].

The apparatus consists of (a) a Beckmann Model DU monochrometer and hydrogen lamp to provide the incident UV light, (b) a Beckmann diffuse reflectance attachment which contains sample holders and means for focusing the fluorescence from the sample onto a ground glass screen, (c) a Corning 3-69 filter situated adjacent to said screen which passes the fluorescence and filters out reflected exciting radiation, and (d) a detector which is situated adjacent to said filter. The detector is a Dumont 6911 infrared photomultiplier which is used in conjunction with a Hamner Model N401 power supply. The output was measured with RCA Model WV-84C microammeter. The relative emission intensity was determined by exposing the sample to the exciting beam, recording the detector output, exposing the magnesium arsenate:Mn to the same beam, again recording the detector output, and taking a ratio of these readings.

A small correction must be made because the detector is slightly more sensitive to the magnesium arsenate:Mn emission than to the emission from Eu^{+3}. A comparison of the respective fluorescence emission spectra with the detector response curve supplied by the manufacturer shows this correction to amount to 7%. The values in Table I are the measured values multiplied by 1.07.

Measurement of UV Absorption

The reflectance is measured directly and the absorption is taken to be (1- reflectance). The UV reflectance (fraction of incident light which is reflected) is measured with the same apparatus described above for relative emission intensities, with the exception that (a) a Corning 7-54 filter is employed which passes the

reflected UV light and filters out the fluorescence, and (b) a 1P28 photomultiplier is used as detector. The intensity of the incident light is determined by allowing it to reflect off a USP magnesium carbonate block (whose reflectance is taken as unity) into the detector. With the geometry identical, the sample is substituted for the magnesium carbonate block and the ratio of detector readings with sample and carbonate block is taken as the reflectance. The reflectance of the magnesium arsenate:Mn was found to be 0.06; i.e., 94% of the incident UV (2537 Å) is absorbed. From these numbers it is seen that the UV absorption is very insensitive to experimental errors. In this instance, a 100% error in the measured reflectance causes only a 6% error in absorption.

Both absorption and emission were measured at 2537 Å.

Quantum Efficiency

The quantum efficiency of the subject materials relative to that of magnesium arsenate:Mn is readily calculated from the above measurements by means of the formula

$$\frac{Q_{Eu}}{Q_{Ars}} = \frac{Ie_{Eu}/Ie_{Ars}}{Ia_{Eu}/Ia_{Ars}}$$

where the subscripts "Eu" and "Ars" refer to the europium phosphor and magnesium arsenate:Mn respectively, where Ie_{Eu}/Ie_{Ars} is the ratio of emission intensities and I_a, the UV absorption. Introducing the value of 0.71 for Q_{Ars} gives Q_{Eu}. This method of determining quantum efficiencies is discussed by Tregellas-Williams[10].

RESULTS

The results are summarized in Table I. The various hosts that were prepared and the respective Eu^{+3} doping levels are given in the first two columns. (The actual material that was prepared would, for the case of the first entry, be $(Y_{0.9}Eu_{0.1})_2SrO_4$.) The Eu^{+3} concentration at which the brightest emission occurs was found to be in the range of 10's of percents. Within this range there is a

regular variation; the more atoms per formula, the higher the optimum Eu^{+3} concentration. This is illustrated in Figure 1 which shows curves of relative emission intensity versus Eu^{+3} concentration for a number of hosts.

The emission intensity relative to magnesium arsenate:Mn, the UV absorption, and quantum efficiency, all at 2537 Å, are tabulated in columns 3-5, respectively.*

DISCUSSION

Empirical Generalization

A striking result is that the quantum efficiency of the materials, although lower than that of magnesium arsenate:Mn, is of the same order of magnitude as that of this commercial phosphor. It is well known that the efficiency of a new phosphor can generally be improved by a factor of 2 or 3 by optimizing the method of preparation and adjusting composition. The magnesium arsenate:Mn standard (obtained by the NBS from lamp manufacturers) is such an optimized material whereas the europium phosphors of Table I are not. This further narrows the gap between the efficiency of these materials and commercial phosphor.

It may be noted that the hosts include a rather broad range of elements, namely, elements from Groups II, III, IV, V, and VI of the Periodic Table. This suggests the following generalization: Eu^{+3} fluoresces very efficiently (e.g., of the same order as commercial phosphors which presumably have quantum efficiencies in the range 60% to 100%) in all crystalline oxygen-dominated host lattices at room

---

* In Reference 3, quantum efficiencies in excess of 80% are cited. This referred to $(Y_{1-x}Eu_x)_2O_3$ compositions and was based on a quantum efficiency of .85 for magnesium arsenate:Mn, the value in the literature at that time[10]. In Reference 8, a quantum efficiency of unity is cited. This referred also to $(Y_{1-x}Eu_x)_2O_3$ compositions, but under 2400 Å excitation.

temperature under 2537 Å UV where the cations are only Eu^{+3} and one or more from the group Sc, Y, La, Gd, and Lu and where the Eu^{+3} concentration is in the range of 10's of percents. Excluded from this generalization, of course, are such colored hosts as would absorb this emission.

The efficient fluorescence of Eu^{+3}, or for that matter any phosphor "activator" in such a wide variety of hosts, is a new phenomenon. It is of interest to speculate upon the underlying cause for the insensitiveness of fluorescent efficiency to the nature of the host.

Fluorescence Mechanism

It seems likely that the mechanism of fluorescence which gives rise to high quantum efficiency in the variety of hosts is essentially the same in each of these hosts. This requires that all steps in the fluorescence process, absorption, excitation and emission may involve only elements that are common to all the materials; these common elements are europium and oxygen. Emission is known to originate from excited 4f states of Eu^{+3}. The only question then is whether Eu^{+3} is excited directly or whether europium-oxygen states are involved in absorption. For reasons given below, we believe that europium-oxygen states are excited first. The overall mechanism then is postulated to be absorption by europium-oxygen groups resulting in the excitation of charge transfer states (e.g., Eu^{+2}-O^{-}), relaxation of these leaving Eu^{+3} in an excited 4f state and emission from said excited Eu^{+3} ion.

Evidence for Eu-O Charge-Transfer Absorption

1. Competition for Incident UV with Charge-Transfer Absorbers

Charge-transfer absorption involves very large absorption coefficients. In order for europium to fluoresce efficiently, it must be able to compete effectively with other host constituents for the incident UV. Some of these host constituents may be charge-transfer absorbers.

An example of competitive charge-transfer absorption by a host constituent is found in the case of $(Gd_{0.8}Eu_{0.2})_2(MoO_4)_3$. At 77°K the fluorescence emission spectrum of this material shows both the broad band molybdate fluorescence as well as the line emission of Eu^{+3}. This indicates that energy transfer from $MoO_4^{=}$ to Eu^{+3} is not occurring. The quantum efficiency with respect to Eu^{+3} emission (quanta emitted by Eu^{+3}/total quanta absorbed) is found to be approximately 0.6 at this temperature. Therefore, absorption by europium must be greater than the absorption by $MoO_4^{=}$. The absorption by $MoO_4^{=}$ is known to be extremely intense and is believed to involve charge-transfer processes[11]. The absorption coefficient of europium must, therefore, be greater than that of this particular charge-transfer absorber, and it is, therefore, likely that the absorption by europium also involves a charge-transfer process (e.g., excitation of Eu-O states).

2. Interpretation of Reflectance Spectra.

Additional evidence for charge-transfer absorption by europium-oxygen states is implicit in the reflectance spectra of the rare earth oxides shown in Fig. 6 of Reference 8. The spectra of the oxides of Sc, Y, La, and Lu show broad UV absorption bands which are attributable to charge-transfer absorption states involving the rare earth element and oxygen. A similar absorption band is seen in Eu_2O_3, except that it extends slightly further to long wave lengths. This similarity suggests that the band in Eu_2O_3 is due to charge-transfer absorption.

If this band were not due to excitation of Eu-O states, it would have to be due to excitation of Eu^{+3} alone. If this were the case, a similar band should be seen in europium compounds which contain no oxygen such as EuF_3. The reflectance spectrum of EuF_3 is shown in Fig. 2. The broad UV absorption band of Eu_2O_3 is seen not to be present.

Miscellany

1. Energy transfer.

Emphasis has been placed upon localized absorption by Eu-O. We do not wish to imply thereby that absorption by the host and energy transfer to Eu^{+3} is either not occurring or not important. The only assertion being made is that such processes are not the underlying cause for the order of magnitude generalization regarding efficiency. It is very likely, however, that the detailed variation in quantum efficiency from host to host seen in Table I is due primarily to variations in the degree of such competitive absorption by and energy transfer from the host.

2. Role of host cation

The experimental work involved only hosts with the rare earth cations Sc, Y, La, Gd, and Lu. The proposed mechanism does not refer to these at all. Presumably any cation which would serve to dilute the Eu^{+3} and which would not interfere with the optical processes could be used.

3. Mode of excitation.

Experimental work was with 2537 Å UV. From the proposed mechanism it follows that UV anywhere in the range where Eu-O charge-transfer absorption occurs would efficiently excite fluorescence. If our interpretation of the reflectance spectrum is correct, this would be at wave lengths anywhere below approximately 2800 Å (Fig. 6B, Ref. 8). According to the proposed mechanism, the 4f electrons of Eu are very effectively coupled to the host via Eu-O charge-transfer states. The latter are said to have a large absorption coefficient. Thus the excitation cross section of Eu is very large and presumably any means for generating approximately 4-6 e.v. units of excitation in the host would excite fluorescence. These might include x-ray, cathode rays, etc.

REFERENCES

1. G. Urbain, Ann. Chim. Phys. 18, 222-386 (1909) and references cited.
2. Chem. Week, p. 29, Nov. 14, 1964; C & E News, p. 54, Nov. 23, 1964.
3. H. J. Borchardt, J. Chem. Phys. 38, 1251 (1963).
4. N. C. Chang, J. Appl. Phys. 34, 3500 (1963).
5. K. A. Wickersheim and R. A. Lefever, J. Electrochem. Soc. 111, 47 (1964).
6. R. C. Ropp, ibid., 111, 311 (1964).
7. A. Bril and W. L. Wanmaker, ibid., 111, 1363 (1964).
8. H. J. Borchardt, J. Chem. Phys. 39, 504 (1963).
9. A. Bril and W. van Meurs-Hoekstra, Philips Res. Repts. 19, 296 (1964).
10. J. Tregellas-Williams, J. Electrochem. Soc. 105, 173 (1958).
11. F. A. Kroger, "Some Aspects of the Luminescence of Solids," Elsevier Publishing Co., New York, 1948.
12. T. Moeller and G. L. King, J. Am. Chem. Soc. 75, 6060 (1953).
13. S. Geller, Acta. Cryst. 10, 243 (1957).
14. M. L. Keith and R. Roy, Am. Mineral 39, 1 (1954).
15. S. J. Schneider, R. S. Roth, J. L. Waring, J. Res. Natl. Bur. Std. 65A, 345-374 (1961).
16. M. Gmelin-Kraut, Handbuch Anorg. Chem. 6 (1932).
17. D. Guisca and I. Popescu, Soc. Roumaine de Physique Bull. 40 (3) 13 (1939); Sci. Abstr. 43A, 352 (1940).

TABLE I

Eu^{+3} Quantum Efficiencies in Various Host Lattices

Host Lattice	Eu^{+3} Conc.[a]	Ie_{Eu}/Ie_{Ars}[b]	Ia_{Eu}[b]	Q[b]	Firing Temp.	Reference[c]
Y_2SrO_4	0.1	0.43	0.86	0.33	1400°C	---
Gd_2SrO_4	0.1	0.41	0.87	0.31	"	---
$YGaO_3$	0.2	0.45	0.87	0.34	"	---
$LaGaO_3$	0.2	0.17	0.92	0.12	"	12,13
$Y_3Ga_5O_{12}$	0.2	0.50	0.82	0.41	"	14
$Gd_3Ga_5O_{12}$	0.2	0.62	0.82	0.50	"	15
YBO_3	0.2	0.25	0.61	0.27	"	16
$GdBO_3$	0.2	0.33	0.70	0.32	1100°	16
$La(BO_2)_3$	0.2	0.53	0.93	0.38	1000°	16
La_2GeO_5	0.2	0.22	0.93	0.16	1500°	17
Gd_2GeO_5	0.2	0.38	0.87	0.29	1200°	---
$Y_2Ge_2O_7$	0.2	0.38	0.64	0.40	1400°	17
$LaPO_4$	0.2	0.42	0 82	0.34	1200°	16
$GdPO_4$	0.2	0.44	0.72	0.41	"	---
$Sc_2(MoO_4)_3$	0.3	0.17	0.92	0.12	900°	---
$Y_2(MoO_4)_3$	0.2	0.23	0.94	0.16	"	16
$La_2(MoO_4)_3$	0.3	0.15	0.93	0.11	"	16
$Gd_2(MoO_4)_3$	0.3	0.23	0.94	0.16	"	---
$Lu_2(MoO_4)_3$	0.3	0.15	0.95	0.11	"	---
Y_2WO_6	0.1	0.60	0.91	0.44	1400°	ó
$Sc_2(WO_4)_3$	0.2	0.19	0.94	0.14	1000°	ó
$Y_2(WO_4)_3$	0.2	0.14	0.95	0.10	"	o
$La_2(WO_4)_3$	0.4	0.32	0.93	0.23	"	ó
$Gd_2(WO_4)_3$	0.4	0.39	0.93	0.28	"	ć
$Lu_2(WO_4)_3$	0.2	0.17	0.95	0.11	"	ć
Y_2O_3	0.08	0.78	0.80	0.69	1400°	

(a) Expressed as mole fraction of rare earth ions.
(b) Under 2537 Å at room temperature.
(c) Where no reference is given, the host lattice has not been previously reported.

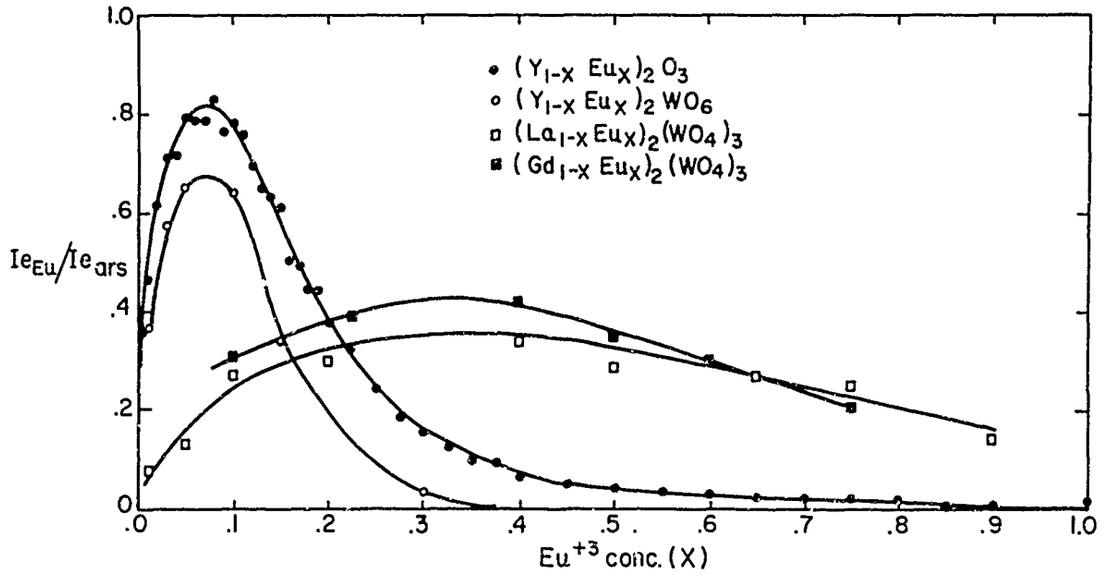

Fig. 1 FLUORESCENCE EMISSION INTENSITY AS A FUNCTION OF Eu^{+3} CONCENTRATION. RELATIVE TO MAGNESIUM ARSENATE: Mn. EXCITATION: 2537 A U.V. T = 25° C.

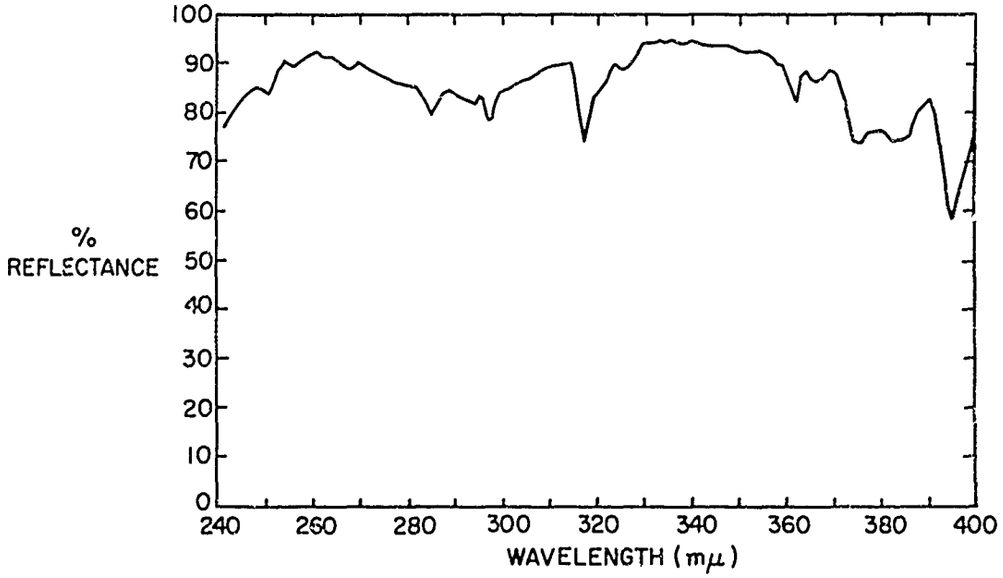

Fig. 2 U.V. REFLECTANCE SPECTRUM OF EuF_3.

ON THE ENHANCEMENT OF THE FLUORESCENCE OF AQUEOUS SOLUTIONS OF NEODYMIUM, SAMARIUM AND DYSPROSIUM CHLORIDES*

Adam Heller

General Telephone & Electronics Laboratories Inc.
Bayside, New York

ABSTRACT

Substitution of H_2O by D_2O enhances the fluorescence of aqueous solutions of the chlorides of trivalent neodymium, samarium and dysprosium. The fluorescence of the two latter weakly absorbing ions is further intensified by energy transfer from water soluble organic compounds in their triplet state. The minimum deuteration enhancement factors are four for neodymium, fourteen for samarium and one hundred for dysprosium. The sensitizing triplets enhance the fluorescence of samarium and dysprosium by an order of magnitude.

The emission spectra of the H_2O, D_2O, sensitized or unsensitized solutions of any of the ions are identical. The dominant emission lines are 10,550 Å for neodymium, 5947 Å for samarium and 4795 Å for dysprosium.

This study was undertaken to evaluate the attainable enhancement of the intensity of luminescence of aqueous solutions of neodymium, samarium and dysprosium and to obtain, through the enhancement techniques, emission spectra of improved resolution. Although the emission spectra of trivalent neodymium, samarium and dysprosium have been studied in detail in various crystalline matrices, little work has been done on the emission of their aqueous solutions. The reason for this may be sought in the extremely weak intensity of emission of the aqueous ions. The weakness of the fluorescence is not due to absorption, since the extinction length of water exceeds 1 cm up to 13,000 Å,[1] but rather to

---

* Work done in part at the Bell Telephone Laboratories, Murray Hill, New Jersey.

radiationless relaxations from the excited states and to insufficient absorption of the pumping radiation by some of the ions. Kropp and Windsor found that the radiationless de-excitation can be at least partially eliminated by substituting D_2O for H_2O.[2,3] A similar effect has been reported in hydrated crystals by Freeman, Crosby and Lawson.[4] Heller and Wasserman[5] suggested that broad pumping bands could be attained in dilute solutions of rare earth ions by energy transfer from organic molecules in their triplet state. In this process aromatic aldehydes and ketones, which are excitable in broad absorption bands, undergo intersystem crossing to their triplet state and lose their energy in a diffusion controlled process to the ion.

The present study extends these results from organic to aqueous solutions, and includes as energy acceptors samarium and dysprosium in addition to the previously investigated terbium and europium ions. The water-soluble compound chosen to sensitize the samarium ion was dipotassium 1,5-dibenzoylnaphthalenedisulfonate. Dysprosium was sensitized by dipotassium 4,4-benzophenone-dimethylenesulfonate. The choice of the sensitizers resulted from considerations of triplet energy and solubility. For efficient energy transfer, it was found desirable to have the triplet energy slightly above, yet close to, the energy required to excite the rare earth ion.[5] The energy of 1-benzoylnapthalene triplet is approximately 20,000 cm^{-1},[6] slightly exceeding the energies of the $^4F_{3/2}$ and $^4G_{5/2}$ states of samarium at 19,000 cm^{-1} and 18,000 cm^{-1}.[8] The energy of benzophenone triplet is approximately 24,000 cm^{-1},[6,7], just above the energy of the $^4F_{9/2}$, $^4I_{15/2}$ and $^4G_{11/2}$ states of dysprosium at about 21,000, 22,000 and 23,000 cm^{-1}.[8]

Experimental

The measurements were carried out on 0.1 M rare earth chloride solutions. Analysis of the 99.9% anhydrous rare earth chlorides indicated a 98% purity of the material by combined rare earth and chloride analysis; the remaining 2% was assumed to be water. The heavy water was 99.7% in deuterium oxide. In the sensitized solutions the concentration of the

sensitizer was 0.01 M. To prevent transferring triplets from being quenched by oxygen and to avoid contact with atmospheric humidity, all operations were carried out in a nitrogen atmosphere. Measurements were made on sealed samples in pyrex ampules of 1 cm diameter. Intensity measurements were reproducible within better than ±10%. The reported excitation spectra correspond to light emitted by a 700-watt Hanovia high-pressure xenon lamp filtered through a 1-64 Corning filter and attenuated by the 1.5 mm wall of the pyrex ampule. The enhancement factor due to sensitization depends on the spectrum of the light source, the cell thickness, and the concentrations of the components. Therefore, the sensitization enhancement factors reported here are rigorously correct only for the particular source, cell and concentrations employed.

The emission spectra are corrected for the detector response of the RCA 7265 and the RCA 7201 photomultipliers used.

Results

Figure 1 shows the emission spectra of neodymium chloride in D_2O and in H_2O. A four-fold enhancement is observed. This and following

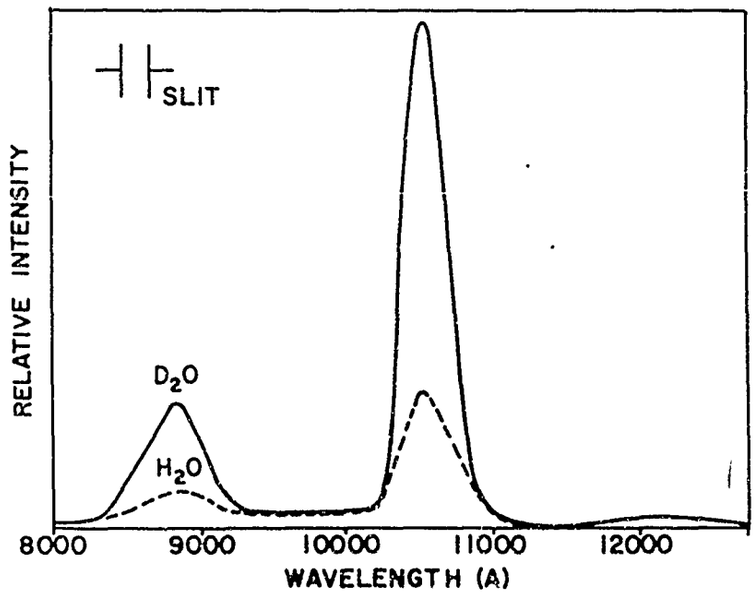

Fig. 1. Emission spectra of 0.1 M $NdCl_3$ in H_2O and in D_2O.

enhancement factors should be regarded only as minimum values, since the H_2O still present may induce nonradiative transitions; its removal should lead to further enhancement of the luminescence. The dominant emission occurs at 10,550 Å and corresponds, by analogy to the results of Dieke and Crosswhite on the energy levels of the free ion,[8] to the familiar $^4F_{3/2} \rightarrow {}^4I_{11/2}$ transition. The second transition observed is $^4F_{3/2} \rightarrow {}^4I_{9/2}$ at 8850 Å. No attempt has been made to sensitize the neodymium emission because the ion has extensive absorption bands for direct pumping. Since the signal-to-noise ratio with the available 7102 photomultiplier was poor, no high-resolution spectroscopy could be done on aqueous neodymium chloride.

The emission spectrum of sensitized samarium chloride in D_2O is shown in Fig. 2. The emission spectra of the ion in sensitized H_2O and in non-sensitized D_2O and H_2O solutions seem to be identical with the emission spectrum in the sensitized D_2O solution. To compare the intensities, the 5947 Å line emissions of the H_2O and non-sensitized solutions are presented. The enhancement due to the deuteration of the solvent is at

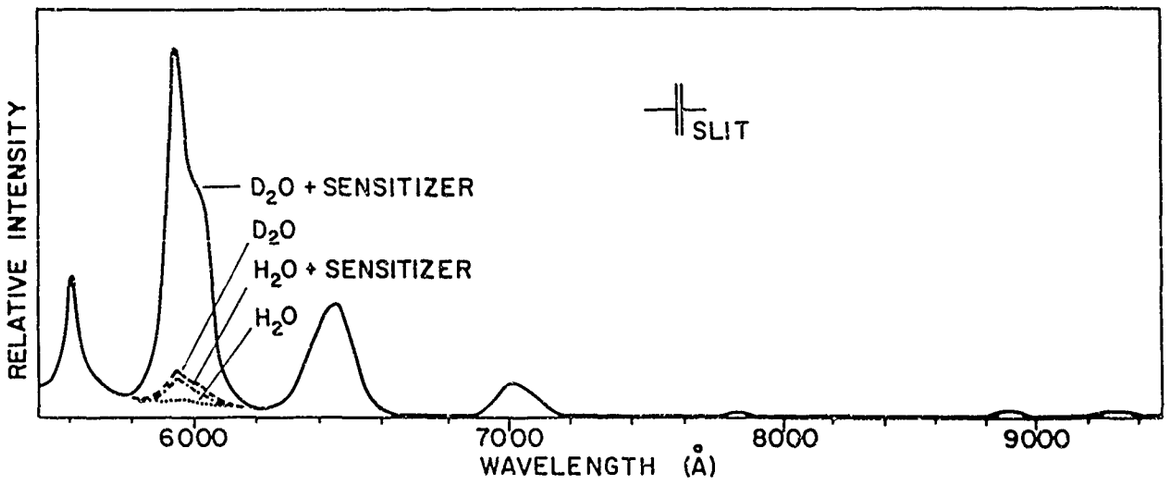

Fig. 2. Emission spectrum of 0.1 M $SmCl_3$ in D_2O sensitized by 0.1 M dipotassium 1,5-dibenzoylnaphthalene disulfonate. The relative intensities of the non-sensitized D_2O, sensitized H_2O and non-sensitized H_2O solutions are indicated for the strongest emission line.

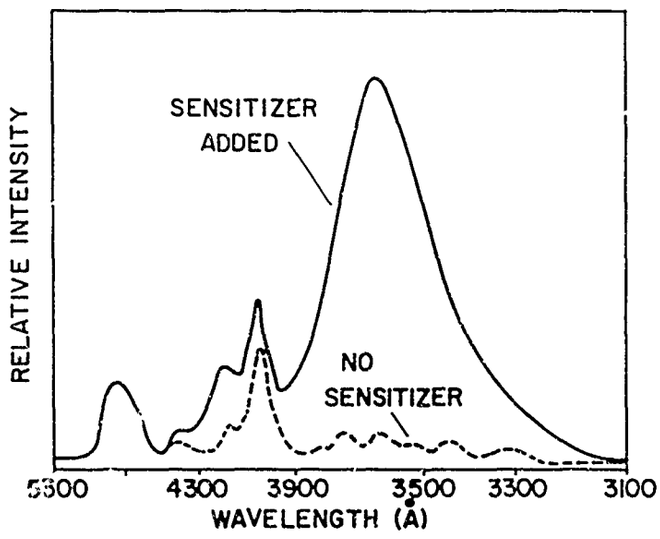

Fig. 3. Excitation spectra for 5947 Å emission of 0.1 M $SmCl_3$ solutions in D_2O. The upper curve shows the excitation spectrum of a solution to which 0.01 M dipotassium 1,5-dibenzoylnaphthalene disulfonate has been added.

least fourteen-fold. The addition of the sensitizer increased the emittance ten-fold, and therefore the lines were intensified one hundred and forty-fold relative to those of the non-sensitized H_2O solution.

The dominant emission occurs at 5947 Å and indicates the presence of at least two lines. Other transitions at 5605, 6455, 7040, 7800, 8870 and 9300 Å have been observed. By analogy with the results on the free ion, these wavelengths correspond to transitions from the $^4G_{5/2}$ state, with the dominant transition terminating in the $^6H_{7/2}$ state.

Figure 3 presents the excitation spectra of sensitized and non-sensitized heavy water solutions of samarium chloride. The excitation lines due to the direct absorption by the ion are observed in both. The sensitized solution has an additional broad pumping band which is attributable to absorption by and energy transfer from the conjugated system of 1,5-dibenzoylnapthalene.

The spectrum of fluorescence of sensitized dysprosium chloride in heavy water is shown in Fig. 4. The limiting lowest enhancement factor

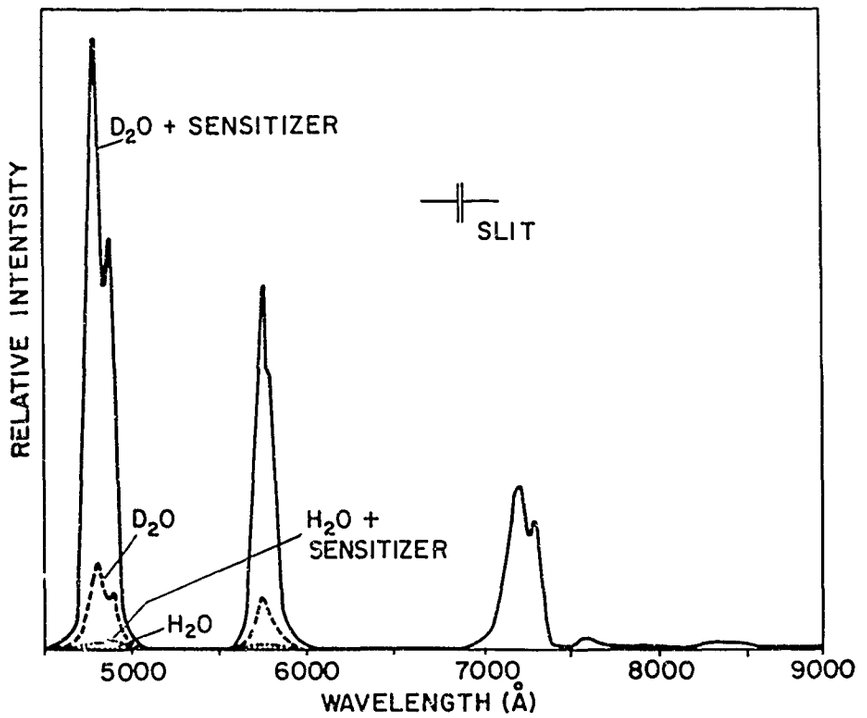

Fig. 4. Emission spectrum of 0.1 M $DyCl_3$ in D_2O sensitized by 0.01 M dipotassium 4,4'-benzophenone-dimethylenesulfonate. The relative intensities for the strongest emission line are indicated for non-sensitized D_2O and sensitized H_2O solutions. The non-sensitized H_2O emission is too close to the baseline to be seen.

due to deuteration is one hundred. Sensitization increases the emittance eight-fold, and therefore results in an overall eight hundred-fold enhancement of the fluorescent radiation relative to that of the unsensitized aqueous solution. The emission wavelengths are 4795, 5735, 7180, 7500 and 8350 Å. The dominant first transition, as well as the third transition, are split into at least two components. These transitions probably orginate in the $^4F_{9/2}$ state and terminate in a series of ^6H states, the dominant transition being $^4F_{9/2} \rightarrow {}^6H_{15/2}$.[8]

Figure 5, which shows the excitation spectra of sensitized and non-sensitized heavy water solutions of dysprosium chloride, resembles Fig. 3. Here again the spectra consist of the dysprosium absorption lines which, in the case of the sensitized solution, are superimposed on the broad pumping band due to the conjugated system of benzophenone.

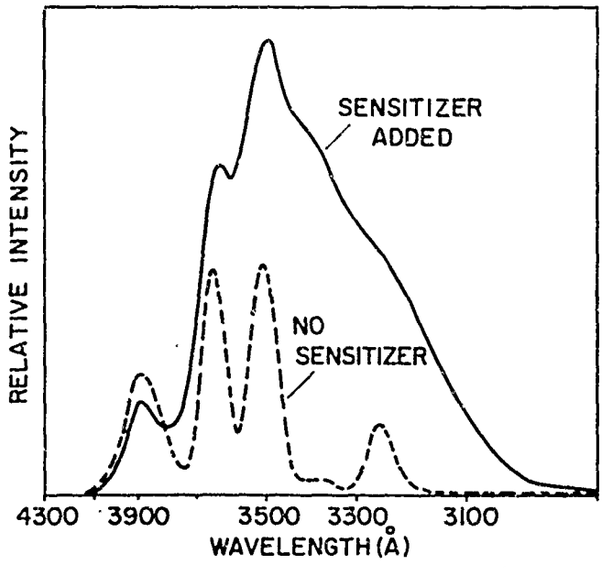

Fig. 5. Excitation spectra for 4795 Å emission of 0.1 M $DyCl_3$ in D_2O. The upper curve shows the excitation spectrum of a solution to which 0.01 M dipotassium 4,4'benzophenone-dimethylenesulfonate has been added.

Discussion

The data presented indicate that the enhancement of the emission by combined deuteration and sensitization may be of two or even three orders of magnitude. The concentration of HDO in a 99.7% D_2O solution is still 0.33 M, exceeding by more than three-fold the rare earth, and more than thirty-fold, the sensitizer concentrations. This relatively high concentration combined with the rapid diffusion of HDO in D_2O suggest that all the present and the previously reported enhancement factors are minimum values. To make them more meaningful, the HDO concentration and the bimolecular quenching constants of the HDO for the rare earth under consideration must be stated. An attempt to measure such a constant is shown in Fig. 6, which describes the quenching of europium perchlorate emission by H_2O. Obviously, the quenching is not proportional to the concentration of H_2O, since small amounts of H_2O cause a strong decline in the fluorescence intensity, and even pure H_2O solutions exhibit some fluorescence. As might be expected and as indicated by the linear dependence of the inverse of the

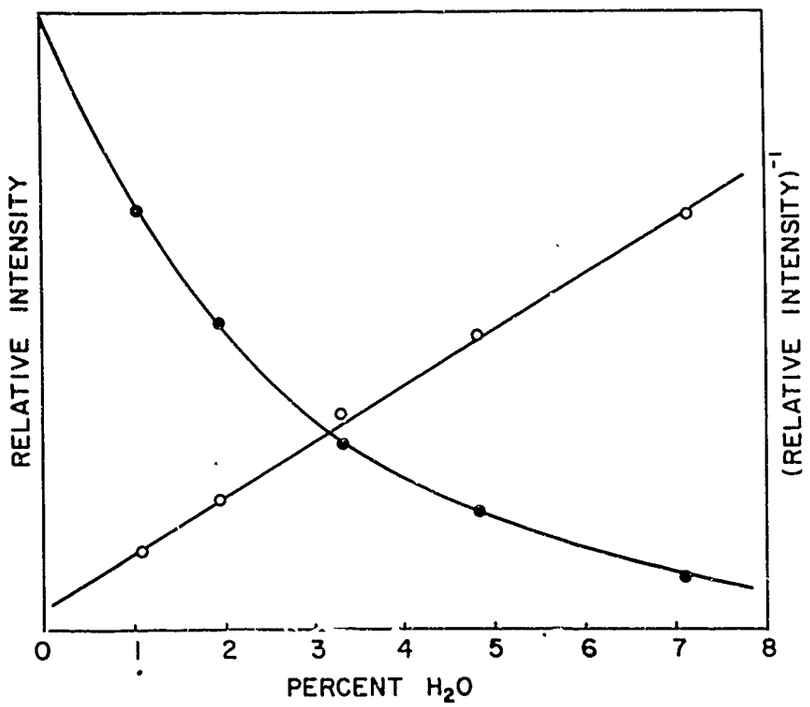

Fig. 6. Variation of the fluorescence intensity of a 0.1 M $Eu(ClO_4)_3$ solution in D_2O with the concentration of the H_2O present. The straight line shows the variation of the inverse of the luminescence with the H_2O concentration.

fluorescence intensity on the H_2O concentration, the Stern Volmer relation is obeyed. The increase in concentration of H_2O required to lower the fluorescence to 50% of its initial value is approximately 2%.

The question may be raised whether the energy transfer between the anionic sensitizer and the rare earth cation is intermolecular or intramolecular. The experimental evidence indicates that the energy transfer is intermolecular: the emission spectra of the rare earths are not changed on sensitization at the sensitizer concentrations employed. Had a new species been formed, a new symmetry would arise, leading to a change in the spectrum. Furthermore, the sensitized emission is quenched by oxygen. Had there been a stable compound between the ion and the energy donor (as occurs in the rare earth-β-diketone chelates), the energy transfer would not be oxygen quenched; this is because the probability of the sensitizer being in the proximity of the rare earth ion would always greatly exceed the probability of its meeting an oxygen

molecule. However, the question on the intermolecular or intramolecular transfer in these aqueous systems depends largely on our definition, as hydrated pairs of rare earth cations and sensitizer anions are undoubtedly present.

Acknowledgment

The author wishes to thank S. Kellner for his assistance, R. Weberling for the analyses, and V. Brophy for assembling the spectroscopic equipment. The helpful comments of A. Lempicki and D. Howell who read the manuscript are appreciated. The author also wishes to express his gratitude to E. Wasserman of the Bell Telephone Laboratories for many stimulating hours of discussion.

References

1. J. G. Bayly, V. B. Kartha and W. H. Stevens, Infrared Physics 3, 211 (1963).
2. J. L. Kropp and M. W. Windsor, J. Chem. Phys. 39, 2769 (1963).
3. J. L. Kropp and M. W. Windsor, J. Chem. Phys. 42, 1599 (1965).
4. J. J. Freeman, G. A. Crosby and K. E. Lawson, J. Molecular Spectroscopy 13, 399 (1964).
5. A. Heller and E. Wasserman, J. Chem. Phys. 42, 949 (1965).
6. W. G. Herkstroeter, A. A. Lamola and G. S. Hammond, J. Am. Chem. Soc. 86, 4537 (1964).
7. G. N. Lewis and M. Kasha, J. Am. Chem. Soc. 66, 2100 (1944).
8. G. H. Dieke and H. M. Crosswhite, Applied Optics 2, 680 (1963).

LOW-TEMPERATURE OPTICAL STUDIES OF RARE-EARTH CYCLOPENTADIENIDES

R. Pappalardo

Cyanamid European Research Institute, Cologny (Geneva)

Switzerland.

ABSTRACT

A systematic study of the optical properties of rare-earth cyclopentadienides was started. These compounds, where the rare-earth ion is bound to a five-membered aromatic ring, are very air sensitive. This required the use of suitable handling techniques in order to take absorption spectra at low temperatures.

Most rare-earth tricyclopentadienides have been studied at 78°K, both as sublimed films and as solutions in 2 Me-THF. The spectrum of $Ndcp_3$ has been studied in detail at liquid helium temperatures.

Many of the undiluted rare-earth cyclopentadienides show fluorescence associated with the aromatic ligand (Gd cp_3; Ce cp_3; La cp_3; Eu cp_2) and broad absorption bands at rather low energies.

A complex chemistry is shown by Ytterbium in its reactions with cyclopentadiene. The composition of sublimed phases is discussed on the basis of their infrared and optical spectra.

* * *

The rare-earth cyclopentadienides [$Ln(C_5H_5)_3$ or $Ln\ cp_3$] and their derivatives are at present the only known metallo-organic compounds of rare-earths.[1,2] In view of this, and of the unusual properties of the cyclopentadienyls of the first transition series, a spectroscopic study of the corresponding rare-earth compounds seemed justified. Here was apparently a class of compounds where

covalency effects or the 4f-electrons might be quite important. Another possibility was that in these compounds the transfer of photon energy from the organic ligand to the 4f-levels might be suitable for energy-conversion processes. For these reasons a study of the optical properties of these systems was begun.

Experimental: Since the compounds in question are air-sensitive, all manipulations were performed under nitrogen or "in vacuo." In the preparation of the samples due attention was given to the purity of reactants and solvents, especially with respect to water impurities. So far we have prepared most of the rare-earth tricyclopentadienides using the procedure introduced by Birmingham and Wilkinson,[1] that is by the metathetical reaction:

$$LnCl_3 + 3\ Na\ cp \xrightarrow{THF} Ln\ cp_3 + 3\ Na\ Cl \qquad (1)$$

Other reactions of this type were carried out in diethyl ether and liquid ammonia.

For most of the products we took spectra with a Cary 14 Spectrophotometer, both at room temperature and at 78°K. The products were either studied as sublimed films or as solutions of such sublimates in tetrahydrofuran or 2-Methyl-tetrahydrofuran. Up to now we have studied at liquid helium temperatures only the spectra[3] of Nd cp_3 in 2-Me-THF. The spectroscopic data in the range of the Cary 14 Spectrophotometer were further supplemented by the IR spectra. For this purpose we used a rather simple device, which incorporated the features of sublimator, IR cell and cryostat. The raw Ln cp_3 were introduced in the device, films were sub-

limed on a sodium chloride plate and the IR spectra taken with a Perkin-Elmer 521. The device was then transferred to the Cary 14 and the samples, always kept in a vacuum, were studied at room temperature and at 78°K. By a suitable modification of the Cary 14 we could also take low-temperature reflection spectra. Some of these reflection spectra compared quite favourably with the diffuse transmission spectra.

Results: We would like to mention now some preliminary results of our survey study of these systems.

a) Bonding effects. First of all, the effect of the bonding to a $C_5H_5^-$ group on the 4f-electronic levels. Already from the solution spectra of Pr cp_3 and Er cp_3 in THF, as reported by Birmingham and Wilkinson[1], for the visible region of the spectrum, one could infer that in the etherates of Ln cp_3 no spectacular alterations of the energetics of the $4f^n$-levels took place. This we confirmed also in the case of sublimed, unsolvated Ln cp_3. As typical examples we could take the cases of Ce cp_3; Ho cp_3 and the unusual strongly coloured Yb cp_3. (Fig 1 to 3).

There are of course shifts in the position of the J-manifolds when one compares these spectra to those of more familiar systems, but they are of the same order of the shifts one observes for instance in a series of halide compounds in going from fluorides to chlorides etc.[4] So the 4f-electrons would seem scarcely affected by the bonding. This is not in contrast with the observed solubility properties and volatility of Ln cp_3 and their derivatives.

The latter do not necessarily imply covalent bonding within the molecule, but simply a weak intramolecular attraction. Ionic bonding is also confirmed by the ease of hydrolitic attack.

b) Fluorescence properties. We observed line fluorescence in undiluted sublimates of Tb cp_3; Sm cp_3 and Dy cp_3 under 3660 A excitation. Eu cp_3 has not been isolated yet. Other undiluted cyclopentadienides show intense band emission. The intense blue fluorescence of Gd cp_3 and a weaker La cp_3 emission have been already reported.[5] Ce cp_3 shows a pronounced red emission (peak at 16900 cm^{-1} at RT; at 18350 cm^{-1} and 15690 cm^{-1} at 78°K). Eu$cp_2 \cdot nNH_3$ shows prior to sublimation an intense yellow emission (peak at 17400 at RT), which becomes red and weaker (16950 cm^{-1} at RT) after removal of the ammonia molecules at the sublimation temperatures of Eu cp_2. Generally we observed for these systems capable of emitting, that the fluorescence of the raw cyclopentadienides was different from those of the sublimed products.

c) Composition of sublimed species. It was stated in the original paper[1] on the preparation of this class of compounds that by sublimation of the reaction products one obtained a non-solvated entity of composition Ln cp_3. This conclusion was essentially based on the determination of the C; H and rare-earth content. Of course, the fact that the compounds we are discussing are very air-sensitive makes it hard to have very accurate analyses. This conclusion on the composition of sublimed species has been recently questioned by Fischer and Fischer[6] on the basis of their IR studies

of rare-earth cyclopentadienides. We had come to a similar conclusion from the interpretation both of our IR data and of those pertaining to the $4f^n$ transitions. As an example we shall mention what situation is met with in the case of Yb tricyclopentadienides, systems we have studied extensively[7]. Inspection of the $^2F_{7/2} \rightarrow {}^2F_{5/2}$ transition of Yb cp_3 in sublimed materials shows three different types of spectra. They have been finally unravelled as belonging to a Yb cp_3. THF species, to a Yb cp_3. NH_3 species and to pure Yb cp_3 (Fig.3 to 5). A surprising conclusion we derived from our data is the following. The final composition of the sublimed species depended on the method used to obtain the rare-earth chloride, required for reaction (1). Two different methods are commonly used to obtain the anhydrous chloride:either treatment of the oxide with NH_4Cl at 300°C and removal of NH_4Cl by sublimation; or dehydration of the rare-earth chloride by thionyl chloride. When one reacted a chloride obtained by the first method, one obtained by sublimation of the raw cyclopentadienide an ammonia adduct. Of this we have conclusive evidence for the case of Er cp_3 and Yb cp_3. We did not look into it closely, but there are indications that this might be true for Nd cp_3 too. Incidentally, the ammonium chloride method was used by Birmingham and Wilkinson in their work[1].

d) <u>Divalent cyclopentadienides:</u> Fischer and Fischer[8] made use of the solubility of Eu metal in liquid ammonia, in order to prepare Eu cp_2 by direct reaction with cyclopentadiene. We applied this

method to the other rare-earth metal soluble in liquid ammonia, that is Yb. Apart from an ammoniate Yb $cp_3 \cdot nNH_3$, which sublimes at $\sim 120°C/10^{-3}$ mm Hg, two more species of high sublimation temperatures were obtained. It is not quite conclusive that the latter are pure Yb cp_2. We found in effect that the sublimates still exhibited the Yb^{3+} lines at $\sim 1\,\mu$. Another method for obtaining Yb cp_2 will be reported soon.(7) It is based on the treatment of Yb cp_2Cl or Yb cp_3 with Na; K or even Yb metal in THF. We have not checked yet whether this method can be extended to other trivalent lanthanides, not soluble in liquid ammonia. It is an interesting possibility for Sm and Tm and would allow to see how the $4f \rightarrow 5d$ transitions are affected by the presence of cyclopentadienyls.

e) Absorption bands in rare-earth cyclopentadienides. Broad absorption bands appear in the spectra of Ln cp_3 at unusually low-energy. Typical are the cases of Ce cp_3; Gd cp_3 and La cp_3 with bands located at 23600 and 26400 cm^{-1}; 25770 cm^{-1}; 28990 cm^{-1} respectively. This meant for instance that the absorption lines of Gd^{3+} in its tricyclopentadienide could not be observed, since they are masked by a broad absorption band.(5) A most striking example of the presence of low-energy absorption bands is that of Yb cp_3 which is dark green because of two absorption bands at 15400 cm^{-1} and 25700 cm^{-1}. An effect related to these absorption bands of Ln cp_3 is that under 3660 Å excitation band emission is observed whenever there are no $4f^n$ levels to which photon energy might be

transferred.

Three possible mechanisms could be operating. The absorption bands could either be due to 4f → 5d transitions, or to $\pi \rightarrow \pi^*$ transitions within the five-membered ring, or finally to charge transfer from the ligand to the central lanthanide. Both the molar extinction coefficient of the bands in question(observed value for Yb cp_3: $\varepsilon \sim 700$; $\varepsilon \sim 55$)and the presence of band emission for Gd^{3+}, Ce^{3+} and Eu^{2+} are more in line with the second alternative. The emission would then correspond to transitions from a triplet level of the ligand to the singlet ground state.

(1)J.M.Birmingham and G.Wilkinson, J.Am.Chem.Soc.78,42(1956).

(2)R.E.Maginn,S.Manastyrskyj and M.Dubec,J.Am.Chem.Soc.,85,672 (1963).

(3)R.Pappalardo,Helv.Phys.Acta 38,178(1965).

(4)C.K.Jørgensen, Orbitals in Atoms and Molecules,Academic Press 1962,page 146-57.

(5)R.Pappalardo and S.Losi, J.Inorg.Nucl.Chem.27, 733(1965).

(6)E.O.Fischer and H.Fischer,J.Organomet.Chem.3,181(1965).

(7)F.Calderazzo, R.Pappalardo and S.Losi, to be published.

(8)E.O.Fischer and H.Fischer, Angew.Chem.76,52(1964).

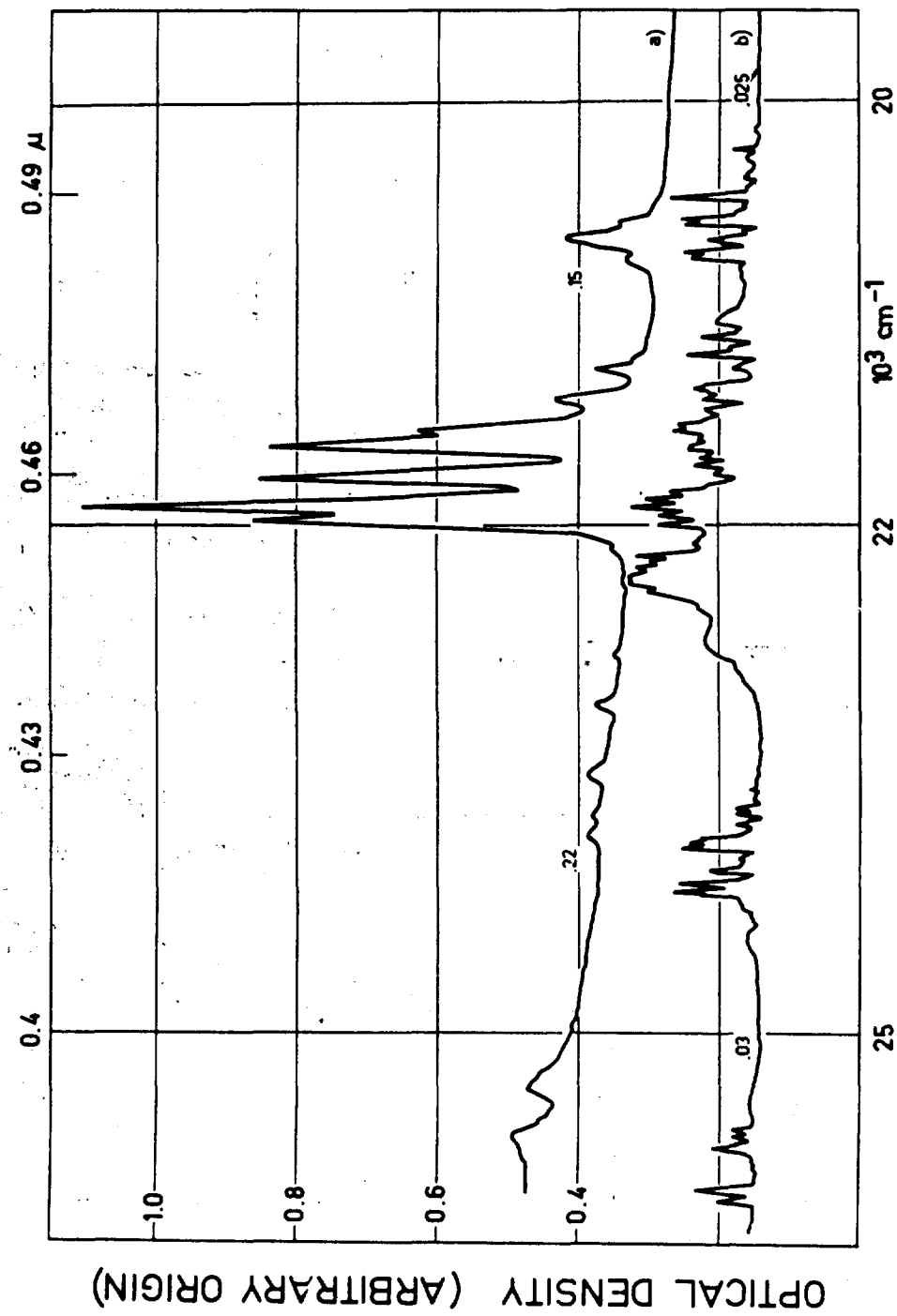

Fig.1.(Top).Diffuse transmission at 78°K. of sublimed Ho cp_3.
(Bottom).For comparison,reflection spectrum of Ho_2O_3 at 78°K.

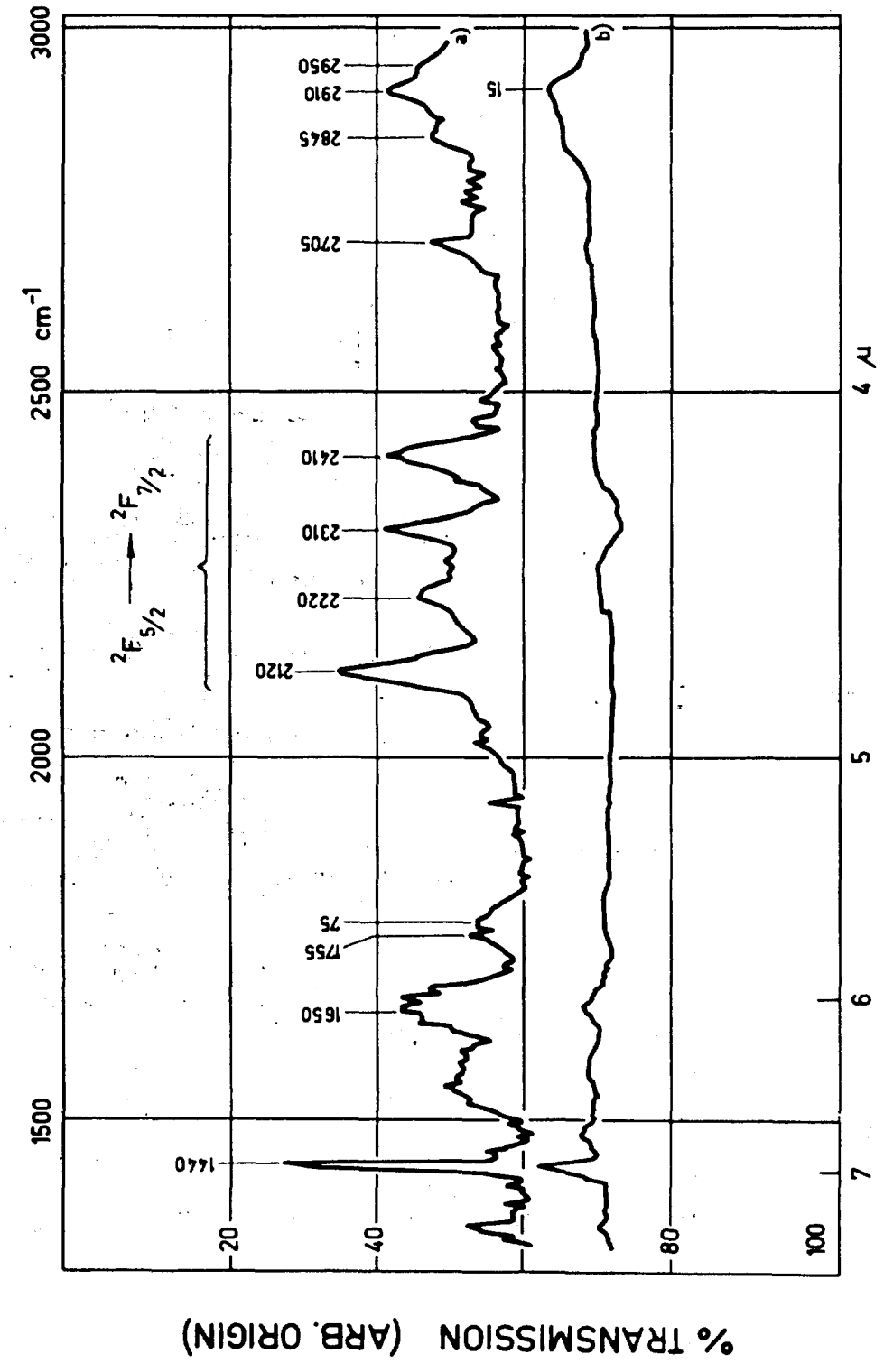

Fig.2.(Top).Sublimed Ce cp_3 at room temperature.
(Bottom) For comparison, Yb cp_3 at room temperature.(Sublimed material).

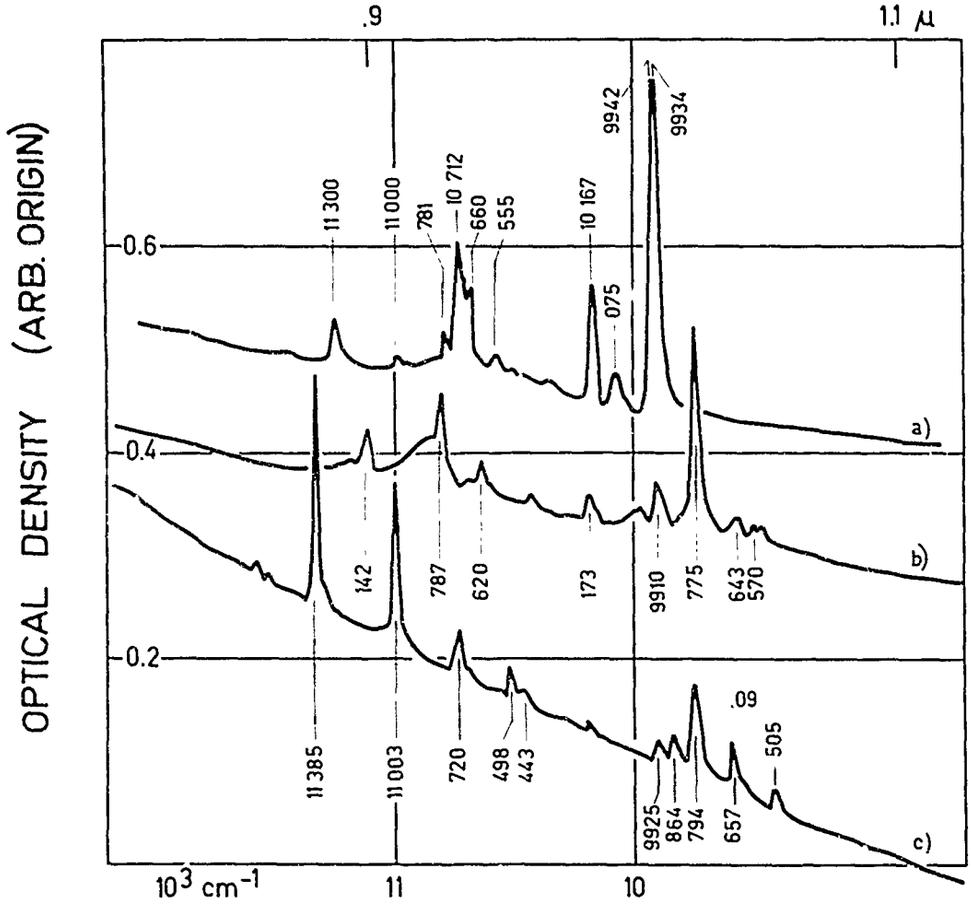

Fig.3. a)Diffuse transmission at 78°K of sublimed Yb $cp_3 \cdot NH_3$. b)Same, sublimed Yb $cp_3 \cdot THF$.
c) Same, Yb cp_3.

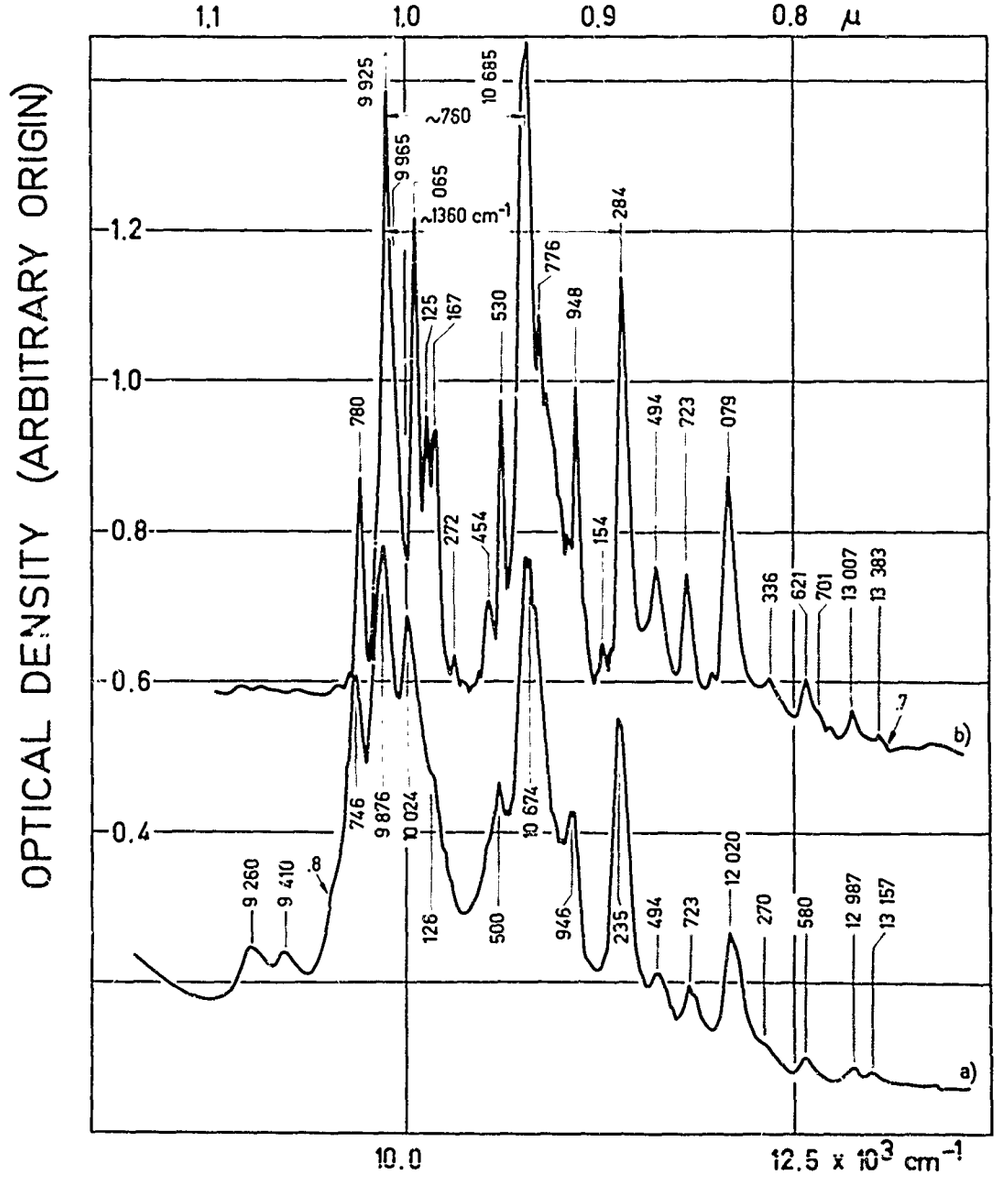

Fig.4. Reflection spectra of sublimed, green Yb $cp_3 \cdot nNH_3$.
a) At room temperature. b) At 78°K. On the low-frequency side two lines at 9,260 and 9,410 cm^{-1} disappear on cooling. Possible vibrational frequencies of 760 cm^{-1} and 1360 cm^{-1} are also indicated.

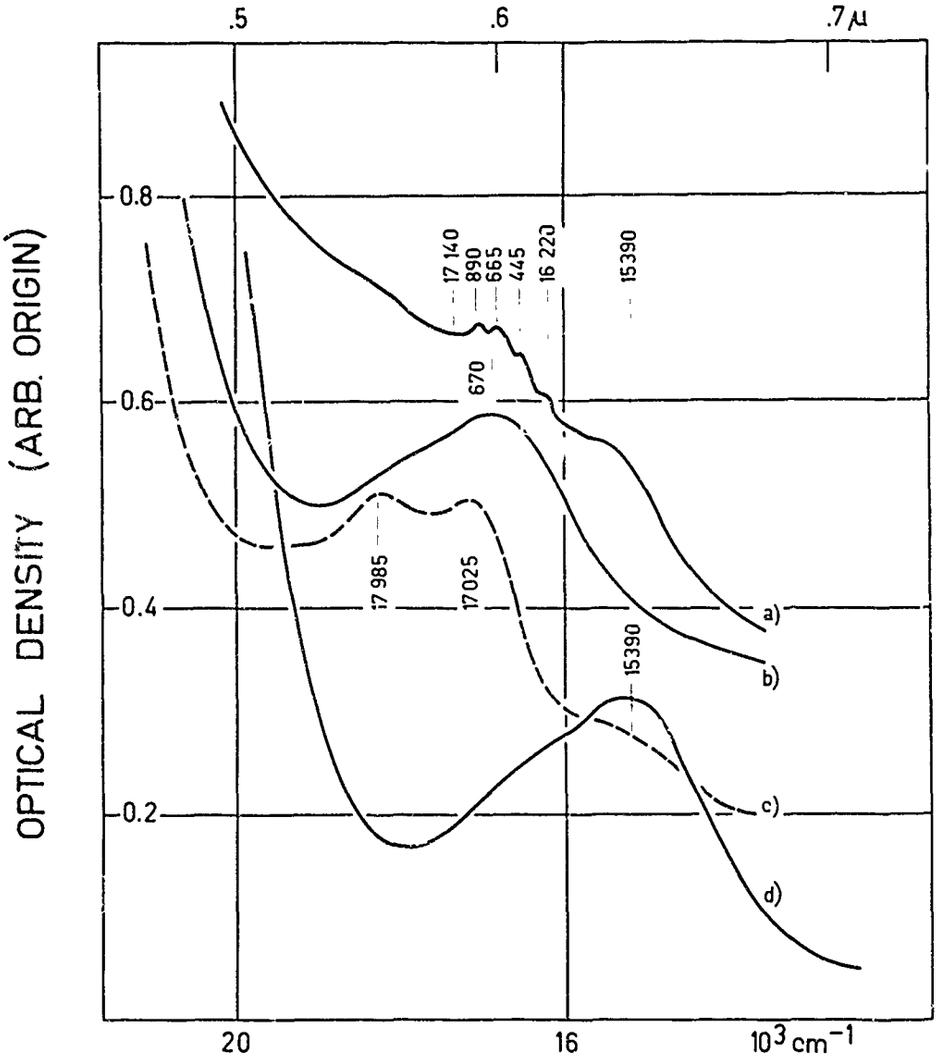

Fig.5. Detail of the absorption in the red region of the spectrum for various Yb^{3+} tricyclopentadienides. a) Sublimed Yb cp_3 at 78°K. b) Sublimed Yb $cp_3 \cdot nNH_3$ at room temperature. c) Same, at 78°K. d) Yb $cp_3 \cdot THF$ in THF solution, room temp.

SPECTROSCOPIC STUDY OF CERIUM IN YTTRIUM GALLIUM AND YTTRIUM IRON GARNET

K. A. Wickersheim

Research Laboratories
Lockheed Missiles & Space Company
Palo Alto, California

and

R. A. Buchanan

Infrared Division, Research Department
U. S. Naval Ordnance Laboratory
Corona, California

ABSTRACT

A fundamental problem in magnetism is the origin and description of the exchange interaction between magnetic ions. The development of an exchange field formalism, applicable to the rare earth ions in the rare earth iron garnets, is reviewed. It is shown that further progress depends upon a more complete solution of the crystal field problem and on the acquisition of more experimental exchange splittings for specific rare earth ions. The advantages of using cerium as a "probe" to provide the necessary information are discussed. Cerium and ytterbium are compared, and spectroscopic results for cerium substituted into both yttrium gallium and yttrium iron garnet are presented. Especially noteworthy are (a) the large size of the crystal field splittings (of the order of 1500 cm^{-1} for the J = 7/2 state), (b) the large size of the exchange splittings of the Kramer's doublets (of the order of 200 cm^{-1}) and (c) the general sharpness of the cerium spectra.

Introduction

While the work we plan to discuss in this paper is of recent vintage, it represents a continuation of a program which has been in progress for a number of years. The program had its origins in the calculations of White and Andelin[1] who first attempted to treat simultaneously the effects of the electrostatic (crystal) field and the exchange field on the energy levels of the rare earth ions in the rare earth iron garnets. The simplifying assumptions made by these workers, both with regard to the cubic symmetry of the crystal field and the isotropy of the exchange interaction, have not been borne out in subsequent work. However, the general predictions of large level shifts and splittings showing a strong dependence upon the orientation of the net magnetization have been fully confirmed.

The program was given life and definition with the advent of explicit experimental data on actual exchange field effects. The most complete information was obtained from near infrared[2,3] and far infrared[4] spectroscopic investigations of ytterbium iron garnet.[5] The spectroscopic studies demonstrated that the exchange splittings of a Kramer's ion can be observed directly, the splittings being surprisingly anisotropic with regard to exchange field orientation (See Figure 1). It was found that the g-tensors obtained for ytterbium in yttrium gallium garnet[6] apply, at least in the first approximation, to the iron garnet as well, and that a large part of the anisotropy in the splittings must therefore come from anisotropy in the exchange interaction itself. (We note that Wolf[7] had correctly anticipated that such

anisotropy might exist.)

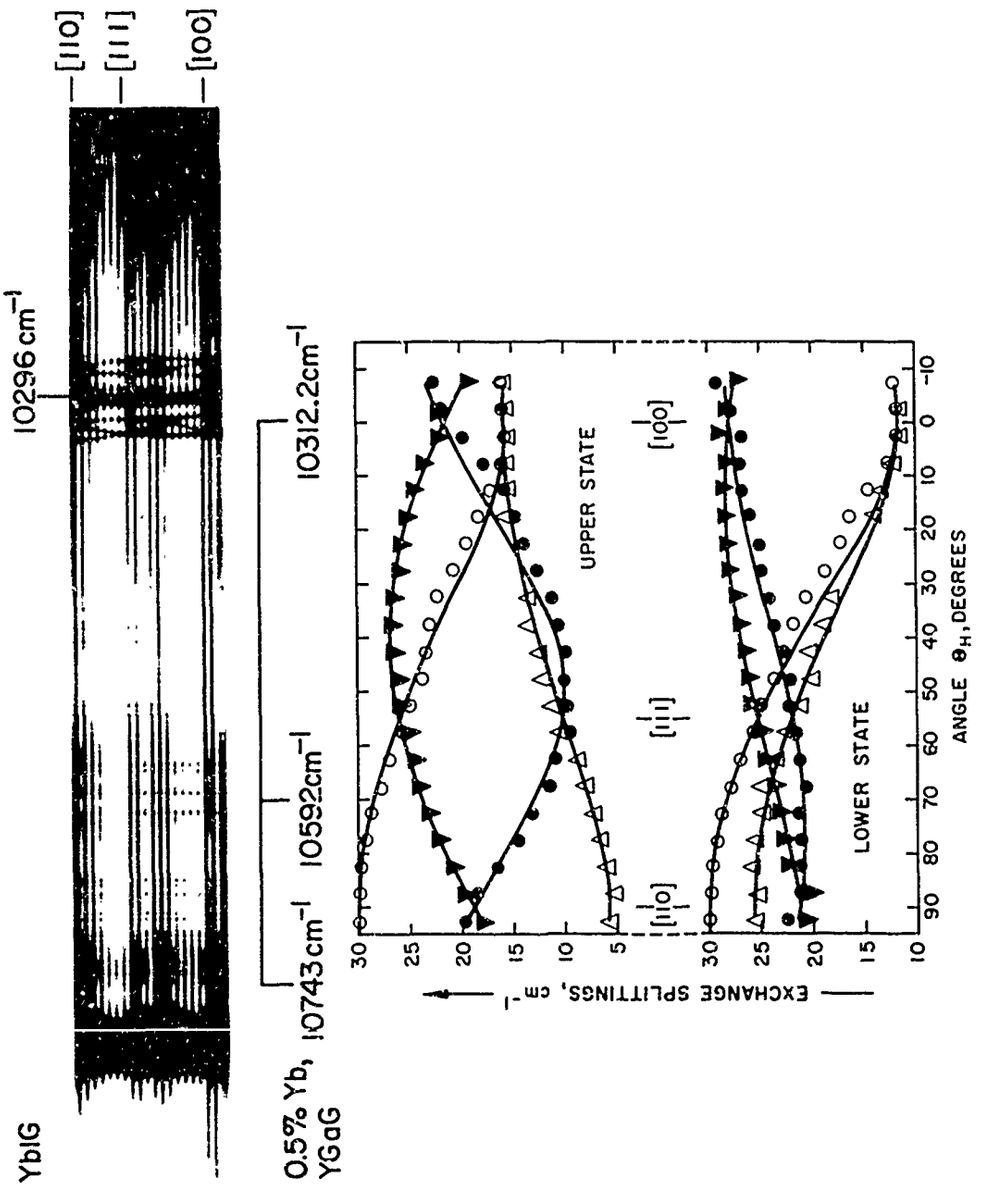

Figure 1. Liquid nitrogen temperature spectrum of ytterbium iron garnet as a function of exchange field orientation. The splittings of the terminal states, derived from the sharp-line pattern near 10,300 cm^{-1}, are shown below.

A rudimentary exchange potential formalism was developed on the basis of the optical information.[3] This potential was obtained via a harmonic series expansion consistent with the site symmetry of the rare earth ion with only the two leading (anisotropic) terms being retained. The net result was an exchange potential exhibiting orbital dependence. This formalism was made to predict correctly, with three adjustable parameters, the exchange splittings for both the ground state and an excited state of the ytterbium ion in the iron garnet. The numerical agreement of the fit may well have been fortuitous, but the prediction of correct topology, especially for the excited state, suggested strongly the merit of the exchange potential approach.

Levy[8] has recently proposed a much more complete formalism in which the rare earth-iron exchange interaction is characterized by as many as 10 exchange potential parameters. With a specific model of the rare earth-iron exchange interaction, these parameters could in principle be derived. However, no such model exists. In the absence of a detailed model, the parameters must be determined empirically. At the present time an empirical determination of so many parameters is equally impossible since there is neither a sufficiently complete solution to the crystal field problem to allow the calculation of a reliable set of starting wave functions, nor are there enough independent pieces of data on the exchange splittings for any rare earth in the iron garnets. It is to the experimental aspects of this dual problem that we now address ourselves.

We have chosen to build on the ytterbium results, while at the same time increasing our understanding of the rare earth series as a

whole, by undertaking a careful study of the spectra of trivalent cerium in yttrium gallium and yttrium iron garnet. Cerium and ytterbium, though near the opposite ends of the rare earth series, have intimately-related energy level schemes. (See Figure 2). The ions

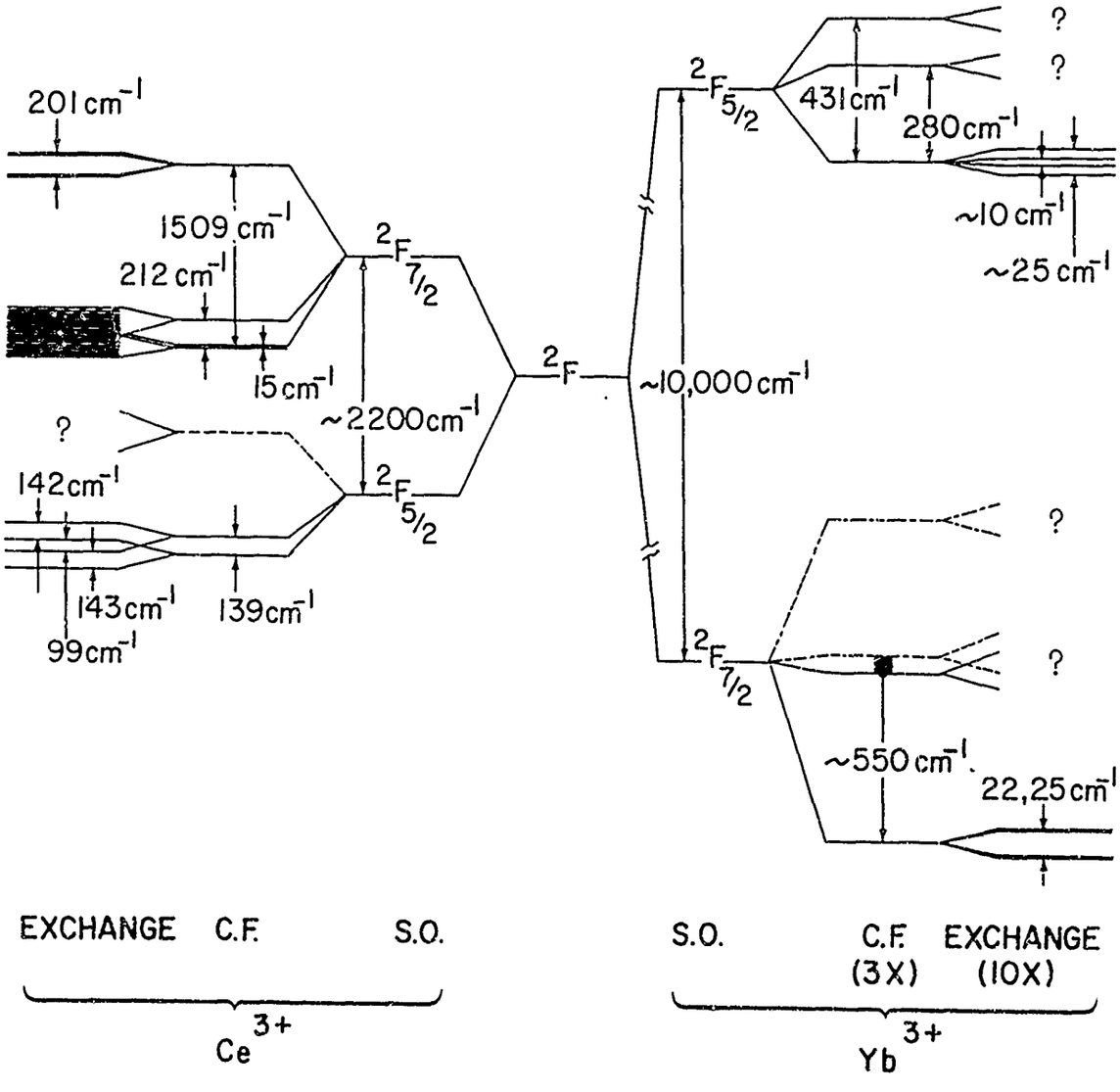

Figure 2. Energy level schemes for cerium and ytterbium in the garnets, showing spin-orbit, crystal field and exchange field effects, the latter obtained with no applied magnetic field.

differ, however, in the magnitude of the spin-orbit interaction, the relative positions of the J=5/2 and J=7/2 manifolds and the relative sequence of crystal-field-split levels within the two J-manifolds. Other dissimilarities resulting from differences in ion size relative to site dimensions, from differences in shielding of the 4f levels, and from differences in the relative magnitudes of the spin-orbit and crystal field effects for the two ions are also to be anticipated. The purpose of this paper is to describe how, despite these differences, the study of cerium seems likely to further our approach to a satisfactory picture of exchange in the garnets.

Experimental Proceudres

Crystals of yttrium gallium garnet and yttrium iron garnet, doped with cerium, were grown from lead oxide-lead fluoride fluxes. While the intended doping level (i.e. the ratio of cerium to yttrium in the melts) was 5 mole-percent, the level of incorporation is almost certainly lower because of the large size of the Ce^{3+} ion. It would appear from absorption spectra that more cerium enters the iron garnet than the gallium garnet.

The cerium spectra were obtained with a Cary Model 14B spectrophotometer, the samples being cooled by conduction in a metal dewar of conventional design.

For studies (in the iron garnet) of the cerium spectrum as a function of exchange field orientation, a special liquid nitrogen dewar was constructed, this dewar having a tip small enough to fit between

the pole pieces of a 4000 oersted magnet. The entire assembly was constructed in such a way as to fit into the normal sample chamber of the Cary spectrophotometer. The sample was physically rotated in increments of 10° with spectra being taken at each angular position.

The spectra of ytterbium iron garnet (Figure 1) which we present for comparison are from prior work,[2] these having been obtained photographically with a Bausch and Lomb dual-grating spectrograph.

Results and Discussion

The full orthorhombic crystal field experienced by the rare earths in the garnet structure requires 9 parameters for its specification. Past workers have used various approximations to reduce the number of parameters.[9] If we take the spin-orbit splitting into account, 10 independent pieces of data are required for a proper empirical determination of all parameters. Since Ce^{3+} and Yb^{3+} each have only 7 4f-electron energy levels, and thus 6 energy separations, we must turn to the anisotropic g-tensors (3 principal values each) for sufficient input data. Computational programs, designed to utilize such a combination of experimental information, are being prepared.

Unfortunately, for ytterbium only two levels are sufficiently sharp to allow the g-tensors to be determined.[6] Five energy levels (four separations) have been observed with certainty for ytterbium, but some dispute remains as to the relative distribution of levels in the ground state manifold.[10] Even with the proper identification of levels, we have the bare minimum of data for the crystal field

calculation.

For cerium, on the other hand, six energy levels have been located and four of these are sufficiently sharp for Zeeman effect analysis. Thus for this ion we expect a redundancy of information for the solution of the crystal field problem. In the liquid helium spectrum of cerium in the gallium garnet (Figure 3) we observe four transitions (at 2161, 2176, 2373 and 3670 cm^{-1}) from the ground state to the four levels of the J=7/2 manifold. A second level of the J=5/2 manifold, 131 cm^{-1} above the ground state, is revealed by the temperature-dependent band observed at liquid nitrogen temperatures near 3539 cm^{-1}.

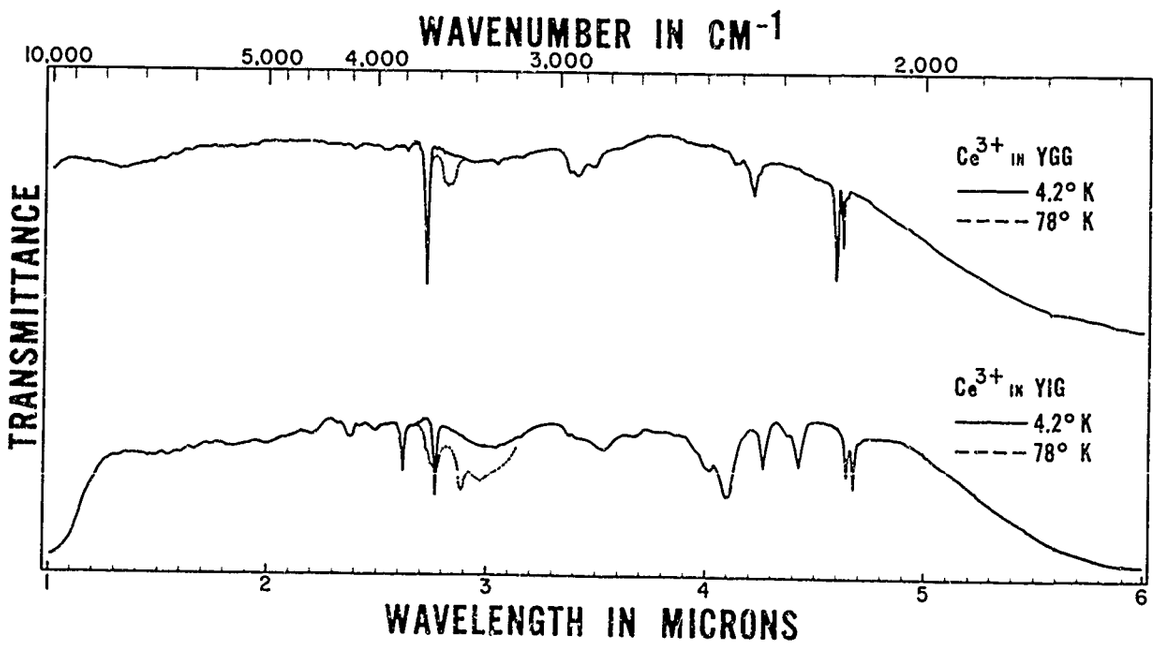

Figure 3. Low temperature spectra of cerium in yttrium gallium and yttrium iron garnet. Sample thicknesses are 8.3 and 1.5 mm respectively. Absorptions in the region from 3.0 to 3.8 microns are also present in crystals containing no cerium.

The more interesting features of the spectra are (a) the close proximity of the three lowest levels of the J=7/2 state, (b) the remarkably large crystal field splitting of that state - perhaps the largest yet observed for a rare earth ion, and (c) the sharpness of not only the two longer wavelength lines, but of the shortest wavelength line as well. The last feature we attribute to the unusual size of the crystal field splittings, the uppermost level here falling well above the region of expected vibronic (vibrational plus electronic) levels associated with the lower energy states of the J=7/2 manifold. Thus the expected broadening resulting from resonance with the vibronic levels is not observed for this particular electronic state. This is most fortunate, for it is this uppermost state of cerium which corresponds to the ground state of ytterbium and thus forms our strongest link with prior results.

The increased amount of data available for Ce^{3+} as opposed to Yb^{3+} is also apparent in the iron garnet spectra (see Figure 3). The exchange splittings of the cerium levels can be discerned if one compares the gallium garnet and iron garnet spectra. Note for example the obvious splitting of the 2.7 micron line at $4.2^{o}K$. The size of these splittings - of the order of 200 cm^{-1} compared with 10 to 30 cm^{-1} for ytterbium iron garnet - is another of the surprising results of this study. We expect to be able to analyze the splittings for perhaps as many as 5 states of cerium, in the process obtaining more than the 10 pieces of input data required to test Levy's exchange potential formalism.

We have carried out a preliminary analysis of the splitting of the uppermost state. While the splitting of this state is far larger than that found for the ground state of ytterbium, the relative anisotropy of the splittings (principal values for the splitting tensor ranging from 165 to 225 cm^{-1}) is markedly less. Despite these differences, the topological similarity of the splittings for the corresponding states of the two ions is apparent.

The exchange splittings of the low-lying levels of cerium, as presently interpreted, also show some unusual features. The splittings of the two lowest levels are sufficiently large to exceed the crystal field separation observed in the gallium garnet. Thus we will apparently have to treat these as components of a 4-level system rather than as two exchange-split Kramer's doublets.

The next step in this program will be to obtain the g-tensors for as many of the cerium states (in the gallium garnet) as possible - this being done in part via spin resonance and in part via optical (Zeeman effect) techniques. When the maximum available data have been obtained, crystal field calculations will be carried out.

The analysis of the iron garnet exchange splittings must also be completed. The applicability of the gallium garnet g-tensors should be checked via high field experiments. We then expect to be able to combine the wave functions obtained from the gallium garnet crystal field calculation with the analysis of the exchange splitting tensors obtained from the iron garnet and obtain empirically the full set of exchange constants required by Levy's formalism.

Acknowledgements

We gratefully acknowledge the assistance of Dr. R. A. Lefever, who grew the crystals used in this study, of Professor R. L. White, who has provided continuing stimulation and advice from the inception of this work, and of Dr. G. F. Herrmann, who, with Dr. J. J. Pearson, is pursuing the theoretical aspects of the problem.

References

1. R. L. White and J. P. Andelin, Jr., Phys. Rev. 115, 1435 (1959).
2. K. A. Wickersheim and R. L. White, Phys. Rev. Letters 4, 123 (1960); K. A. Wickersheim, Phys. Rev. 122, 1376 (1961).
3. K. A. Wickersheim and R. L. White, Phys. Rev. Letters 8, 483 (1962).
4. A. J. Sievers, III and M. Tinkham, Phys. Rev. 124, 321 (1961).
5. These and related investigations are summarized in Volume 1, Chapter 7 of "Magnetism," Academic Press, New York (1963).
6. The ground state values were obtained (independently) by D. Boakes, G. Garton, D. Ryan and W. P. Wolf, Proc. Phys. Soc. (London) 74, 663 (1959) and J. W. Carson and R.L. White, J. Appl. Phys. 31, 535 (1960), both groups of workers using spin resonance techniques. The g-values for the excited state were determined by H. M. Crosswhite of Johns Hopkins University (private communication) via optical Zeeman effect studies.
7. W. P. Wolf, Proc. Phys. Soc. (London) 74, 665 (1959).

8. P. M. Levy, Phys. Rev. 135, A 155 (1964).

9. See for example, the following:

R. Pappalardo and D. L. Wood, J. Chem. Phys. 33, 1734 (1960);

J. F. Dillon and L. R. Walker, Phys. Rev. 124, 1401 (1961);

J. J. Ayant and J. Thomas, J. Phys. Soc. Japan Suppl. B-1, 448 (1963); M. T. Hutchings and W. P. Wolf, J. Chem. Phys. 41, 617 (1964); J. A. Koningstein and J. E. Geusic, Phys. Rev. 136A, 711, 717 and 726, (1964).

10. In this regard, contrast the Yb^{3+} level spacings suggested by D. L. Wood, J. Chem. Phys. 39, 1671 (1963) with the earlier and still widely-accepted arrangement shown in Figure 2 of this paper.

SOME NEW ELECTRON-TRANSFER SPECTRA OF TRIVALENT LANTHANIDES

John C. Barnes and Hugh Pincott

Chemistry Department, Queen's College, Dundee, Scotland

ABSTRACT

Electron transfer spectra are presented for the compounds $LnPO_4$, $Ln_2(CO_3)_3$, $Ln_2(oxalate)_3\ 10\ H_2O$ and several compounds containing sulphate or halide ion. Ln = Sm, Eu and Yb. The consequence of change in coordination number and structure are discussed. Oxyanion have very similar optical electronegativities, which do not correlate with their oxidation potentials.

A change of ligand or co-ordination number produces only small changes in the 4f→4f transitions of the trivalent lanthanides. By looking far enough into the ultra-violet, and selecting the metals which have accessible divalent states, we can sometimes find other transitions which are broader, of higher extinction coefficient, and much more dependent on ligand. Jørgensen[1] has shown that these transitions can be assigned to electron transfer from an orbital located mainly on the ligands to one which is essentially metal 4f in origin. These spectra can be interpreted by the same arguments that Jørgensen has used with electron transfer in transition metal complexes.[2]

If we are to see these bands, which have $\epsilon \sim 100$, the ligand must be transparent well into the ultra-violet or else must have a low optical electronegativity such as diethyldithiocarbamate.[1, 3] The donor group must also be adjacent to the metal ion; the introduction of a solvent sheath as in the well-known $Ln(H_2O)_9^{3+}$ unit has the two-fold effect of moving the band to higher energy, normally into the vacuum ultra-violet, and also reducing the orbital overlap so much that the band intensity would be close to zero.

With a given ligand the band is seen at lowest energy with europium, then followed by ytterbium, samarium and thulium (Figure 1), the band energy increasing linearly with $M^{3+} \rightarrow M^{2+}$ redox potential. [4] As far as the metal is concerned the process is reduction, except that the M^{2+} complex produced is in an excited state which loses energy by returning to the ground state of the M^{3+} complex rather than stabilisation of the lower oxidation state.

So far the electron transfer spectra published for the lanthanides refer almost exclusively to complexes in solution. [1, 3] In this paper we shall deal with some solid complexes and compare these where possible with the solution data. We shall confine our remarks to the first electron transfer band although often more than the one can be observed.

EXPERIMENTAL TECHNIQUES AND RESULTS

Powder reflection spectra were measured on a Hilger Uvispek, which was shown to give useful data to 53 kK. The reference was alumina. Solution spectra came from a Unicam S. P. 700 spectrophotometer.

The compounds discussed are $LnPO_4$. $Ln_2(CO_3)_2$, $Ln_2(oxalate)_3$ $10H_2O$, $Ln(NO_3)_3 \cdot 10H_2O$ and series of compounds containing sulphate or halide ions in various environments. These were all prepared and analysed by conventional techniques. In each case Ln signifies La, Eu, Sm, and Yb. Lanthanum shows no electron transfer bands, and is used as a check against false assignment of ligand bands to electron transfer.

The oxalates and nitrates have strong ligand transitions in the ultra-violet and no electron transfer bands could be seen, with the possible exception of $Eu(NO_3)_3 \cdot 6H_2O$. Since oxalates are powerful reducing agents, this emphasises that the ability of a polyatomic ligand to donate an electron in the excited state of a complex is not the same process as is measured by a solution redox potential. [3]

All the other compounds gave spectra which we assign to electron transfer. Justification of these assignments is obtained by plotting the band energies for the range of ligands with one metal against those for the same ligands with a second metal. If the bands are due to electron

transfer the difference in band energy between two metals with the same ligand environments ($\Delta\sigma$) should be independent of the ligand. Figure 2 shows that the correlation for Sm and Eu is very good, the average deviation from the chosen line of unit slope is a 6.5 kK, and the greatest deviation 2.2 kK even when solution data is included with the solids (average $\Delta\sigma_{Eu\text{-}Sm} \equiv \Delta\sigma_1$ = 8.5 kK.). Thus we can be certain that all our data do refer to electron transfer bands, and we have a firm basis for further discussion.

The data for Yb are also plotted against Eu in Figure 1. This time the deviations are more marked, an average point is 1.44 kK from the line of unit slope, and the maximum deviation is 5.0 kK. The very large deviations are for solid compounds and their effect is always to increase $\Delta\sigma_{Eu\text{-}Yb} \equiv \Delta\sigma_2$ from the average value of 5.0 kK.

DISCUSSION

Correlation between metals

In the most naive terms the worsening of the correlation of band energies of Yb against Eu compared with Sm against Eu can be stated as "Sm and Eu are neighbours in the series, Yb is many elements away." The blame cannot be placed directly on the size difference between the ions since this is essentially independent of environment and must figure in $\Delta\sigma$ for all complexes, in solution or in the solid phase. However, one of the consequences of the lanthanide contraction is that the crystal structure of a compound often changes somewhere between La and Lu. This will lead to a change in coordination and probably a fall in coordination number in the latter part of the series. One example of this is the series of hydrated sulphates. Lanthanum gives $La_2(SO_4)_3 \cdot 9H_2O$, but along the series $8H_2O$ is the rule.[5] In the lanthanum compound some of the La^{3+} ions are 12 coordinate but the heavier elements have 9 as the maximum coordination number.

Reducing the number of donor ligands is known to produce a blue shift in the first electron transfer band. For example[6] the first band in $CuBr_4^{2-}$ is at 16.9 kK whereas in $Cu(H_2O)_5Br^+$ no intense transition is seen until 35.4 kK.

The compounds $LnCl_3 \cdot 6H_2O$ and $Ln_2(SO_4)_3 8H_2O$ are reported[5,7] to have the same crystal structure for Ln = Sm, Eu and Yb, and the values of $\Delta\sigma_2$ obtained are; 4.5 kK and 5.5 kK, very close to the average value 5.0 kK. The compounds $YbCl_3$ and YbOCl, however, are known to differ in structure from their Sm and Eu analogues although the inner coordination spheres do not seem to be established for either of the Yb compounds. These are two cases where $\Delta\sigma_2$ is much larger than the average value, 9.0 kK for $YbCl_3$, and 8.9 kK for YbOCl. We suggest that the coordination numbers will prove to be smaller in the Yb compounds than the established value of 9 for the Sm and Eu analogues.

Support for this argument is obtained by doping Sm, Eu and Yb (5%) into LaOCl. The bands all shift (Table 2) but $\Delta\sigma_2$ is now 3.8 kK, a slightly less than average value, while $\Delta\sigma_1$ remains constant within 0.6 kK. A similar experiment doping into $LaCl_3$ is less conclusive; $\Delta\sigma_2$ became 4.3 kK, but a reasonable value for $\Delta\sigma_1$ can only be obtained by using the position of the second intense transition in $La_{0.95}Sm_{0.05}Cl_3$.

Correlation between ligands

Oxyanions

Phosphate, hypophosphite, carbonate, sulphate and selenate are all rather similar ligands in that an approaching metal ion finds only the backsides of covalently bonded oxygen atoms with which to interact. The energies of the oxygen lone-pairs which function as donor orbitals cannot differ very greatly in these ions and this is supported by the similar electron transfer band energies (Table 1).

The oxidation potentials of these ligands vary widely and hence cannot be of great importance in determining the electron transfer band position; one might predict that the anhydrous perchlorates would show bands at about the same energies. As further support for this we can

quote a band at 40.8 kK in $Eu(NO_3)_3 \cdot 6H_2O$, and one at 41.5 kK in europium oxynitrite (prepared as described by Sherwood).[8] These are thought to be electron transfer bands since they are not found in the La compound. At the appropriate energies for the samarium and ytterbium compounds the ligands are absorbing too strongly for the weak electron transfer bands to be seen.

Table 1 shows that the three solid sulphate compounds of each metal have their bands at very similar energies. This suggests that the inner coordination sphere cannot change very greatly from the hydrate to the anhydrous salt or the sodium-lanthanide double sulphate. Detailed x-ray structures are not available for any of these compounds at present; but in $La_2(SO_4)_3 \cdot 9H_2O$ sulphate appears in the inner coordination sphere.[9] The solution spectra for $LnSO_4^+$ show bands at similar energies, supporting the belief that the solution species contain a sulphate group in the inner coordination sphere. More evidence for this comes from studies of the ethyl sulphates. In $Eu(SO_4Et)_3 \cdot 9H_2O$ no electron transfer band is seen below 50 kK; the crystal is known to contain only water attached directly to the metal ion.[10] Likewise, in aqueous solution we find no electron transfer band except at very high concentrations of $EtSO_4^-$ (σ = 44.8 kK) presumably under these conditions the equilibrium

$$Eu(H_2O)_9^{3+} + EtSO_4 \rightleftharpoons Eu(H_2O)_n\ SO_4Et^{2+} + (9-n)\,H_2O$$

displaced some way to the right.

The small variation within the solid sulphate spectra appear to be random and no correlations can be drawn at present.

Halides

The spectra of all the compounds and solutions containing halogen are summarised in Table 2. The range of values for a given halogen with a metal is far greater than that observed for sulphate. As mentioned earlier an increase in the number of donor atoms coordinated to the metal produces a red shift in the electron transfer spectrum. The change from two coordinated chloride ions in $EuCl_3 6H_2O$ to five in EuOCl and nine in $EuCl_3$ moves the band 3.3 kK and 12.3 kK

respectively to lower energy.

A blue shift was observed when the reducible lanthanides were doped into $LaCl_3$, whereas a red shift occurred in doped LaOCl. We have argued[11] that in the oxychlorides the europium can approach one halogen more closely than in the pure EuOCl since the field at the metal is assymetric; produced by halide layer on one side of the metal and a layer of oxide ions on the other.[12] In the trihalides the metal is completely surrounded by halide,[13] and if the lattice spacings of the halide are preserved the europium-halogen distance must increase, giving rise to the observed blue shift.

Comparison between chloride, bromide and iodide for both oxyhalide and trihalide produces the surprising result that the bromide and iodide spectra appear far closer to the chlorides than would be expected from Jørgensen's extensive studies of transition metal hexa- and tetra halides, where a separation of 6.0 kK is usual between chloride and bromide and 10 kK between bromide and iodide.[2] We have suggested an explanation for the oxyhalides[11] in terms of the transferred electron coming from a halide in the next layer, the distance of which from the metal atom increases rapidly down the series Cl, Br, I.[12]

A similar explanation might be offered for the trihalides if the donor orbital is located mainly on the three halogen atoms about the waist of the EuX_9^{6-} units, i.e. X_{II} in Figure 3. The distance $M - X_{II}$ will increase more rapidly than $M - X_I$ with halogen radius from packing requirements. In $EuBr_3$ one of the X_{II} bromide atoms is over 4 A from the metal.[13]

We hope to test this hypothesis by investigating the polarization of the electron transfer band in single crystal spectra in the near future.

Thanks are due to the Department of Scientific and Industrial Research and the Society of the Sigma Xi for apparatus and the Chemistry Department, Queen's College, for a studentship (H. P.).

REFERENCES

1 Jørgensen, C.K. Molecular Physics (1962) 5, 271.

2 Jørgensen, C.K. "Orbitals in atoms and Molecules," Academic Press, London, 1962.

3 Barnes, J.C., J. Chem. Soc., (1964) 3880.

4 Barnes, J.C. and Day, P., J. Chem. Soc. (1964) 2886.

5 Geller, S., Acta Cryst. (1957) 10, 713.

6 Barnes, J.C. and Hume, D.N. Inorg. Chem. (1963) 2, 444.

7 Zachariasen, W.H. Acta Cryst. (1961), 14, 234.

8 Sherwood, G.R., J. Amer. Chem. Soc. (1944), 66, 1228.

9 Hunt, B.H., Rundle, R.E., and Stosick, A.J. Acta Cryst. (1954) 7, 106.

10 Ketelaar, J.A.A., Physica (1937) 4, 619.

11 Barnes, J.C. and Smith, D.W., To be published.

12 Zachariasen, W.H., Acta Cryst. (1948) 1, 265.

13 Sillen, L.E. Svensk Kem Tidskr (1941) 53, 39.

TABLE 1

Reflection spectra of complexes with oxyanions

Energy of first electron transfer band in Kilo Kaysers

Compound	Ln = Sm	Eu	Yb
$Ln\,PO_4$	52.0	43.5	48.4
$Ln_2(CO_3)_3$	52.1	42.4	47.8
$Ln_2(SO_4)_3$ anhyd.	50.8	42.2	48.5
$Ln_2(SO_4)_3\,8H_2O$	50.3	41.7	47.2
$Na_2SO_4 \cdot Ln_2(SO_4)_3 \cdot nH_2O$	50.3	42.5	46.5
$Ln\,SO_4^{+}$ (solution)	48.4	41.7	44.5
$Ln\,SeO_4^{+}$ (solution)	-	44.0	-
$Ln\,H_2PO_2^{2+}$ (solution)	-	45.8	-

TABLE 2

Electron transfer spectra in kK of lanthanide halide complexes.

Compound	Ln = Sm	Eu	Yb
$LnCl_3$	37.2	28	37.0
$La_{0.95}Ln_{0.05}Cl_3$	39.2	34.7	38.5
$LnBr_3$	34.5	26	28.2
LnI_3	-	25.0	-
$LnCl_3 \cdot OH_2O$	48.1	40.3	44.5
LnOCl	46.5	37.0	45.9
$La_{0.95}Ln_{0.05}OCl$	44.0	33.9	37.7
LnOBr	44.5	36.1	43
$La_{0.95}Ln_{0.05}OBr$	42.0	33.7	36.4
Cl^- in EtOH solution	45.7	36.2	41.0
Br^- in EtOH solution	40.2	31.2	35.5

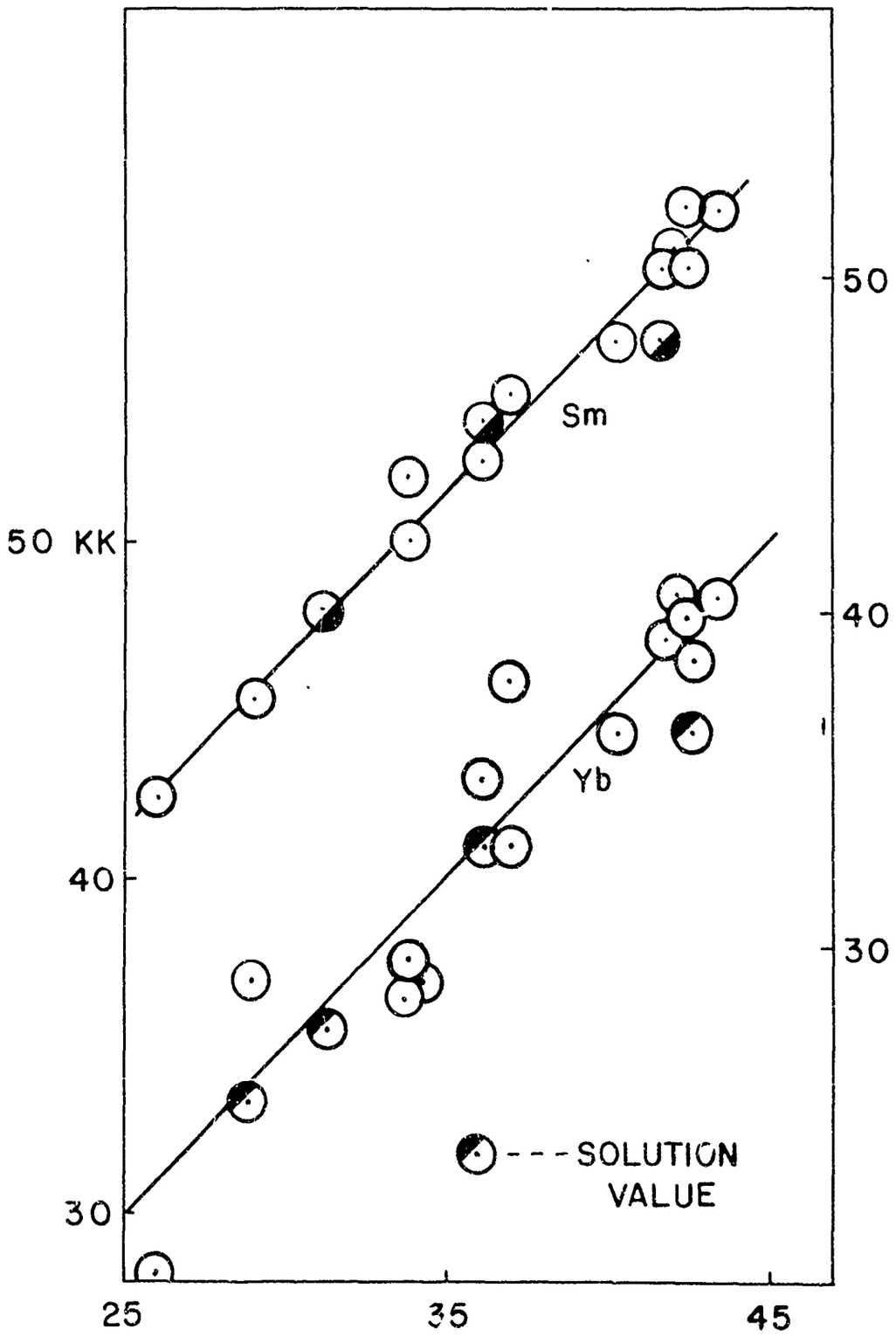

Fig. 1. Diffuse reflectance spectra of $Na_2SO_4 \cdot Ln_2(SO_4)_3 \cdot nH_2O$.

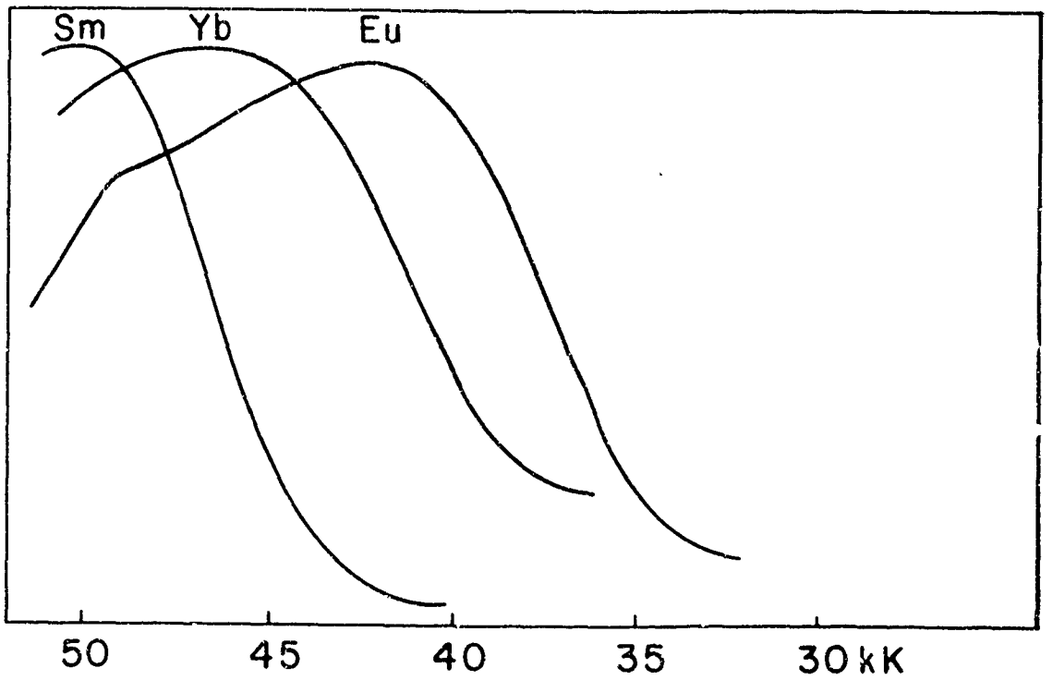

Fig. 2. Energy of first electron transfer transitions for Sm and Yb compounds plotted against the spectra of the corresponding Eu compounds.

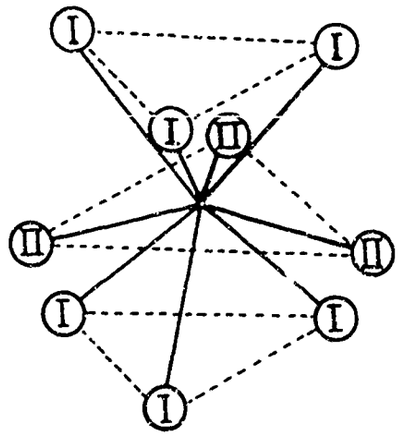

Fig. 3. Arrangement of Halide Ions in nine-coordinate LnX_3 Structures. (The distances M-X_I and M-X_{II} are shown as equal for clarity.)

OPTICAL AND PHYSICAL PROPERTIES OF SINGLE CRYSTAL LANTHANUM TRIFLUORIDE

Hugh M. Muir* and William Stein

Varian Associates, Palo Alto, California

ABSTRACT

Optical and physical measurements made on high purity single crystal LaF_3 indicate its potential as a valuable optical window material. The excellent transmission over a very broad spectrum extending from $\sim$ 1300 Å in the vacuum ultraviolet to $\sim$ 13 μ in the intermediate infrared, coupled with a high degree of chemical and physical stability, makes LaF_3 extremely attractive for a wide range of optical applications. Some of the critical purification and crystal growth conditions necessary for the synthesis of the high purity, optical grade LaF_3, as well as the optical and physical parameters, are presented.

* Presently at Department of Materials Science, Stanford University.

1. INTRODUCTION

Over the past 25 years very little in the way of new optical materials has been witnessed for the spectrum range extending from the vacuum ultraviolet (~1100 Å) to the intermediate infrared (~10.0 μ). Optical glasses presently available have a very limited usefulness outside of the visible spectrum, and currently only cover a range of approximately 3000 Å to 2.0 μ. Research now in progress on some chalcogenide glasses indicate they may be of some importance in the 12.0 - 14.0 μ region.

For years synthetic optical fluoride crystals such as LiF, CaF_2, BaF_2 and MgF_2 of select quality have been the old line material systems that fulfill the preponderance of optical requirements over the 1100 Å to 10.0 μ range. There are, however, some inherent optical and physical weaknesses in all of these systems, namely, their relative softness, lack of chemical and thermal stability, and individually limited transmission ranges, which allow considerable room for improvement.

During the course of an evaluation at Varian of single crystal LaF_3 as an experimental laser host, it became apparent that LaF_3 possessed several unique optical and physical properties which indicated that it could become an important replacement for several of the optical fluoride crystal systems now in use. This paper is a presentation of preliminary optical and physical data for the optical grade, single crystal LaF_3 grown in a hydrogen fluoride atmosphere.

2. EXPERIMENTAL

a) LaF_3 Starting Material

Anhydrous rare-earth fluorides first became important in the early 1950's through the research efforts of Spedding and Daane[1] at the A.E.C. Ames Laboratory in the preparation of the first really high purity rare-earth metals. It was determined in this research that the water content of the fluoride was extremely critical to the control of the

gaseous impurity content of the reduced metal. The degree of purity of the starting LaF_3 material for optical applications must be at least an order of magnitude better than that now accepted for high purity metals production. Commercially available "anhydrous" rare-earth fluorides still do not meet the specifications required for an optical grade LaF_3. Light scattering centers in LaF_3, assumed to be La_2O_3 and/or LaOF, cause excessive transmission losses, especially in the vacuum ultraviolet regions. Their elimination requires the use of special processing techniques.

The initial stage of the fluoridation process that has been developed for optical grade LaF_3 is quite similar to the one described by Carlson and Schmidt[2] for the preparation of anhydrous rare-earth fluorides. High purity 99.997% La_2O_3, purchased from Linsay Chemical Company and Research Chemicals Company, is used as the starting material. Fig. 1 is a schematic of the fluoridation apparatus employed. Anhydrous hydrogen fluoride, carried by argon, is passed over the freshly ignited La_2O_3 at a temperature of $\sim$ 800°C for a period of six to eight hours to complete the following reaction:

$$La_2O_3 + 6HF \xrightarrow{800°C} 2LaF_3 + 3H_2O$$

The resulting product, in a fine powder form, is approximately 99.99% converted. In order to get below the 100 ppm oxygen impurity level required from optical considerations, a second stage to the fluoridation process has been developed. In this stage LaF_3 is brought to a melt, under a hydrogen fluoride atmosphere, and a zone refining pass is made through a thermal gradient. This phase of the process provides a polycrystalline ingot with the total oxygen impurities reduced to approximately 50 ppm, which is acceptable for the actual single crystal growth.

b) LaF_3 Single Crystal Growth

Commerical optical fluoride crystals presently available are

grown either in a high vacuum or an inert atmosphere. The most commonly employed crystal growing technique for these systems is the Bridgman-Stockbarger method. LaF_3 has been grown at Varian employing several techniques, namely, the Störber, Czochralski, as well as the Bridgman. To date the best results, both from an optical and physical viewpoint, have been obtained employing the Bridgman technique. To insure excellent optical and physical properties in the lanthanide fluorides, it has been found necessary to provide an "active ambient atmosphere," in particular a hydrogen-fluoride atmosphere, during the entire growth and annealing cycles.

The list of references pertaining to the growth of fluoride crystals employing active atmospheres is of recent vintage, and is quite meager. In 1961 Catalano and Stratton[3] of the Lawrence Radiation Laboratory described a Störber growth technique of CoF_2 and MnF_2 in a static hydrogen fluoride atmosphere. In 1962 and 1964 Muir and Stein[4,5] detailed the growth of LaF_3 and other rare-earth fluorides employing a dynamic hydrogen fluoride atmosphere with Bridgman, Störber, and Czochralski growth techniques. Guggenheim of the Bell Telephone Laboratories published a paper in 1963[6] in which a Bridgman technique was employed utilizing a static hydrogen fluoride atmosphere for the growth of Ca, Ba, Li and La fluoride crystals. The most recent publication is one by Robinson of the Hughes Research Laboratories describing a Bridgman-Stockbarger method for the growth of $LaF_3:Nd^{3+}$ laser crystals in a dynamic HF atmosphere.[7]

Fig. 2 is a schematic presentation of the crystal growing furnace employed in our Bridgman growth studies. The furnace is of a stainless steel, double-walled, water cooled design. The furnace end plates, also water cooled, are designed as electrical contacts for the graphite resistance electrode as well as hydrogen fluoride gas inlet and outlet ports. A radial sight tube sealed with a LaF_3 window, which is impervious to the reactive hydrogen fluoride atmosphere, is provided for visual and pyrometric observations. The upper radial tube contains

a graphite-tungsten thermocouple for temperature control. Power is supplied by an 18 KVA saturable controlled reactor controlled by a L & N Speedomax proportionating system.

The growth process consists of lowering a conical bottomed crucible filled with zone refined LaF_3 through a sharp thermal gradient in the closely controlled hydrogen fluoride atmosphere. Drop rates are selected depending upon the cross section of the crystal being grown. After the growth cycle is completed, a programmed annealing cycle is utilized to remove strains. The crystal is then ready for cutting, coring and optical polishing.

3. OPTICAL PROPERTIES

Lanthanum trifluoride possesses several unique optical and physical properties that could make it a promising new optical material. Table I lists some of the preliminary optical data obtained for single crystal LaF_3. The optical transmission range of LaF_3 from 1300 Å - 13 μ indicates that it will cover the spectrum now requiring five materials for coverage, namely, LiF, CaF_2, BaF_2, MgF_2 and PbF_2. Its low index of refraction[8] and reflection losses[9] permit its use without costly anti-reflection coatings being required. The optical quality of LaF_3 has been determined to be equivalent to that of a fine optical glass. Fig. 3 is a Twyman-Green interferogram of LaF_3 taken through a crystal 4 cm long. The distortion of the background fringe pattern was found to be so low that the crystal had to be rotated to polarize the pattern in order that it be distinguished from the background. Light scattering centers in LaF_3 have been essentially eliminated when the oxygen content of the crystals is held to 10 - 50 ppm through the careful control of the hydrogen fluoride atmosphere.

Lanthanum fluoride belongs to the hexagonal system and therefore has an optic axis. The associated birefringence can be used in the design of polarizers and quarter wave plates for the vacuum ultraviolet.

4. PHYSICAL PROPERTIES

Lanthanum trifluoride's physical properties are quite remarkable compared with any of the other halide crystal systems now employed. Table II lists some of the physical properties determined for LaF_3 crystals grown in a hydrogen fluoride atmosphere.

LaF_3 has been found to be a very durable single crystal system. Its hexagonal structure is much less prone to cleavage than are the cubic systems; consequently edge chipping is much less of a problem. Dislocation counts of approximately $5 \times 10^3/cm^2$ are considerably below those reported for other single crystal halides, which are normally in the 10^5 - $10^6/cm^2$ range. The Knoop hardness of 450 allows excellent optical finishes to be obtained, with only moderate handling care required to maintain this surface quality. LaF_3 has also been found to be chemically inert, as is evidenced by the data showing low solubility in various acids and bases. Thermal shock resistance has also been determined to be excellent. Optical viewports used on our furnaces, in continuous operation for the past two years under reactive atmospheric conditions, have seen many hundreds of thermal cycles from approximately 150°C to 20°C. No optical degradation has been observed during this period. Crystals with thicknesses ranging from 7 to 13 mm have been rapidly cycled from 20°C to -77°C and back to 20°C many times without fracturing. The excellent compression and rupture strength, along with a fair degree of elasticity and combined with the chemical inertness, should allow very durable windows, lenses, cells, prisms, etc. to be fabricated that will possess long useful lives.

Also of considerable interest is the coefficient of expansion for LaF_3. Fig. 4 details the expansion vs. temperature up to 1100°C. This curve is similar to that of copper, the 300 series of stainless steel, and monel. This characteristic could allow the development of high vacuum, high temperature crystal-to-metal seals, eliminating the somewhat undesirable epoxy, wax and AgCl type seals now required for the other fluoride systems.

5. CONCLUSIONS

Considerable improvements in the optical and physical properties of single crystal LaF_3 have been realized through the use of a dynamic hydrogen fluoride atmosphere during the entire growth and annealing cycles. Further increase in the purity of the starting material and the crystal growth parameters could conceivably extend its useful optical transmission range, especially into the vacuum ultraviolet, and make LaF_3 an optical material of considerable merit.

* * * * * * * *

Acknowledgments

We wish to thank R. D. Fairman and C. S. Pearsall of Varian for providing the polished crystal specimens and physical data measurements, and to thank also Dr. W. Yen of Stanford University and Dr. J. Vanier of Varian for the optical measurements. We would also like to acknowledge the numerous helpful discussions with Professor W. Walker of the University of California, Santa Barbara.

References

1. F. H. Spedding and A. H. Daane, Prog. Nuclear Energy 1, 413 (1956).

2. O. Carlson and F. Schmidt, The Rare Earths (J. Wiley and Sons, Inc. New York, 1961).

3. E. Catalano and G. Stratton, University of California Lawrence Radiation Laboratory Report UCRL-6370 (1961).

4. H. M. Muir and W. Stein, Crystal Technology Corporation Report No. L-145917 (1962).

5. H. M. Muir and W. Stein, AIME Materials Conference, Los Angeles, May, 1964.

6. H. Guggenheim, J. Appl. Phys. 32, 1337 (1961).

7. M. Robinson and C. Asawa, Electrochemical Society 127th Meeting, San Francisco, May, 1965.

8. G. Haas, T. B. Ramsey and R. Thun, J. Opt. Soc. Am. 49, 116 (1959).

9. W. Walker, University of California, Santa Barbara, priva e communication.

TABLE I

GENERAL OPTICAL PROPERTIES OF LaF_3

Transmittance Cutoff (0.43mm Thick Polished)	$\sim$ .13 - 13μ at 25% T
Optical Activity	$\sim 90^0$ Rotation
Reflection Loss	$\sim$ 5%
Light Scattering	$\ll$ 1.0%

Refractive Index:

Wavelength (microns)	Index At 20^0C
0.4	1.60
0.8	1.580
1.2	1.567
2.0	1.555
2.2	1.552

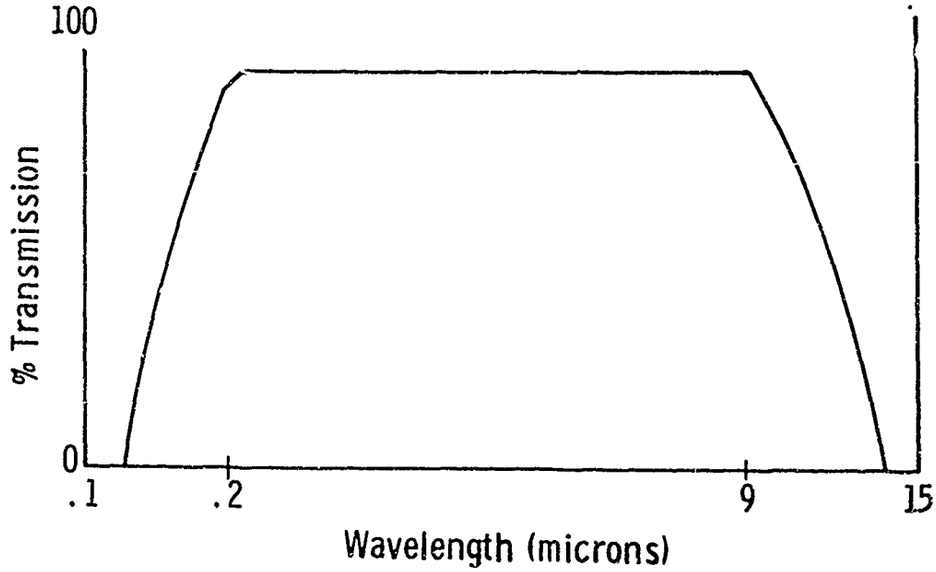

TABLE II

GENERAL PHYSICAL PROPERTIES OF LaF_3

Melting Point (^0C)	1493
Density (gm/cm^3)	5.966
Structure	Hexagonal ($P6_3/mcm$)
Lattice Constants (a_0)	7.184 Å
Lattice Constants (C_0)	7.351 Å
Dislocation Density ($counts/cm^2$)	$3\text{-}5 \times 10^3$
Radiation Resistance (Rads)	5×10^5
Dielectric Constant (IMC)	14
Hardness (Knoop)	~450
Expansion Coefficient (10^{-6})	15
Rupture Modulus (psi)	8000
Elasticity Modulus (psi)	12×10^6
Compressive Strength (psi)	100,000
Thermal Conductivity ($Cal/(sec)(cm^2)(^0C/cm)$)	0.025
Solubility (100^0C/100 hours):	
H_2O	None
1/2 N NaOH	None
1/2 N HCl	.2 gm/100 gm
1/2 N H_2SO_4	.18 gm/100 gm
1/2 N HNO_3	.25 gm/100 gm

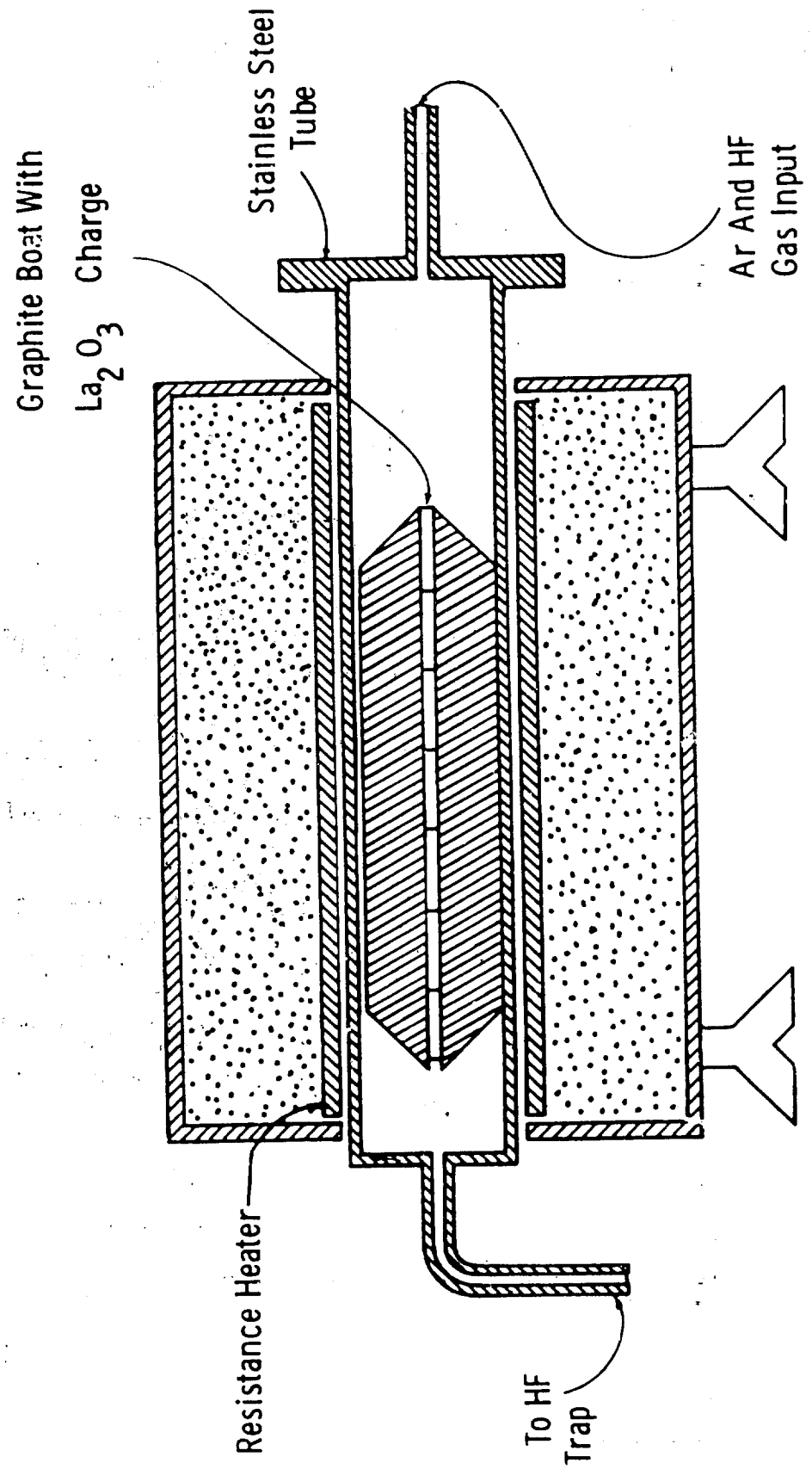
Graphite Boat With
La_2O_3 Charge
Stainless Steel
Tube
Ar And HF
Gas Input
Resistance Heater
To HF
Trap

FIGURE 1

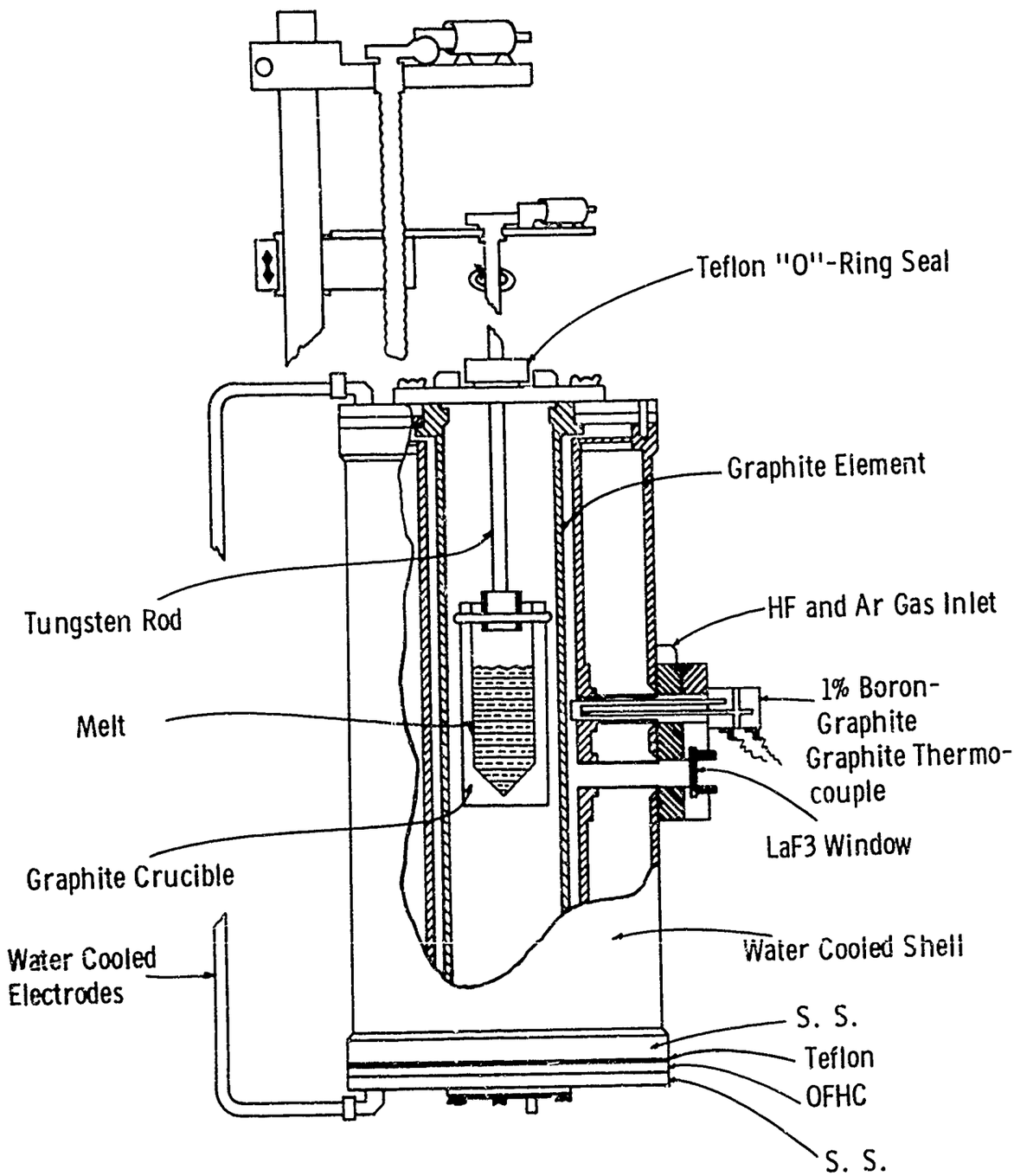
Teflon "O"-Ring Seal
Graphite Element
Tungsten Rod
HF and Ar Gas Inlet
1% Boron-
Graphite
Graphite Thermo-
couple
Melt
LaF3 Window
Graphite Crucible
Water Cooled Shell
Water Cooled
Electrodes
S. S.
Teflon
OFHC
S. S.

FIGURE 2

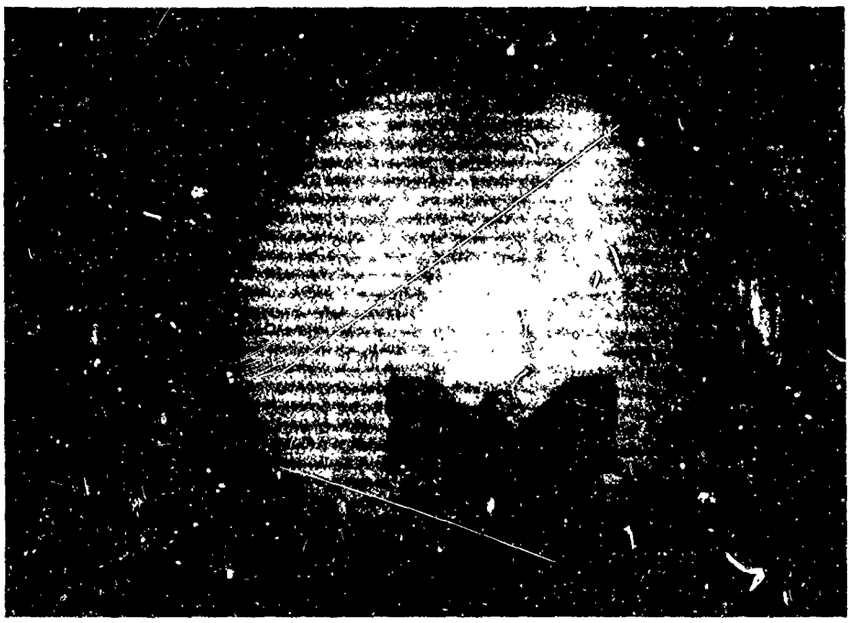

TWYMAN-GREEN INTERFEROGRAM OF VARIAN-MADE
LaF_3. 10% Pr^{3+} ROD 1" x 1/4" D
(Photograph courtesy of Dr. R. H. Kingston, Lincoln Laboratory.)

FIGURE 3

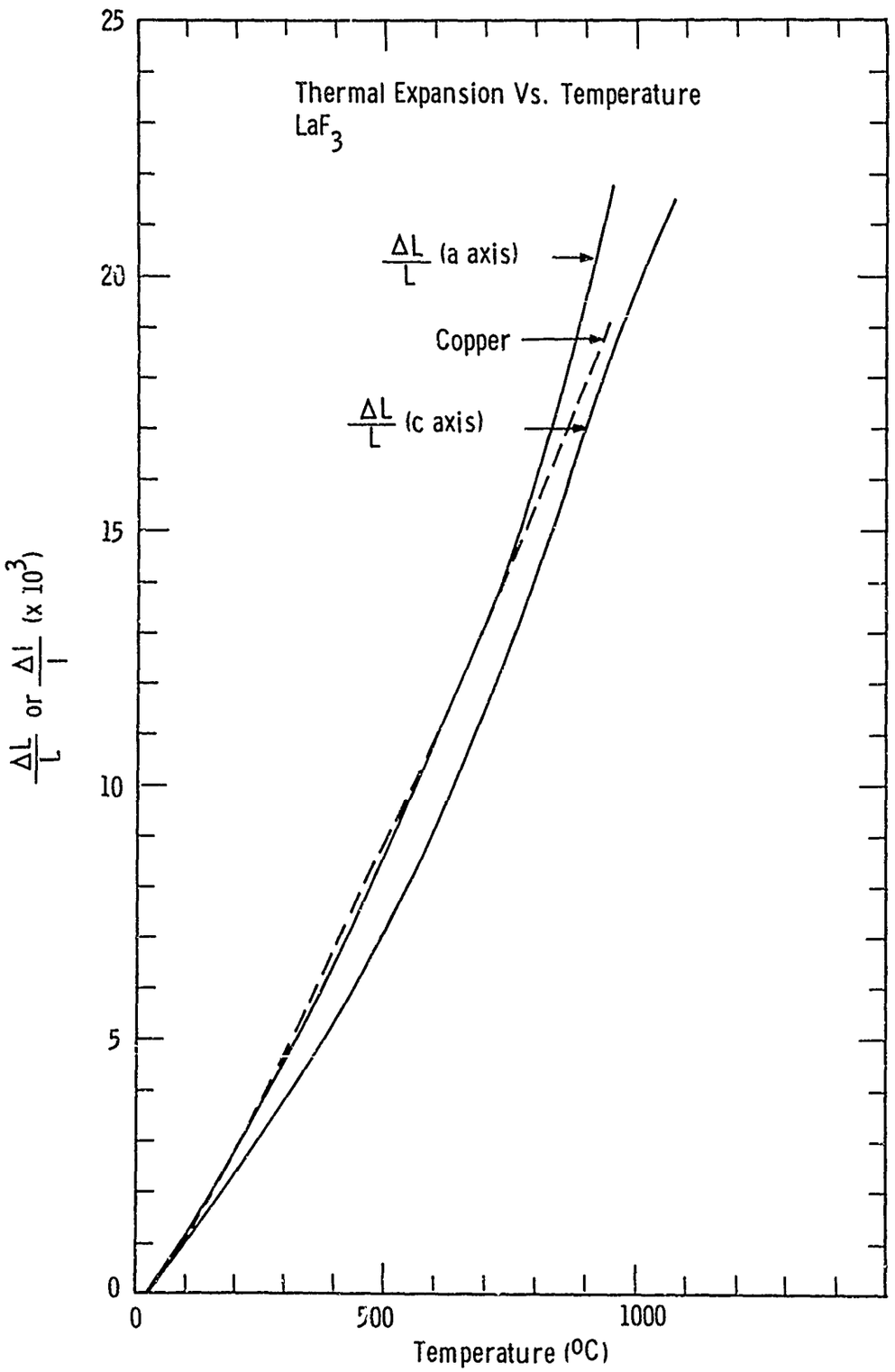
Thermal Expansion Vs. Temperature
LaF3
ΔL/L (a axis)
Copper
ΔL/L (c axis)
ΔL/L or Δl/l (x 10^3)
Temperature (°C)
0
5
10
15
20
25
0
500
1000

FIGURE 4

LOCALIZED H^- MODES IN RARE EARTH TRIFLUORIDES IN VIBRONIC SPECTRA

G.D. Jones and R.A. Satten

University of California, Los Angeles

Crystals of LaF_3, PrF_3 and NdF_3 doped with hydrogen and deuterium have been studied spectroscopically. Two strong polarized fundamentals and their combinations have been observed in the infra-red for both H^- and D^-. The fundamentals appear also polarized in the vibronic spectrum of pure NdF_3 coupled to several electronic transitions. Extra electronic lines appearing only in the doped crystals occur on the long wavelength side of the usual rare earth electronic transitions. From frequency differences, these extra levels are the parent states for the local mode vibronic transitions. The displacement of the extra electronic lines from the usual electronic transitions is mainly due to a changed crystalline field and covalency arising from the replacement of H for F, and is greater for higher levels. In addition the extra electronic levels have slightly different frequencies for hydrogenated and deuterated crystals. This isotope shift depends in both magnitude and sign on the particular electronic level and ranges from 0.4 cm^{-1} for $^4F_{3/2}$ to -2.9 cm^{-1} for $^4F_{7/2}$. This effect is accounted for by a large difference in zero point amplitude for H^- and D^- localized modes which, through the electron-vibration interaction, perturbs each electronic level to a different extent.

SPECTRAL CHARACTERISTICS OF Nd^{3+} AND Er^{3+} TRIETHYLENETETRAMINEHEXAACETIC ACID COMPLEXES

E. A. Boudreaux and A. K. Mukherji

Department of Chemistry, Louisiana State University in New Orleans, New Orleans, Louisiana 70122

ABSTRACT

A new series of stable rare earth chelates with triethylenetetramine-hexaacetic acid (TTHA) have been prepared in aqueous solution. Those of Nd^{3+} and Er^{3+} show particularly striking intensification of the $^4G_{5/2}$ and $^4G_{11/2}$ absorption bands respectively.

In all cases the rare earth ion--TTHA stoichiometry is 1:1, and on making reasonable assumptions about the complex having the common nine-fold coordination of D_{3h} symmetry, the rationalization of these observations in terms of a weak covalent bonding interaction does not seem reasonable. However, the mechanism of pseudo-quadrupole interaction at the rare earth ion may perhaps offer a plausible explanation.

INTRODUCTION

The spectra of rare earth ions are characterized by sharp, well-defined, line-like absorption bands occurring through the near infrared, visible and ultraviolet regions, depending upon the particular ion involved. The many bands found in these regions are generally of low intensity ($\epsilon_{max} \leqslant 7.0$) and there is an abundance of evidence supporting the fact that they are associated with f-f transitions of a particular f^n configuration.

These features in the absorption spectra of rare earth ions are consistent with the properties of 4f orbitals penetrating the atom core to a considerable extent and are well shielded from environmental perturbations by the outer filled 5s and 5p orbitals. Thus, even in what may be considered the strongest complexes, the above spectral features are not significantly altered, except for small ligand field splittings of the order of 100 cm^{-1}. There are, however,

some cases in which certain absorption bands are intensified by as much as two to five times the molar extinction coefficient of the aqueous ion. Furthermore, less dramatic effects are sometimes observed in which one or more bands are broadened and the band contour modified. These latter effects have been invoked as evidence for the involvement of 4f electrons in some degree of covalent bonding(1), and in accord with these views the small splittings have been reinterpreted recently on more quantitative grounds(2).

In most cases where enhancement of absorption intensity is observed, the involved ground state $\longrightarrow$ excited state transition rigorously obeys the selection rule $\Delta J \pm 2$. In view of these observations, it has been suggested(3) that the enhancements may be due to pseudo-electric quadrupole radiation field across the rare earth ion, for which the selection rule is $\Delta J \leqslant 2$. For Nd^{3+} and Er^{3+} this is identifiable with the transitions $^4I_{9/2} \longrightarrow {}^4G_{5/2}$ and $^4I_{15/2} \longrightarrow {}^4G_{11/2}$ respectively.

According to this theory, the oscillator strength, P, for a given transition $\psi_J \longrightarrow \psi_{J'}$ is given by

$$p = \sum_{\lambda=2,4,6} \lambda T_\lambda < \psi_J \left| \underset{\sim}{U}^{(\lambda)} \right| \psi_{J'} >^2$$

where λ is the frequency of the transition, $U^{(\lambda)}$ is a unit tensor operator of rather complex form, and T_λ parameters gauging the magnitude of the effect which are apparently associated in some way with the time dependence of the transition. Furthermore, T_2 of the various T_λ is particularly sensitive to the environment and is henceforth employed as a measure of the relative magnitudes of the various factors possibly contributing to an increase in the oscillator strength of a particular transition. The importance of T_2 is further varified in the fact that $\underset{\sim}{U}^{(2)} \equiv 0$ unless $\left| J-J' \right| \leqslant 2$.

The four principle phenomenological effects contributing to T_2 are:

1. forced electric dipole radiation as a result of the motion of the ion in the solvent producing a charge at some distance R from the ionic nucleus, giving

rise to $T_2^{(1)}$;

2. mixing of vibrational modes into the electronic wave functions producing electric fields at the ionic nucleus, for which the contribution is $T_2^{(2)}$;
3. contribution to $T_2^{(3)}$ via pure electric quadrupole radiation in a homogeneous dielectric environment;
4. electric quadrupole fields at the ion in an inhomogeneous dielectric environment, contributing to $T_2^{(4)}$.

Each of these effects has already been considered in some detail(3) with respect to the oscillator strength of the $^4I_{9/2} \longrightarrow {}^4G_{5/2}$ transition of Nd^{3+}, which has been evaluated as 1.05×10^{-5} in aqueous solutions(4). If it is assumed that P is increased by a factor of four, then $T_2 = 8.8 \times 10^{-20}$ sec. Reasonable estimates to the upper limit of each of the effects (1.-4.) leads to the following results. For $T_2^{(1)}$ to have the value 8×10^{-20} sec. requires unrealistic assumptions regarding the solvent interaction. Similarly, $T_2^{(2)} \approx 10^{-22}$ sec. and is thus not considered a principal factor. Lastly, values of $T_2^{(3)}$ fall short by a factor of 10^5 whether or not weak covalent bonding effects are considered, while estimates of $T_2^{(4)}$ appear to be the correct order of magnitude based even on the simplest model.

EXPERIMENTAL

Aqueous $NdCl_3$ and $ErCl_3$ solutions were prepared from 99.9 per cent pure salts (Michigan Chemical Corp.). These were standardized by EDTA titrations using Xylenol Orange indicator.

A 0.2 M TTHA (Geigy Chemical Corp.) was prepared by dissolving 9.89 gm of the pure solute in 40 ml. of distilled water, to which was added (constant stirring) 30 ml. of 1.5 M NaOH. The solution was then heated to approximately 80°C for 20 minutes so as to insure complete dissolution, and then made up to 100 ml. total volume after cooling to ambient temperature.

Appropriate volumes of the rare earth chloride and TTHA solutions were thoroughly mixed and then set aside a few minutes for complete equilibration. The spectra of these solutions were then scanned against distilled water on a Beckman DK-1 spectrophotometer.

RESULTS AND DISCUSSION

Aqueous solution spectra of Nd^{3+} and Er^{3+}, and spectra with 1:0.5 and 1:1 rare earth ion to TTHA ratios are presented in Figures 1 and 2.

Although in the Nd^{3+} spectra (Fig. 1) several bands appear to be modified at a maximum Nd^{3+} to TTHA ratio of 1:1, the $^4G_{5/2}$ band shows significant enhancement in intensity. the $^4G_{5/2}$ and $^4G_{7/2}$ bands are, however, separated only by a few wave numbers(5) and hence appear as a single band at 573 mμ. However, Er^{3+} with its $4f^{11}$ configurations is three electrons short of a full f^{14} configuration, thus its spectral terms are the same as those of Nd^{3+} except for an inversion in the order of multiplets. Hence, the $^4I_{15/2} \longrightarrow {}^4G_{11/2}$ transition occurs at 372 mμ, and is furthermore not complicated by an overlapping band of different multiplicity as in the case of Nd^{3+}. It is this band which shows the most pronounced enhancement in the 1:1 Er^{3+}-TTHA complex (see Fig. 2).

The TTHA molecule has the structural formula

$$(HO_2CCH_2)_2N(CH_2)_2\underset{\displaystyle CH_2\\ \displaystyle COOH}{N}\text{-}(CH_2)_2\text{-}\underset{\displaystyle CH_2\\ \displaystyle COOH}{N}\text{-}(CH_2)_2\text{-}N\text{-}(CH_2\text{-}COOH)_2$$

and thus as a decadentate ligand has a maximum potential coordination number of ten with respect to a rare earth ion. Simple structural models show that this ligand would not have to be subjected to much strain in order to achieve an optimum configuration for maximum coordination. However, there is the alternative possibility that the coordination may involve only the terminal carboxyl groups, their respective nitrogen atoms and three additional water molecules, to

give a $M(TTHA)(H_2O)_3^-$ complex analogous to the known $La(EDTA)(H_2O)_3^-$ complex(6). Since the water molecule is such a strong coordinating ligand for rare earths, this latter assumption is adopted in further discussion.

Although it has already been pointed out that electric quadrupole effects may be of prime importance, it is none the less of interest to attempt at least a qualitative explanation of the observed effects in terms of the weak covalent interaction mechanism suggested by Jørgensen, et.al.(2). On the assumption that both $Nd(TTHA)(H_2O)_3^-$ and $Er(TTHA)(H_2O)_3^-$ are symmetrical complexes having point group symmetry D_{3h}, the transformation properties of the seven f symmetry orbitals of the rare earth ion and the σ group orbitals of the ligands may be derived as shown in Table I. The bonding is then considered to arise through antibonding combination of the form where ψ_{4f} is the appropriate atomic f orbital and ψ_σ

$$\psi mo = a\,\psi_{4f} - b\,\psi_\sigma$$

the σ-group orbitals of the ligands. The interaction is strongest when $b > a$ thus spreading electron density onto the ligands. The relative ordering of the resulting ψmo's is an indication of which f orbitals attain added stabilization.

It is conceivable that mixing of the lowest lying ψmo with a non-bonding f orbital could further remove the forbidden character inherent in pure f-f transitions, and thus enhance the intensity of the involved absorption band. A qualitative representation of this effect is presented in Figure 3. The diagram is constructed empirically relative to the data derived for the neodymium and erbium ethyl sulfates(2). The $\delta_1(e')$, $\pi(e')$ and $\phi(a_2')$ are assigned as singularly occupied f orbitals having orbital quantum numbers appropriate to ^4G transitions. For $Nd(TTHA)(H_2O)_3^-$ this scheme places the $\sigma(a_1'')$ antibonding orbital some 50 cm^{-1} above the $\phi_1(a_2')$ non-bonding orbital, while this separation is at least 100 cm^{-1} in $Er(TTHA)(H_2O)_3^-$. Thus the enhancement of the $^4G_{5/2}$ band in Nd^{3+} should be greater than that of the $^4G_{11/2}$ in Er^{3+}. However, this is apparently not the case since the ratio of the molar extinction coefficient of $Nd(TTHA)(H_2O)_3^-$ to that of the aqueous Nd^{3+} ion is about 2.4, while this ratio for $Er(TTHA)(H_2O)_3^-$ to the aqueous Er^{3+} ion is 4.0.

Consequently this simple interpretation does not seem to provide an adequate explanation of the observed effects.

A logical explanation may indeed lie in the mechanism of pseudoquadrupole radiation in the environment of an inhomogeneous dielectric as pointed out earlier, but the data necessary to test this hypothesis is unattainable for the cases in point. Nevertheless, if this mechanism is indeed reasonable, then it is anticipated that the intensity of the transition should increase regularly with increasing polarizability of the environment, particularly in those cases where the interaction of the environment with the rare earth ion is chemically similar.

The absorption spectra of Nd^{3+} and Er^{3+} acetylacetonates in various solvents having widely different dielectric properties have been reported by Moeller and Ulrich(7). Although these data may be subject to some criticism owing to the lack of knowledge of the exact extent of hydration of the solutes, the reported analytical data nevertheless seem consistent with the formulations $Nd(C_5H_7O_2)_3$ and $Er(C_5H_7O_2)_3$. Furthermore, the fact that these particular complexes may have been hydrated seems rather unlikely in view of the solvents in which they were dissolved. The pertinent data are reproduced in Table II, and the solvents have been grouped according to their chemical similarity. The effective molar polarizabilities, (α_m)eff were calculated from the Clausius-Mosotti equation employing dielectric constants available from the literature. In addition to the molar polarizabilities of the solvents themselves, the differences in polarizabilities between the various solvents and acetylacetone, $\Delta(\alpha_m)$eff, are also reported. These data show no apparent correlation between trends in molar extinction coefficients, ϵ_{max}, and either solvent polarizability or $\Delta(\alpha_m)$eff. In fact in some instances the anticipated trends are even reversed.

Although these findings are by no means sufficient to say conclusively that the mechanism of pseudoquadrupole interaction is not primarily responsible for the effects observed in the spectra of the Nd^{3+} and Er^{3+} TTHA complexes, they do give cause for some skepticism in accepting this as the ultimate explanation. In the light of these results, it seems more reasonable to conclude that a combination of factors; i.e. covalent interaction, pseudoquadrupole, vibrational and induced dipole effects, each properly weighted in its own right, collectively contribute to the net effect.

Acknowledgments: The authors gratefully acknowledges the support of the Petroleum Research Fund of the American Chemical Society under the auspices of Grant No. 1367-B awarded to A. K. Mukherji and Grant No. 1748-B awarded E. A. Boudreaux.

REFERENCES

1. L. I. Katzin and M. L. Barnett, J. Phys. Chem., 68, 3779 (1964).

2. C. K. Jørgensen, R. Pappalardo and H. H. Schmidtke, J. Chem. Phys., 39, 1422 (1963).

3. C. K. Jørgensen and B. R. Judd, Mol. Phys. 8, 281 (1964).

4. J. Hoogschagen and C. J. Gorter, Physica, 14, 197 (1948).

5. B. G. Wybourne, J. Chem. Phys. 32, 639 (1960).

6. J. L. Hoard, B. Lee and M. D. Lind, J. Am. Chem. Soc., 87, 1612 (1965).

7. T. Moeller and W. F. Ulrich, J. Inorg. and Nucl. Chem., 2, 164 (1956).

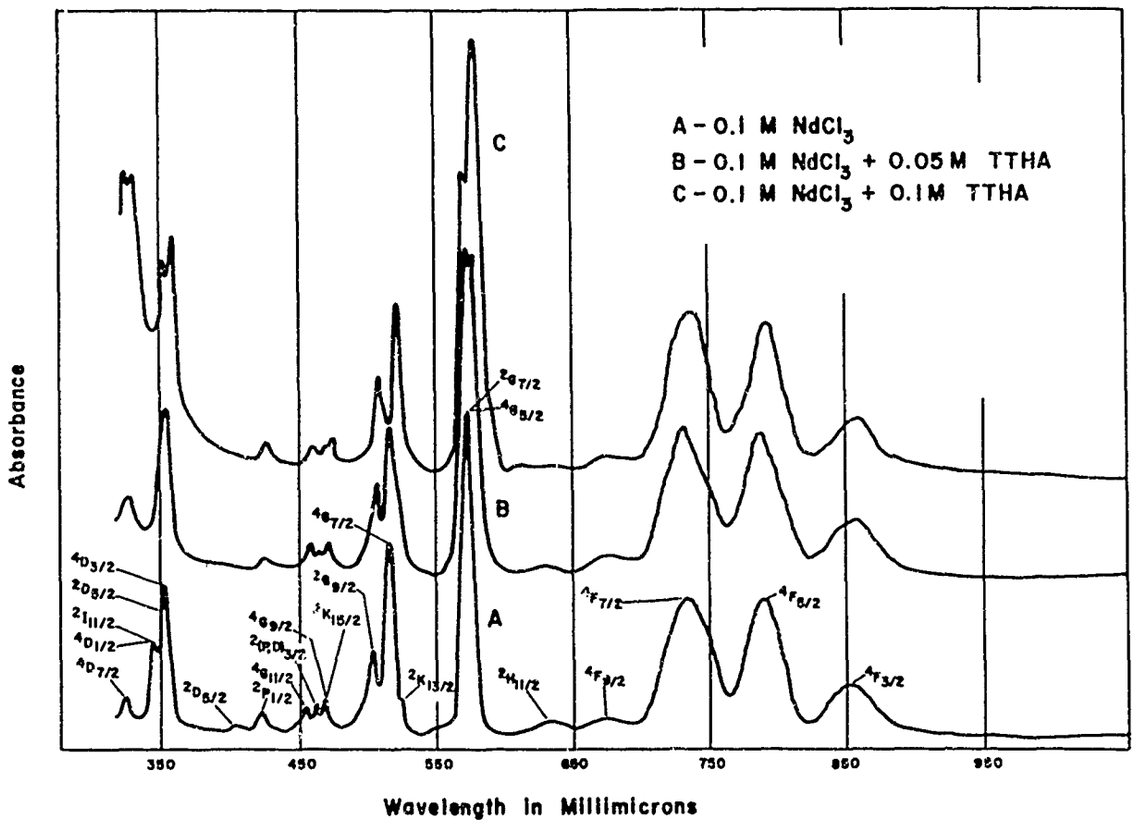

Fig. 1

Absorption Spectra of Nd^{3+}

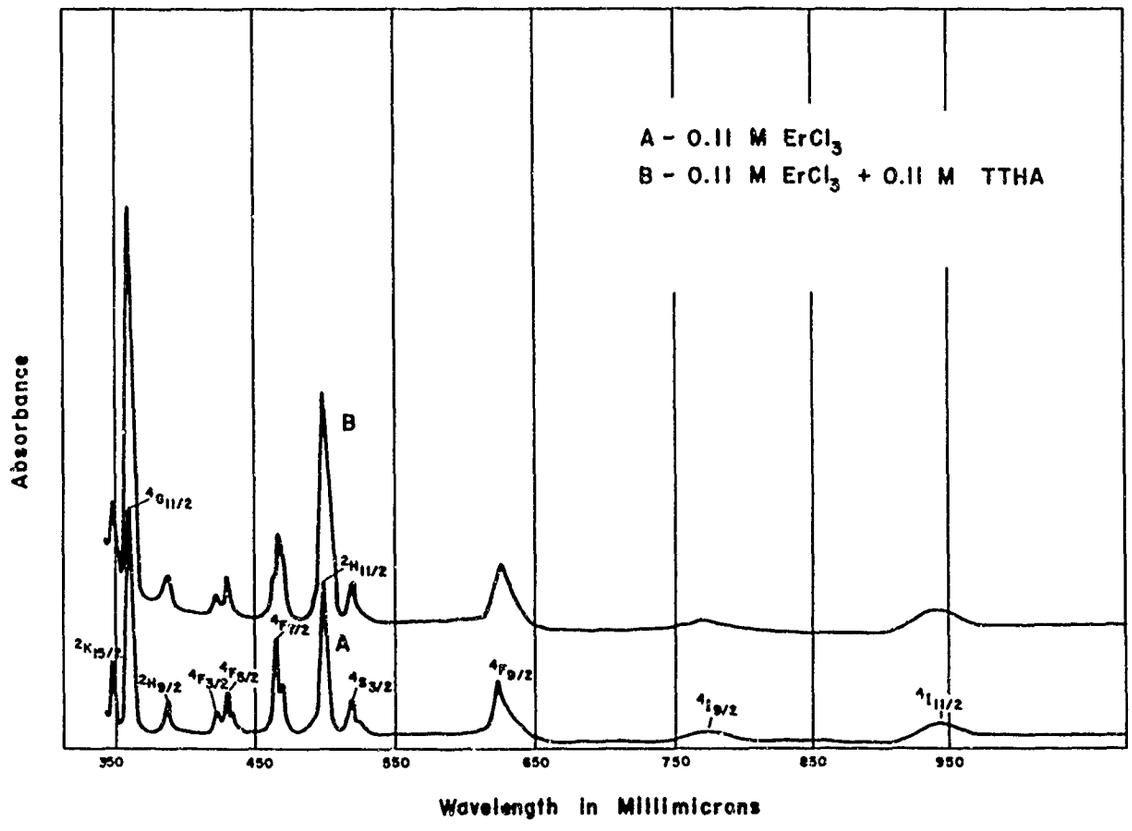

Fig. 2

Absorption Spectra of Er^{3+}

EMPIRICAL ONE ELECTRON ENERGIES OF $Nd(TTHA)(H_2O)_3^-$, (A) AND $Er(TTHA)(H_2O)_3^-$, (B) RELATIVE TO THEIR ETHYLSULFATES*

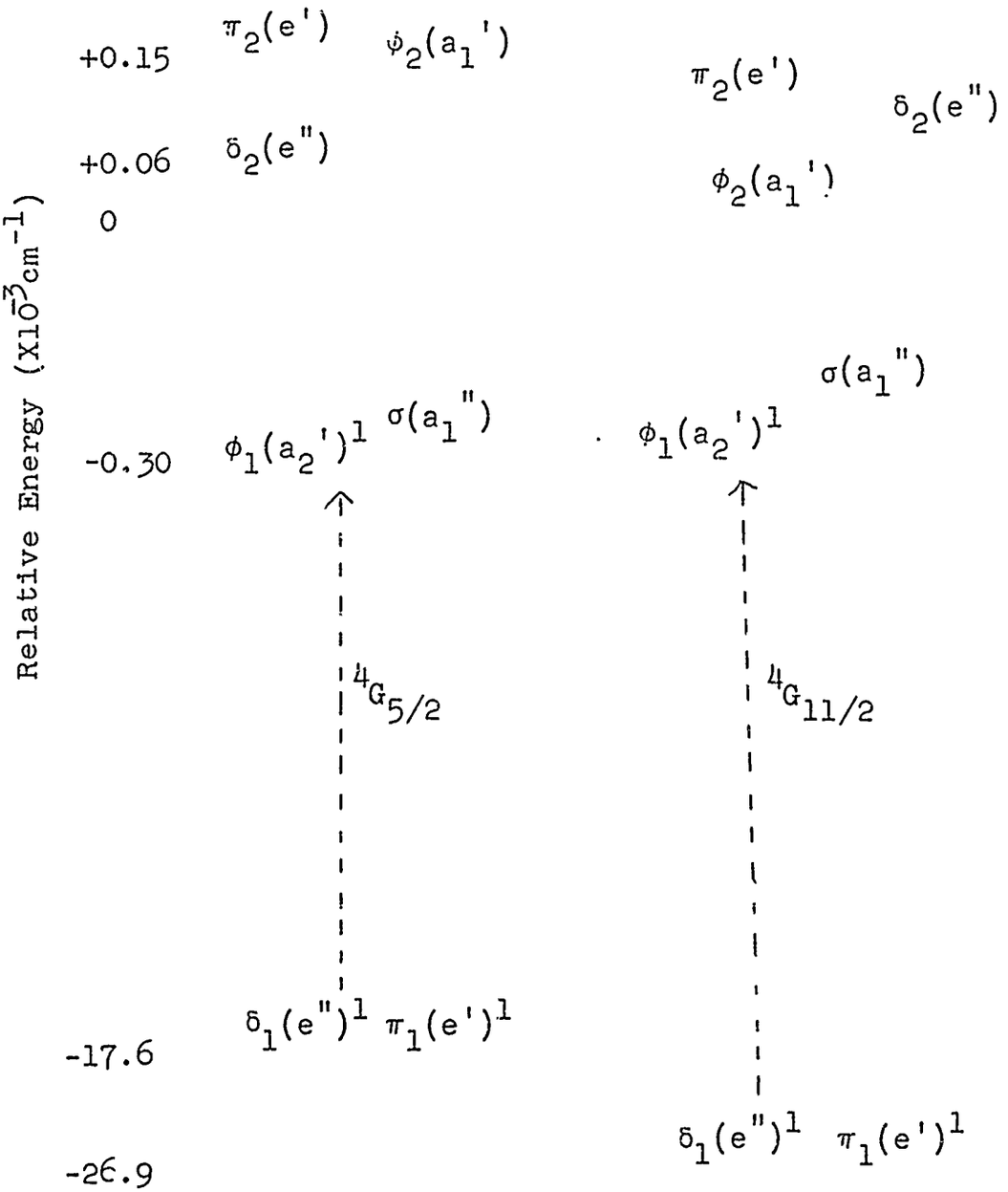

*See Reference (2).

Figure 3

CENTRAL ATOM (M) f-ORBITALS AND LIGAND ORBITAL COMBINATION (X) FOR MX_9 IN D_{3h} SYMMETRY*

TABLE I

$\lambda = \lvert M \rvert$ [a]	(M) Orbital[b]	Symmetry Character[c]	(X_9) Group Orbitals[d]
0	$f_z(5z^2 - 3r^2)$	$\sigma(a_1'')$	$1/\sqrt{6}\,(\sigma_4 + \sigma_5 + \sigma_6 - \sigma_7 - \sigma_8 - \sigma_9)$
1	$f_y(5_z{}^2 - r^2)$	$\pi_2(e')$	$1/\sqrt{2}\,(\sigma_2 - \sigma_3)$ $1/2\,(\sigma_5 - \sigma_6 + \sigma_8 - \sigma_9)$
1	$f_x(5z^2 - r^2)$	$\pi_1(e')$	Nonbonding
2	$f(xyz)$	$\delta_2(e'')$	$1/2\,(\sigma_5 - \sigma_6 - \sigma_8 + \sigma_9)$
2	$f_z(x^2 - y^2)$	$\delta_1(e'')$	Nonbonding
3	$f_x(x^2 - 3y^2)$	$\phi_2(a_1')$	$1/\sqrt{3}\,(\sigma_1 + \sigma_2 + \sigma_3)$ $1/\sqrt{6}\,(\sigma_4 + \sigma_5 + \sigma_6 + \sigma_7 + \sigma_8 + \sigma_9)$
3	$f_y(3x^2 - y^2)$	$\phi_1(a_2')$	Nonbonding

*After Jørgensen, Pappalardo and Schmidtke, J. Chem. Phys. 39, 1422 (1963).

a. The orbital quantum number

b. The constant factor $1/r^3$ and a normalizing factor have been omitted in each case.

c. The symmetry designation of the f-orbitals.

d. The σ-orbital combinations for 2P oxygen orbitals.

CHANGES IN MOLAR EXTINCTION COEFFICIENTS FOR Nd^{3+} AND Er^{3+} ACETYLACETONATES

$Nd(C_5H_7O_2)_3$: TABLE II

Solvent	λ(mμ)	$\epsilon_{max.}$	$(\alpha m)^a eff$	$\Delta(\alpha m)^b eff$
MeOH	585	21.6	14.7	21.6
EtOH	584	25.4	20.5	15.8
n-ButOH	584	20.4	30.5	5.8
CCl_4	586	21.1	11.1	25.2
$CHCl_3$	585	23.4	17.8	18.5
Benzene	586	25.2	10.5	25.8
Toluene	586	22.9	13.3	23.0

$Er(C_5H_7O_2)_3$:

Solvent	λ(mμ)	$\epsilon_{max.}$	$(\alpha m)eff$	$\Delta(\alpha m)^b eff$
MeOH	379	36.0	14.7	21.6
EtOH	378	25.1	20.5	15.8
n-ButOH	378	29.8	30.5	5.8
CCl_4	378	35.2	11.1	25.2
$CHCl_3$	378	38.6	17.8	18.5
Benzene	378	29.6	10.5	25.8
Toluene	378	29.3	13.3	23.0

a) The effective molar polarizability calculated from the molecular Clausius-Mosotti equation.

b) The difference in the effective molar polarizability between the solvent and acetylacetone ($\alpha m = 36.3$).

SOME CHROMOGENIC REAGENTS FOR THE LANTHANOIDS*

Arun K. Dey, Surendra N. Sinha†, Satendra P. Sangal and Kailash N. Munshi

Chemical Laboratories, University of Allahabad, Allahabad, India.

ABSTRACT

The use of Alizarin Red S, Chromotrope 2B, 4-(2-pyridylazo) resorcinol, 2-(p-sulphophenylazo)-1:8-dihydroxy-naphthalene-3:6-disulphonate, Thoron, Chrome Azurol S, Aluminon and Xylenol Orange, as chromogenic reagents for the lanthanoids has been described. They are sensitive, but not selective for the rare earths. Xylenol Orange and 2-(p-sulphophenylazo)-1:8 dihydroxynaphthalene 3:6-disulphonate are particularly suitable, the former being highly sensitive and the latter being more tolerant towards other cations.

INTRODUCTION

The methods for the detection and determination of metal ions with colourless reagents have recently been found to be inadequate for analytical purposes in view of the increasing demand for sensitivity. Hence, there is growing tendency to employ organic coloured reagents, especially dyes, which are usually more sensitive. For the rare earth elements, the following chromogenic reagents have been described in recent years : Alizarin Red S (23), Tiron (24), Arsenazo I (12), Arsenazo III (25), Pyrocatechol Violet (31),

* Supported by grants from the Council of Scientific and Industrial Research, New Delhi.

† Present address : Erie County Laboratory, 462 Grider Street, Buffalo-15, N.Y. (U.S.A.)

1-(2-pyridylazo) 2-naphthol (28), Thymolphthalexan (20), Bromopyrogallol Red (9) and Haematoxylin (27).

The present paper describes the use of some organic chromogenic reagents, studied in these laboratories, which form coloured chelates with the lanthanoids, and are therefore useful in colorimetric analysis.

EXPERIMENTAL

Instruments : All measurements were made with a Unicam SP 500 spectrophotometer using 1 cm glass cells. A Leeds and Northrup direct reading pH indicator with a glass-calomel electrode system was used for pH measurements.

Metal Solutions : Standard solutions of the rare earths (Johnson Matthey and Co.) were prepared by dissolving either their oxides or chlorides in dilute hydrochloric acid, and then diluting to the required extent.

Reagent Solutions : The standard solutions of the reagents were made by dissolving known weights of pure samples in water. Xylenol Orange was dissolved in 10% aqueous ethanol. All the reagents were obtained from British Drug Houses, except PAR which was of E.Merck make.

Table 1. Chromogenic Reagents for the Rare Earths

Chemical name	Trivial name	Abbreviated name
1. 3"-Sulpho-2":6-dichloro-3:3'-dimethyl-4-hydroxyfuchsone-5:5'-dicarboxylic acid (sodium salt)	Chrome Azurol S	CAS
2. 3:3'-bis N:N-di(carboxymethyl) aminomethyl-o-cresolsulphonphthalein	Xylenol Orange	DCAC
3. Ammonium aurintricarboxylate	Aluminon	AAC
4. 4-(2-Pyridylazo)-resorcinol	...	PAR

5. 2-(p-Sulphophenylazo)-1:8-dihydroxynaphthalene-3:6-disulphonic acid (sodium salt)	...	SPADNS
6. p-Nitrobenzene azochromotropic acid (sodium salt)	Chromotrope 2B	CTB
7. 1-(o-arsonophenylazo)-2-naphthol-3:6-disulphonic acid (sodium salt)	Thoron	APANS
8. 1:2-dihydroxyanthraquinone 3-sulphonic acid (sodium salt)	Alizarin Red S	ARS

Conditions of Study : All experiments were performed in an air conditioned room at 25°±1°C. The total volume of all the mixtures were kept 25 ml and pH was adjusted at a constant level by the addition of suitable amounts of hydrochloric acid or sodium hydroxide. In the case of PAC, mannitol was added to prevent the separation of the lakes. In view of the high value of the absorbance of some of the reagents at the wavelengths of maximum absorbance of the corresponding chelates, the observations were recorded at wavelengths where the differences between the absorbances of the chelates and of the reagent alone, were appreciable.

Rate of Colour Formation and Stability of Colour at Room Temperature : In some cases colour formation was instantaneous, while in others 10 to 30 minutes were required to develop the full intensity. Therefore, the absorbance measurements were performed after equilibration for a period of one hour in each case. Once the mixture attains the maximum colour intensity, the absorbance does not change even after standing for 24 hours.

Order of Addition of the Reagent : The effect of the order of addition of the reactants has hardly any effect on the sensitivity of the reaction or on the absorbance values.

Influence of Temperature : Temperature has no effect on the colour intensity from 5°-90°C, but if the mixtures are boiled for a long time the lakes tend to precipitate.

Effect of Reagent Concentration : Mixtures were prepared with constant metal ion and varying reagent concentrations. The absorbances were noted at definite wavelengths. At least 4-6 times excess of the reagent is necessary to develop the maximum colour intensity.

Absorption Maxima of the Chelates : Several mixtures containing metal ion : ligand in the ratio of (a) 0:1, (b) 1:0.5, (c) 1:1, (d) 1:2, (e) 1:3 and (f) 1:4, were prepared at fixed pH and absorbances were measured between 350 and 650 mμ. The wavelength of maximum absorbance in (a) indicated the λ_{max} of the reagent, while the λ_{max} of the chelate was found from the spectral curves of the other mixtures.

Influence of pH : The ligands used in this work, being dyes, change in colour with the variation of pH. The metal chelates also show changes in colour as the hydrogen ion concentration is varied. A number of mixtures containing known excess of ligands were prepared and pH adjusted to different values. The pH range within which the absorbance (at the λ_{max} of the chelate or at the wavelengths of observation) remains constant is the effective pH range for the photometric determinations.

Beer's Law : Mixtures were prepared by keeping the reagent in excess and adding varying amounts of the metal ions, keeping the total volume constant. The range of concentration for adherence to Beer's law in p.p.m. for each system was determined. From the Beer-law plots, the range of effective photometric determination in p.p.m. was evaluated for each system.

Sensitivity : The sensitivity of the colour reactions has been expressed in μg of element per sq. cm. for absorbance of 0.001, as defined by Sandell. Different mixtures containing excess of the reagent and metal ion in varying concentrations, were prepared and absorbances were noted against reagent blank. The sensitivity index was then calculated.

RESULTS AND DISCUSSION

The results obtained from a study of the various reagents and their chromogenic reactions with the rare earths, are briefly described in the following account.

Alizarin Red S

Several workers have studied the chromogenic reactions of ARS with the lanthanoids (5,8,11,23,30). In continuation with our studies (19) of the ARS chelates of scandium (III) and yttrium (III), we have now obtained the analytical data of the rare earths with ARS. The results are summarized in table 2.

Table 2. Photometric Determinations with ARS

Composition of the chelates - Metal:Reagent = 1:2; pH of study 4.0; Wavelength of study 530 mμ; λ_{max} of ARS = 420 mμ; Molar excess of the reagent = 4-fold.

Rare earth (III)	Wavelength maximum (mμ)	Range for effective determination (p.p.m.)	Optimum pH range	Sensitivity Index $\mu g/cm^2$
Sc	500	0.3 - 12.0	3.5 - 4.3	0.020
Y	510	0.6 - 25.0	4.0 - 4.5	0.089
La	520	1.0 - 8.0	3.7 - 4.5	0.087
Ce	520	1.0 - 8.0	3.7 - 4.5	0.093
Pr	525	1.0 - 8.0	3.7 - 4.3	0.090
Nd	520	1.0 - 8.0	3.7 - 4.3	0.072
Sm	520	1.0 - 8.0	3.7 - 4.3	0.100
Eu	530	1.0 - 8.0	3.7 - 4.3	0.100
Gd	520	1.0 - 8.0	3.7 - 4.3	0.078
Tb	520	1.0 - 9.0	3.7 - 4.5	0.070
Dy	530	1.0 - 9.0	4.0 - 4.5	0.080
Ho	530	0.8 - 17.0	4.0 - 4.5	0.082
Er	530	0.8 - 15.0	3.7 - 4.3	0.083
Tm	520	0.8 - 10.0	3.7 - 4.3	0.084
Yb	520	0.8 - 10.0	3.7 - 4.3	0.086
Lu	520	0.9 - 12.0	4.0 - 4.5	0.086

Chromotrope 2B

The excellent chromogenic and chelating properties of CTB and our earlier studies of their metal chelates (18), prompted the present study and we have, for the first time, observed the formation of coloured chelates of the lanthanoids with CTB. A summary of the work is given in table 3.

Table 3. Photometric Determinations with CTB

Composition of the chelates - Metal:Reagent = 1:1; pH of study 6.0; Wavelength of study 580 mμ; λ_{max} of CTB = 515 mμ; Molar excess of the reagent = 4-fold.

Rare earth (III)	Wavelength maximum (mμ)	Range for effective determination (p.p.m.)	Optimum pH range	Sensitivity Index $\mu g/cm^2$
Sc	530	0.3 - 3.0	5.5 - 6.5	0.022
Y	530	0.5 - 5.0	5.5 - 6.5	0.044

Contd...

La	540	0.5 - 9.0	5.5 - 6.5	0.139
Ce	540	0.6 - 10.0	5.7 - 6.5	0.093
Pr	535	0.6 - 10.0	5.7 - 6.5	0.070
Nd	540	0.7 - 8.0	5.5 - 6.5	0.070
Sm	530	2.0 - 8.0	5.5 - 6.3	0.070
Eu	530	0.7 - 15.0	5.5 - 6.5	0.080
Gd	530	0.7 - 6.0	5.7 - 6.7	0.100
Tb	540	0.5 - 5.0	5.7 - 6.5	0.100
Dy	530	0.7 - 9.0	5.7 - 6.5	0.080
Ho	545	0.8 - 9.0	5.8 - 6.5	0.082
Er	540	0.8 - 10.0	5.8 - 6.3	0.083
Tm	540	0.8 - 10.0	5.7 - 6.5	0.084
Yb	540	0.8 - 12.0	5.7 - 6.5	0.086
Lu	540	0.8 - 15.0	5.7 - 6.5	0.088

4-(2-Pyridylazo) Resorcinol

PAR has recently been suggested as a chromogenic reagent for the determination of metal ions (3,10). This reagent belongs to the same family as 1-(2-pyridylazo) naphthol (PAN) but has the added advantage of being soluble in water. We have earlier reported (16) the analytical data for the spectrophotometric determination of the rare earths with PAR, which are summarised in table 4.

Table 4. Photometric Determinations with PAR

Composition of the chelates - Metal:Reagent = 1:2; pH of study 6.2; λ_{max} of PAR = 410; Molar excess of the reagent = 4-fold.

Rare earth (III)	Wavelength maximum (mμ)	Range for effective determination (p.p.m.)	Optimum pH range	Sensitivity Index $\mu g/cm^2$
Y	515	0.5 - 4.0	5.5 - 7.0	0.029
La	515	0.4 - 6.0	5.8 - 7.0	0.043
Ce	515	0.4 - 7.0	6.0 - 7.0	0.053
Pr	515	0.4 - 7.0	6.0 - 7.0	0.056
Nd	515	0.5 - 6.0	6.0 - 7.0	0.028
Sm	515	0.5 - 6.0	6.0 - 7.0	0.025
Eu	515	0.5 - 6.0	6.0 - 7.0	0.034
Gd	515	0.5 - 6.0	6.0 - 7.0	0.036
Tb	515	0.4 - 7.0	6.0 - 7.0	0.039
Dy	515	0.4 - 7.0	6.0 - 7.0	0.032
Ho	515	0.4 - 7.0	6.0 - 7.0	0.041
Er	515	0.5 - 6.0	6.0 - 7.0	0.025
Tm	515	0.5 - 6.0	6.0 - 7.0	0.033

Contd...

Yb	515	0.5 - 6.0	6.0 - 6.8	0.043
Lu	515	0.5 - 6.0	6.0 - 7.0	0.045

2-(p-Sulphophenylazo)-1:8-dihydroxynaphthalene 3:6-disulphonate

The use of SPADNS in the determination of thorium and zirconium has been described (1,2). The formation of coloured chelates with the rare earths have been reported for the first time from these laboratories (17). Similar to the other known reagents for the rare earths, this reagent is not selective but is quite sensitive under the conditions described. The results are given in table 5.

Table 5. Photometric Determinations with SPADNS

Composition of the chelates - Metal:Reagent = 1:1; pH of study 6.0; Wavelength of study 580 mμ; λ_{max} of SPADNS = 515 mμ; Molar excess of the reagent = 6-fold

Rare earth (III)	Wavelength maximum (mμ)	Range for effective determination (p.p.m.)	Optimum pH range	Sensitivity Index $\mu g/cm^2$
Y	555	0.3 - 2.5	5.7 - 6.5	0.018
La	545	0.5 - 3.8	5.7 - 6.5	0.033
Ce	545	0.5 - 3.8	5.7 - 6.5	0.035
Pr	550	0.4 - 4.0	5.8 - 7.0	0.035
Nd	550	0.3 - 4.0	5.8 - 6.3	0.020
Sm	565	0.3 - 4.0	5.8 - 6.3	0.017
Eu	560	0.3 - 4.0	5.7 - 6.3	0.022
Gd	560	0.3 - 4.0	5.7 - 6.3	0.024
Tb	560	0.4 - 4.0	5.8 - 7.0	0.026
Dy	560	0.3 - 4.0	5.8 - 6.5	0.023
Ho	565	0.4 - 4.0	5.8 - 6.5	0.027
Er	565	0.3 - 4.0	5.8 - 6.5	0.016
Tm	560	0.4 - 4.0	5.8 - 6.3	0.024
Yb	565	0.4 - 4.0	5.7 - 7.0	0.034
Lu	565	0.4 - 4.0	5.7 - 7.0	0.036

Thoron

Some observations are available on the chromogenic reactions of rare earths with thoron (13,14). A detailed study of the lanthanoid chelates of thoron has now been done and table 6 describes the results.

Table 6. Photometric Determinations with APANS

Composition of the chelates - Metal:Reagent = 1:2; pH of study 4.0; Wavelength of study 545 mμ; λ_{max} of APANS = 480 mμ; Molar excess of the reagent = 4-fold

Rare earth (III)	Wavelength maximum (mμ)	Range for effective determination (p.p.m.)	Optimum pH range	Sensitivity Index $\mu g/cm^2$
Sc	500	0.3 - 2.0	3.7 - 4.5	0.022
Y	500	0.4 - 10.0	3.7 - 4.5	0.042
La	515	0.6 - 12.0	4.0 - 4.5	0.046
Ce	500	0.6 - 8.0	3.7 - 4.5	0.070
Pr	500	0.8 - 8.0	3.7 - 5.0	0.094
Nd	500	0.6 - 9.0	3.7 - 5.0	0.090
Sm	500	0.8 - 9.0	3.5 - 4.5	0.075
Eu	500	0.8 - 10.0	3.7 - 4.5	0.076
Gd	500	1.0 - 9.0	3.7 - 4.5	0.100
Tb	500	0.8 - 12.0	3.7 - 4.5	0.071
Dy	500	1.0 - 9.0	3.7 - 5.0	0.080
Ho	500	1.0 - 8.0	3.7 - 5.0	0.082
Er	500	0.8 - 15.0	3.5 - 4.5	0.083
Tm	500	1.0 - 9.0	3.7 - 5.0	0.084
Yb	500	1.0 - 9.0	3.7 - 5.0	0.086
Lu	500	1.0 - 10.0	3.7 - 5.0	0.087

Chrome Azurol S

CAS forms coloured chelates with many metals (7). The chromogenic reactions of the lanthanoids with CAS were noted for the first time in these laboratories and details of the experimental findings are recorded in table 7.

Table 7. Photometric Determinations with CAS

Composition of the chelates - Metal:Reagent = 1:1; pH of study 6.0; λ_{max} of CAS = 420 mμ; Molar excess of the reagent = 4-fold.

Rare earth (III)	Wavelength of study (mμ)	Range for effective determination (p.p.m.)	Optimum pH range	Sensitivity Index $\mu g/cm^2$
Sc	560	1.0 - 8.0	5.5 - 6.3	0.050
Y	500	1.0 - 7.0	5.7 - 6.5	0.092
La	520	1.0 - 6.0	5.7 - 6.3	0.139
Ce	520	0.7 - 6.0	5.7 - 6.5	0.093

Contd...

Pr	500	1.0 - 8.0	5.7 - 6.5	0.075
Nd	520	0.7 - 8.0	5.7 - 6.3	0.070
Sm	520	0.8 - 8.0	5.7 - 6.3	0.075
Eu	550	0.5 - 7.0	5.5 - 6.5	0.056
Gd	520	0.8 - 8.0	5.7 - 6.5	0.078
Tb	520	0.8 - 8.0	5.5 - 6.5	0.053
Dy	540	0.8 - 8.0	5.7 - 6.3	0.069
Ho	550	1.0 - 8.0	5.8 - 6.5	0.082
Er	520	1.0 - 9.0	5.8 - 6.3	0.167
Tm	520	0.6 - 6.0	5.8 - 6.3	0.113
Yb	550	1.0 - 8.0	5.8 - 6.5	0.113
Lu	550	1.0 - 9.0	5.8 - 6.3	0.140

Aluminon

Aluminon, like CAS, gives a large number of colour reactions with metal ions (7). Corey and Rogers (6) reported that AAC forms coloured products with scandium. In the present paper details of the experimental findings are worked out for the spectrophotometric determination of the rare earths, and the results are given in table 8.

Table 8. Photometric Determinations with AAC

Composition of the chelates - Metal:Reagent = 1:1; pH of study 6.0; λ_{max} of AAC = 520 mμ; Molar excess of the reagent = 4-fold.

Rare earth (III)	Wavelength maximum (mμ)	Range for effective determination (p.p.m.)	Optimum pH range	Sensitivity Index μg/cm^2
Y	540	0.5 - 12.0	5.5 - 6.5	0.029
La	540	1.0 - 9.0	5.5 - 6.5	0.069
Ce	540	0.6 - 10.0	5.5 - 6.5	0.070
Pr	540	0.6 - 14.0	5.5 - 6.5	0.056
Nd	540	0.5 - 15.0	5.5 - 6.5	0.057
Sm	540	0.4 - 18.0	5.5 - 6.5	0.070
Eu	540	0.4 - 18.2	5.5 - 6.5	0.038
Gd	540	0.4 - 18.8	5.5 - 6.5	0.039
Tb	540	0.4 - 19.0	5.5 - 6.5	0.039
Dy	540	0.4 - 19.4	5.5 - 6.5	0.040
Ho	540	0.4 - 19.7	5.5 - 6.5	0.041
Er	540	0.4 - 20.0	5.5 - 6.5	0.042
Tm	540	0.5 - 23.3	5.5 - 6.5	0.042
Yb	540	0.5 - 24.0	5.5 - 6.5	0.043
Lu	540	0.5 - 25.0	5.5 - 6.5	0.043

Xylenol Orange

Xylenol Orange has been used in the determination of various rare earths including yttrium (26,29), praseodymium (27), neodymium (27,28), samarium (4,22,27), gadolinium (4), dysprodium (4), holmium (27), and ytterbium (4). We have also worked out in detail (15) the analytical data for the colorimetric determination of rare earths with DCAC. The results are reproduced in table 9.

Table 9. Photometric Determinations with DCAC

Composition of the chelates - Metal:Reagent = 1:1; pH of study 5.0; λ_{max} of DCAC = 440 mμ; Molar excess of the reagent = 4-fold.

Rare earch (III)	Wavelength maximum (mμ)	Range for effective determination (p.p.m.)	Optimum pH range	Sensitivity Index $\mu g/cm^2$
Y	580	7.5 - 50	4.7 - 5.5	0.015
La	580	10.0 - 75	4.8 - 5.3	0.022
Ce	585	12.5 - 75	4.8 - 5.3	0.023
Pr	585	12.5 - 75	4.8 - 5.3	0.028
Nd	580	7.5 - 75	4.7 - 5.4	0.014
Sm	585	7.5 - 100	4.8 - 5.3	0.007
Eu	585	7.5 - 100	4.8 - 5.3	0.016
Gd	580	7.5 - 100	4.8 - 5.3	0.020
Tb	580	10.0 - 100	4.8 - 5.4	0.026
Dy	580	10.0 - 100	4.7 - 5.3	0.020
Ho	580	10.0 - 100	4.7 - 5.5	0.016
Er	580	10.0 - 100	4.7 - 5.4	0.013
Tm	580	10.0 - 100	4.7 - 5.4	0.010
Yb	580	12.5 - 112	4.7 - 5.4	0.021
Lu	580	12.5 - 115	4.7 - 5.4	0.019

Unfortunately none of these reagents described here, are specific for the individual rare earth metals. The reagents known so far give colour reactions with all the elements of the family, producing almost similarly coloured chelates. However, chromatography and ion exchange separation procedures enable a sharp separation of the individual

lanthanoids. So the main requirements of the reagents are now : (i) high sensitivity, (ii) water solubility to avoid organic solvent extraction and (iii) reproducibility.

The above mentioned criteria are satisfied by the reagents investigated in this work. DCAC is the most sensitive, but also gives colour reactions with many other metal ions. SPADNS is quite sensitive and has a lesser tendency of colour formation with elements other than the rare earths. These two reagents particularly show possibilities of use as suitable chromogenic reagents for the lanthanoids.

REFERENCES

1. Banerjee, G., Z. analyt. Chem., 148, 349 (1955).
2. Banerjee, G., Analyt. Chim. Acta, 16, 62 (1957).
3. Busev, A.I. & Chang, F., Talanta, 1, 101 (1962).
4. Buděšínský, B. & Bezděková, A., Z. analyt. Chem., 196, 172 (1963).
5. Charlot, G., Analyt. Chim. Acta, 1, 218 (1947).
6. Corey, R.B. & Rogers, N.W., J. Amer. Chem. Soc., 49, 2167 (1927).
7. Dey, A.K., Microchim. Acta, Benedetti-Pichler Anniversary Number, 414 (1964).
8. Erble, A.R. & Lerner, M.W., Analyt. Chem., 27, 1551 (1955).
9. Herrington, J. & Steed, K.C., Analyt. Chim. Acta, 22, 180 (1960).
10. Iwamoto, R., Bull. Chem. Soc. Japan, 34, 605 (1961).
11. Kolthoff, I.M. & Elmquist, R., J. Amer. Chem. Soc., 53, 1121 (1931).

12. Kuteinikov, A.F. & Lankoi, G.A., Zhur. analit. Khim., 14, 686 (1959).

13. Kuznetsov, V.I., Zhur. Obshchei Khim., 10, 1512 (1940).

14. Lane, W.J., Thesis, Iowa State College (1957); vide Chem. Abstracts, 52, 10796 (1958).

15. Munshi, K.N. & Dey, A.K., Chemist-Analyst, 53, 105 (1964).

16. Munshi, K.N. & Dey, A.K., Analyt. Chem., 36, 2003 (1964).

17. Munshi, K.N. & Dey, A.K., Microchem. J., 8, 152 (1964).

18. Munshi, K.N. & Dey, A.K., J. Inorg. Nucl. Chem., 26, 1603 (1964).

19. Munshi, K.N., Sinha, S.N., Sangal, S.P. & Dey, A.K., Microchem. J., 7, 473 (1963).

20. Prajasnar, D., Chem. analit. (Warsaw), 7, 861 (1962).

21. Prajasnar, D., Chem. analit. (Warsaw), 8, 71 (1963).

22. Prajasnar, D., Chem. analit. (Warsaw), 6, 885 (1961).

23. Rinehart, R.W., Analyt. Chem., 26, 1820 (1954).

24. Sarma, B., J.Sci.Ind.Research (India), 14B, 538 (1955)

25. Savvin, S.B., Zavodskaya Lab., 29, 131 (1963).

26. Serdyuk, L.S. & Smirnaya, V.S., Zhur. analit. Khim., 19, 451 (1963).

27. Sharma, T.B. & Raghava Rao, Bh.S.V., J.Sci.Ind. Research (India) 14B, 450 (1955).

28. Shibata, S., Analyt. Chim. Acta, 28, 388 (1963).

29. Tonosaki, K. & Otomo, M., Bull. Chem. Soc. Japan, 35, 1683 (1962).

30. Wenger, P.W., Duckert, R. & Rusconi, Y., Helv. Chim. Acta, 28, 925 (1945).

31. Young, J.P., White, J.C. & Ball, R.G., Analyt. Chem., 32, 928 (1960).

UNCLASSIFIED
Security Classification

DOCUMENT CONTROL DATA — R&D

(Security classification of title, body of abstract and indexing annotation must be entered when the overall report is classified)

1. ORIGINATING ACTIVITY *(Corporate author)*
Iowa State University
Department of Physics
Ames, Iowa

2A. REPORT SECURITY CLASSIFICATION
☒ Unclassified
Other — Specify

2B. GROUP

3. REPORT TITLE
Rare Earth Research Conference 5th Ames, Iowa 30 Aug-1 Sep 1965 Books 1-6. Spectra Bk 1; Solid State Bks 2,4 & 6; Chemistry Bk 3; Metallurgy Bk 5

4 DESCRIPTIVE NOTES *(Type of report and inclusive dates)*
☐ Scientific Report ☒ Final Report ☐ Journal Article ☐ Proceedings ☐ Book

5. AUTHOR(S) *(Last name, first name, initial)*
(Legvold Sam Dr (PI)

6. REPORT DATE AS PRINTED	7A. TOTAL NO. OF PAGES	7B. NO. OF REFS
September 1965	718	811

8A. CONTRACT OR GRANT NO.
AF-AFOSR-812-65

B. PROJECT NO. 9760-01

C 61445014

D.

9A. ORIGINATOR'S REPORT NUMBER(S) *(if given)*

9B. OTHER REPORT NO.(S) *(Any other numbers that may be assigned this report)*
AFOSR 65-1917
AD

10 AVIALABILITY/LIMITATION NOTICES
Distribution of this document is unlimited

☒ Available from DDC
☒ Available from CFSTI
☐ Available from Source
☐ Available Commercially

11. SUPPLEMENTARY NOTES *(Citation)*

12. SPONSORING MILITARY ACTIVITY
AF Office of Scientific Research (SRC)
Office of Aerospace Research
Washington, D. C. 20333

13 ABSTRACT

A total of 69 papers were presented at the Rare Earth Research Conference. The papers, with abstracts, are contained in 6 volumes. Book 1 deals with spectra; Books 2, 4, and 6, solid state; Book 3, chemistry; and Book 5, metallurgy. (U)

DD FORM 1473
1 JAN 64

UNCLASSIFIED
Security Classification

Security Classification

14. KEY WORDS	LINK A		LINK B		LINK C	
	ROLE	WT	ROLE	WT	ROLE	WT
Metallurgy Rare Earth Elements Solid States Spectra Symposia						

INSTRUCTIONS

1. ORIGINATING ACTIVITY. Enter the name and address of the contractor, subcontractor, grantee, Department of Defense activity or other organization *(corporate author)* issuing the report.

2a. REPORT SECURITY CLASSIFICATION: Enter the overall security classification of the report. Indicate whether "Restricted Data" is included. Marking is to be in accordance with appropriate security regulations.

2b. GROUP: Automatic downgrading is specified in DoD Directive 5200.10 and Armed Forces Industrial Manual. Enter the group number. Also, when applicable, show that optional markings have been used for Group 3 and Group 4 as authorized.

3. REPORT TITLE: Enter the complete report title in all capital letters. Titles in all cases should be unclassified. If a meaningful title cannot be selected without classification, show title classification in all capitals in parenthesis immediately following the title.

4. DESCRIPTIVE NOTES: If appropriate, enter the type of report, e.g., interim, progress, summary, annual, or final. Give the inclusive dates when a specific reporting period is covered.

5. AUTHOR(S): Enter the name(s) of author(s) as shown on or in the report. Enter last name, first name, middle initial. If military, show rank and branch of service. The name of the principal author is an absolute minimum requirement.

6. REPORT DATE: Enter the date of the report as day, month, year; or month, year. If more than one date appears on the report, use date of publication.

7a. TOTAL NUMBER OF PAGES: The total page count should follow normal pagination procedures, i.e., enter the number of pages containing information.

7b. NUMBER OF REFERENCES: Enter the total number of references cited in the report.

8a. CONTRACT OR GRANT NUMBER. If appropriate, enter the applicable number of the contract or grant under which the report was written.

8b, &, & 8d. PROJECT NUMBER. Enter the appropriate military department identification, such as project number, subproject number, system numbers, task number, etc.

9a. ORIGINATOR'S REPORT NUMBER(S): Enter the official report number by which the document will be identified and controlled by the originating activity. This number must be unique to this report.

9b. OTHER REPORT NUMBER(S): If the report has been assigned any other report numbers *(either by the originator or by the sponsor)*, also enter this number(s).

10. AVAILABILITY/LIMITATION NOTICES: Enter any limitations on further dissemination of the report, other than those imposed by security classification, using standard statements such as:

(1) "Qualified requesters may obtain copies of this report from DDC."

(2) "Foreign announcement and dissemination of this report by DDC is not authorized."

(3) "U. S. Government agencies may obtain copies of this report directly from DDC. Other qualified DDC users shall request through

_____."

(4) "U. S. military agencies may obtain copies of this report directly from DDC. Other qualified users shall request through

_____."

(5) "All distribution of this report is controlled. Qualified DDC users shall request through

_____."

If the report has been furnished to the Office of Technical Services, Department of Commerce, for sale to the public, indicate this fact and enter the price, if known.

11. SUPPLEMENTARY NOTES: Use for additional explanatory notes.

12. SPONSORING MILITARY ACTIVITY: Enter the name of the departmental project office or laboratory sponsoring *(paying for)* the research and development. Include address.

13. ABSTRACT: Enter an abstract giving a brief and factual summary of the document indicative of the report, even though it may also appear elsewhere in the body of the technical report. If additional space is required, a continuation sheet shall be attached.

It is highly desirable that the abstract of classified reports be unclassified. Each paragraph of the abstract shall end with an indication of the military security classification of the information in the paragraph, represented as *(TS)*, *(S)*, *(C)*, or *(U)*

There is no limitation on the length of the abstract. However, the suggested length is from 150 to 225 words.

14 KEY WORDS: Key words are technically meaningful terms or short phrases that characterize a report and may be used as index entries for cataloging the report. Key words must be selected so that no security classification is required. Identifiers, such as equipment model designation, trade name, military project code name, geographic location, may be used as key words but will be followed by an indication of technical context. The assignment of links, roles, and weights is optional.